University of Denver
Digital Commons @ DU

Electronic Theses and Dissertations | Graduate Studies

1-1-2018

The Investigation of Lactoferrin Nitration: Quantification, Function, and Inhibition

Amani Yahya Alhalwani
University of Denver

Follow this and additional works at: https://digitalcommons.du.edu/etd

 Part of the Biochemistry Commons, and the Environmental Chemistry Commons

Recommended Citation

Alhalwani, Amani Yahya, "The Investigation of Lactoferrin Nitration: Quantification, Function, and Inhibition" (2018). *Electronic Theses and Dissertations*. 1452.
https://digitalcommons.du.edu/etd/1452

This Dissertation is brought to you for free and open access by the Graduate Studies at Digital Commons @ DU. It has been accepted for inclusion in Electronic Theses and Dissertations by an authorized administrator of Digital Commons @ DU. For more information, please contact jennifer.cox@du.edu,dig-commons@du.edu.

The Investigation of Lactoferrin Nitration: Quantification, Function, and Inhibition

Abstract

Lactoferrin (LF) is an iron-binding glycoprotein of molecular mass ca. 80 kDa that is predominantly found in mammalian body fluids. Lactoferrin is a multifunctional protein that has a wide range of properties such as antibacterial, antiviral, anti-inflammatory, and anti-allergic functions. Tyrosine residues in the protein play a part in many lactoferrin functions. Protein tyrosine nitration modification represents an oxidative and nitrosative stress process which can be caused by the exposure of proteins to oxidants from air pollution or disease. Understanding the way nitrated lactoferrin interacts with the biochemical environment of the body is thus important to the broader goal of understanding and preventing lactoferrin-related diseases, including certain ocular diseases. The main goal of this set of linked studies was to investigate the process by which LF may be nitrated, to observe changes in its protein structure and function, and to investigate a possible route to block the nitration process.

In the first project discussed here, nitrated lactoferrin was synthesized using two different nitration agents: sodium peroxynitrite and tetranitromethane. After nitration, spectroscopic analysis showed formation of nitrotyrosine with an increase in absorbance intensity at 350 nm, as well as attenuation in fluorescence intensity at an excitation wavelength of 280 nm. A sandwich ELISA protocol was developed to quantify the amount of nitrotyrosine in nitrated lactoferrin samples. The results show that the increase in the amount of nitrotyrosine depends on the molar ratio of nitrating agents added to the reaction. This study represents the first time that nitrotyrosine in lactoferrin had been selectively detected. In the second project, a broth microplate antibacterial susceptibility assay was applied to determine changes in the antibacterial function of lactoferrin brought about after nitration. The results reveal a reduction in the naturally present antibacterial activity of LF, which scales linearly with the increase in nitration molar ratios. In the third project, ergothioneine was used to inhibit the nitration reaction using several protein models, as well as to examine it as a potential therapeutic target for nitrosative stress-related diseases. The results illustrated that ergothioneine diminished the nitration production and protected the protein antibacterial activity. Collectively, these findings suggest that the nitration of tyrosine residues within lactoferrin can be important with respect to several physiological processes. Thus, further understanding the interaction between nitrated LF and the biochemical environment may aid in future research toward clinical diagnoses and in the development of therapies for diseases involving nitration of lactoferrin.

Document Type

Dissertation

Degree Name

Ph.D.

Department

Chemistry and Biochemistry

First Advisor

John Alexander Huffman, Ph.D.

Second Advisor

Rebecca Powell

Third Advisor

Michelle Knowles

Keywords

Atmospheric pollution, Ergothioneine, Lactoferrin, Nitrotyrosine, Ocular disease, Protein nitration

Subject Categories

Biochemistry | Chemistry | Environmental Chemistry

Publication Statement

Copyright is held by the author. User is responsible for all copyright compliance.

This dissertation is available at Digital Commons @ DU: https://digitalcommons.du.edu/etd/1452

THE INVESTIGATION OF LACTOFERRIN NITRATION: QUANTIFICATION, FUNCTION, AND INHIBITION

_____

A Dissertation

Presented to

the Faculty of Natural Sciences and Mathematics

University of Denver

_____

In Partial Fulfillment

of the Requirements for the Degree

Doctor of Philosophy

_____

by

Amani Yahya Alhalwani

June 2018

Advisor: John Alexander Huffman, PhD

©Copyright by Amani Yahya Alhalwani 2018

All Rights Reserved

Author: Amani Yahya Alhalwani
Title: THE INVESTIGATION OF LACTOFERRIN NITRATION: QUANTIFICATION, FUNCTION, AND INHIBITION
Advisor: John Alexander Huffman, PhD
Degree Date: June 2018

Abstract

Lactoferrin (LF) is an iron-binding glycoprotein of molecular mass ca. 80 kDa that is predominantly found in mammalian body fluids. Lactoferrin is a multifunctional protein that has a wide range of properties such as antibacterial, antiviral, anti-inflammatory, and anti-allergic functions. Tyrosine residues in the protein play a part in many lactoferrin functions. Protein tyrosine nitration modification represents an oxidative and nitrosative stress process which can be caused by the exposure of proteins to oxidants from air pollution or disease. Understanding the way nitrated lactoferrin interacts with the biochemical environment of the body is thus important to the broader goal of understanding and preventing lactoferrin-related diseases, including certain ocular diseases. The main goal of this set of linked studies was to investigate the process by which LF may be nitrated, to observe changes in its protein structure and function, and to investigate a possible route to block the nitration process.

In the first project discussed here, nitrated lactoferrin was synthesized using two different nitration agents: sodium peroxynitrite and tetranitromethane. After nitration, spectroscopic analysis showed formation of nitrotyrosine with an increase in absorbance intensity at 350 nm, as well as attenuation in fluorescence intensity at an excitation wavelength of 280 nm. A sandwich ELISA protocol was developed to quantify the amount of nitrotyrosine in nitrated lactoferrin samples. The results show that the increase

in the amount of nitrotyrosine depends on the molar ratio of nitrating agents added to the reaction. This study represents the first time that nitrotyrosine in lactoferrin had been selectively detected. In the second project, a broth microplate antibacterial susceptibility assay was applied to determine changes in the antibacterial function of lactoferrin brought about after nitration. The results reveal a reduction in the naturally present antibacterial activity of LF, which scales linearly with the increase in nitration molar ratios. In the third project, ergothioneine was used to inhibit the nitration reaction using several protein models, as well as to examine it as a potential therapeutic target for nitrosative stress-related diseases. The results illustrated that ergothioneine diminished the nitration production and protected the protein antibacterial activity. Collectively, these findings suggest that the nitration of tyrosine residues within lactoferrin can be important with respect to several physiological processes. Thus, further understanding the interaction between nitrated LF and the biochemical environment may aid in future research toward clinical diagnoses and in the development of therapies for diseases involving nitration of lactoferrin.

Acknowledgements

I would like to express appreciation to the mentorship of Dr. J. Alex Huffman. I sincerely appreciate his patience throughout my graduate studies and his precious advice. I am extremely grateful to committee members; Dr. Michelle K. Knowles, Dr. Brian Majestic, and Dr. Rebecca Powell who assisted and guided me through the process to accomplish this graduate study. Also, a big thanks to Dr. Michelle K. Knowles, Dr. John E. Repine, Dr. Brian Cowen, Dr. John Latham, Dr. Scott Horowitz, Dr. Scott Barbee, and Dr. Angila Hebel for their contributions, thoughtful sharing of knowledge and information. I am grateful to Dr. Ying Chen for her invaluable scientific advice and friendship. I would like to thank the funding support from a grant by the University of Denver Knoebel Institute for Healthy Aging (KIHA) and the scholarship support from King Saud bin Abdulaziz University for Health Sciences (KSAU-HS). A special thanks to my friends who provided skillful help and friendship. I am grateful to all past and current members of the Huffman group for their support at all times.

I dedicate this work to the memory of my mother in heaven, Mrs. Weedad T. Nusier. I would like to give sincerest thanks to my father, Mr. Yahya A. Alhalwani for his emotional support no matter what path I choose. I would like to extend special thanks to my sisters and brothers for the constant support they've provided to me.

Heartfelt thanks to my husband, Dr. Mohammed Khojah, for his patience and continual support of my academic endeavors over the past years. I would like to warmly thank my children who bring me such happiness and keep me on my toes. My children

have grown up watching me study and manage both family and work. Each has contributed immeasurably to our family happiness in their own special way. I hope I have been a good mother and that I have not lost too much during my studies.

Table of contents

List of figures

List of abbreviations

A……..absorbance

APS……..……...ammonium persulfate

BCA……bicinchoninic acid assay

Bestsel……..… β-Structure Selection

BSA……bovine serum albumin

ca……calculated

CAM……..….. chloramphenicol

CD…….circular dichroism

Cys……..……. cysteine

EEM…….excitation emission matrix

ELISA……..…enzyme linked immunosorbent assay

Ergo……..……..Ergothioneine

et.al……and coworkers

HEPES……..……4-(2-Hydroxyethyl)piperazine-1-ethanesulfonic acid, N-(2-Hydroxyethyl)piperazine-N′-(2-ethanesulfonic acid)

His……histidine

Kan……..……kanamycine

LF……..lactoferrin

LPS……..lipopolysaccharide

Met ……..methionine

NO_2……nitrogen dioxide

NLF…….…….nitrated lactoferrin

NTyr……...3-nitrotyrosine

O. D……...optical density

$ONOO^-$…….…….peroxynitrite

PAGE…… polyacrylamide gel electrophoresis

Phe……...phenylalanine

RT……..room temperature

s…….standard diviation

SDS…….……..sodium dodecyl sulfate

TMB…….....3,3’,5,5’-tetramethylbenzidine

TNM……tetranitromethane

Trp……tryptophan

Tyr…….tyrosine

UV-Vis……..ultraviolet-visible

Chapter one: Introduction

1.1 Overview of lactoferrin

1.1.1 Background of lactoferrin

Lactoferrin (LF) is a protein found widely within the physiological system of mammals. LF was discovered in 1939 by M. Sørensen and S. P. L. Sørensen in bovine milk. An alternative name for lactoferrin is lactotransferrin due to a similar structural homology to transferrin, (Masson, et al. 1971). This name was proposed by Blanc and Isliker in 1961 (Blanc, et al. 1961). It exists in mammals and is found mainly in granules of neutrophils and is present in secreted fluid such as tears, milk, and saliva (Masson, et al. 1966). It is produced by acinar epithelial cells and neutrophils (Baggiolini, et al. 1970; Spitznagel, et al. 1974).

1.1.2 Structure of lactoferrin

LF is a monomeric glycoprotein with molecular weight 80 kDa and containing 703 amino acids residues (Metz-Boutigue, et al. 1984). It consists of two globular lobes (C and N) which are connected via an α-helix (Metz-Boutigue, et al. 1984; Adlerova, et al. 2008). The net charge of LF is positive (González-Chávez, et al. 2009). LF is able to bind and transfer non-heme iron (Fe^{3+}) ions (Metz-Boutigue, et al. 1984; Baker, et al. 1990).

1.1.3 Iron binding sites on lactoferrin structure

Each globular lobe has identical composition and function. The lobes contain two domains: the N-lobe has N1 and N2 domains and the C-lobe has C1 and C2 domains, e.g. Figure 1. a in (García-Montoya, et al. 2012). Each globular lobe in LF has one active binding site to bind to Fe^{3+}, which makes each mole of LF bind to two moles of Fe^{3+} (Adlerova, et al. 2008). The binding site in each lobe comprises of four amino acids which are: two tyrosines (Tyr), one aspartic acid (Asp), and one histidine (His). Particularly, Asp-61, Tyr-93, Tyr-193, and His 254 in the N-lobe and Asp-396, Tyr-436, Tyr-529, and His 598 in the C-lobe (Anderson, et al. 1989b). These amino acids provide negative charges to balance the Fe^{3+} charge via the two phenolate oxygens from Tyr, one carboxylate oxygen from Asp, and one imidazole nitrogen from His, and the arginine (Arg) side chain with the N-terminus helix provides positive charges to balance CO_3^{2-} charge, shown in Figure.1 b in (García-Montoya, et al. 2012).

The N-lobe of the protein has an open binding cleft which closes when it binds to metal. The C-lobe cleft remains closed with or without binding to metal. Also, LF changes the form of the lobes due to binding. LF has a closed form when it binds to Fe^{3+}; LF has an open form when it is free to bind, shown in Figure 1. A and B in (Latorre, et al. 2010). LF has three iron binding forms: not bound to iron (apolactoferrin), and bound to two irons (hololactoferrin) (Latorre, et al. 2010).

1.2 Lactoferrin function

1.2.1 Lactoferrin function dependent on iron

LF receptors bind to iron in LPS (lipopolysaccharide) within the bacterial wall and inhibits the growth (Krewulak, et al. 2008). Also, LF binds to glycosaminoglycans of eukaryotic cell and prevent viruses from binding, see Figure 3 in (González-Chávez, et al. 2009).

Some biological functions are determined by LF, such as antioxidant properties provided to the cell via the production of hydroxyl radicals within leukocytes (Kanyshkova, et al. 2001). LF shows some of these biological functions because of the iron-binding capacity of the protein. The antioxidant function of LF, for example, relates iron-binding properties to hydroxyl radicals production in leukocytes, which the protein accomplishes without releasing O_2 and H_2O_2 (Kanyshkova, et al. 2001).

1.2.2 Lactoferrin function independent of iron

LF is able to attach to the surfaces of many types of cells via surface properties such as monocytes (Birgens, et al. 1983). The main part of LF molecule that binds to the cell surface is the N-terminal lobe. For example, LF competes with binding activity of lipopolysaccharides (LPS) in the bacteria wall to bind to immature dendritic cells from (CD14) receptors deficient mice and prevent inflammation (Baveye, et al. 1999).

1.2.3 The surface properties of lactoferrin

The LF protein has an isoelectric point (pI~ 9) which makes it a cationic surface. Additionally, LF has properties to bind to the macromolecule independent from the iron binding site (Baker, et al. 2009). Several of LF antimicrobial functions are associated to the surface cationic charge, which is mainly in the N-lobe (Valenti, et al. 2005).

1.3 Lactoferrin functions.

LF has two known mechanisms for antibacterial functions. The LF antibacterial mechanism that remains unknown is the interaction which prevents the bacteria from attaching to the host cell receptors (González-Chávez, et al. 2009). The bactericidal function shows the direct interaction of charge on the LF molecule, e.g. Figure 5 in (Baker, et al. 2005) to the bacteria surface (Baker, et al. 2005). The bacteriostatic function is related mainly to iron-binding properties which inhibits bacterial growth via binding to the iron in the environment which is essential for the growth (Jenssen, et al. 2009). LF shows bacteriostatic action against *E. coli*, *B. subtilis*, *B. stearothermophilus*, *S. albus*, *S. aureus*, and *P. aeruginosa* (Oram, et al. 1968; Masson, et al. 1966).

1.3.1 Anti-inflammatory properties

LF is called an acute-phase protein because it increases in concentration during most of the inflammation reaction (Kanyshkova, et al. 2001). LF plays a crucial role in inflammation by inhibiting the inflammation receptors (Conneely 2001). By binding to specific receptors of the target cell surface, LF protects them from the damage by oxidative radicals such as monocytes, macrophages, and hepatocytes (Brock 1995). Also, it inhibits the production of tumor necrosis facor-α (TNF) and interleukin-1 (IL-1) in the inflammatory process (Crouch, et al. 1992).

1.3.2 Antioxidant properties

LF in tears protects the corneal epithelial cells from UV damage through inhibition of hydroxyl radical formation (Shimmura, et al. 1996). Furthermore, LF has an antioxidant affect through the iron-binding site to prevent the production of the hydroxyl radical (Wakamatsu, et al. 2008).

1.3.3 Antibacterial mechanisms of lactoferrin

a. Bactericidal mechanism

The cationic charge in LF at the N-terminal binds to the bacteria anion surface lipopolysaccharides (LPS) and causes membrane damage (Roşeanu, et al. 2010). This cationic nature is concentrated on the N-terminus at residues 1-7, the first helix at residues 13-30, and the inter-lobe region, see Figure 2.A and B in (González-Chávez, et al. 2009).

b. Bacteriostatic mechanism

The LF iron-binding site binds to the membrane of gram negative bacteria to destabilize the membrane organization. The bacteria *A. actinomycetemcomitans* requires magnesium cations to organize the membrane by stabilizing LPS and protect the bacterial outer membrane which plays a role in the metabolic function (Kalmar, et al. 1988).

1.4 Protein nitration

1.4.1 Tyrosine nitration reaction

The protein Tyr nitration is the result of covalent reaction by the addition of nitro group into the ortho position in aromatic ring (Riordan, et al. 1966). The specific Tyr nitrating reagent is tetranitromethane (TNM) which produces mainly 3-nitrotyrosine (NTyr) (Sokolovsky, et al. 1966). Also, the peroxynitrite ($ONOO^-$) reagent used nitrate Tyr and other amino acids, and it is suitable for *in vivo* study (Franze, et al. 2005; Shuker, et al. 1993).

1.4.2 Nitration protein and biochemical properties

In vivo protein nitration is caused by reactive nitrogen species (RNS) including peroxynitrite ($ONOO^-$) and nitrogen dioxide (NO_2) to produce 3-nitrotyrosine (NTyr)

(Aulak, et al. 2004). The NTyr is used as a marker to the protein function alteration in many physiological and pathological systems (Turko, et al. 2002; Good, et al. 1998; Kim, et al. 2002; Franze, et al. 2003). After nitration, the pKa value of protein changes from pKa 10 to 7 due to the addition of NO_2 in the protein structure, shown in Figure 1 in (Radi 2013). The reduction on pKa affects protein function (Begara-Morales, et al. 2013). Nitration makes the protein hydrophobic and adds steric hindrance to the protein structure (Savvides, et al. 2002). The nitration process changes protein conformation. For example, α-synuclein protein showed changes in folding conformation *in vitro* (Uversky, et al. 2005). Additionally, nitration has been shown to form the protein oligomerization structure (Kampf, et al. 2015). These changes in the chemical properties can play an important role in protein activity dysfunction.

1.4.3 Protein nitration health implications

The protein nitration has been reported with direct correlation to diseases such as cardiovascular disease (Turko, et al. 2002), neurodegenerative disease (Good, et al. 1998), and ocular disease (Kim, et al. 2002); and indirect exposure to substances such as birch pollen which linked to the increase in allergenic diseases (Franze, et al. 2003). These implications highlight the need for further investigation in the biochemical properties of protein nitration to explore the function changes or addition in the protein.

1.5 LF nitration modification

1.5.1 The effect of chemical modifications to LF function

Protein chemical modification has previously been used to study LF structure and functional activities (Hutchens, et al. 2012). The protein was modified with several site-

specific amino acids such as cysteine, methionine, tryptophan, and tyrosine (Lundblad 2018). LF activities changed due to the type of chemical modifications. For example, amidation chemical modification in LF improved antimicrobial function but acylation eliminated antimicrobial and antiviral properties (Pan, et al. 2007). The nitration chemical modification in LF changes iron-binding properties (Teuwissen, et al. 1973). The focus of this work was on protein nitration specific to tyrosine (Tyr) residues. Protein nitration is an important tyrosine modification because it is linked to oxidative stress, inflammation, aging, and many other diseases (Ogino, et al. 2007; Andreadis, et al. 2003; Tsang, et al. 2009; Elahi, et al. 2009; Yeo, et al. 2008). A study showed a reduction in iron binding of LF after mutation via converted tyrosine residues in both binding sites (Tyr-93, Tyr-193, Tyr-436, and Tyr-529) to alanine residues (Ward, et al. 1996).

1.6 Analytical techniques to characterize protein nitration

Modification of Tyr to NTyr can play an important role in the physiological system, and the ability to detect and quantify the modified residues can be impactful for a number of medically-relevant research endeavors. For example, Ischiropoulos reviewed several methods to determine the NTyr concentration in diseased samples of human and animal tissue (Ischiropoulos 1998). NTyr has been quantified using Western blot (WB) (Hinson, et al. 2000), enzyme-linked immunosorbent assay (ELISA) (ter Steege, et al. 1998), high-performance liquid chromatography (HPLC) (Crow, et al. 1995), and gas chromatography paired with mass spectrometry (GC-MS) (Dalle-Donne, et al. 2006) techniques. Tandem mass spectrometric (MS/MS) analysis is the most sensitive for detecting low concentrations of NTyr and was used to investigate the relationship of nitrated

proteins to many diseases, but requires very high up-front cost (ca. $300k to $1,000k) and high maintenance costs (Yeo, et al. 2008; Reinmuth-Selzle, et al. 2014). To overcome some of the limitations presented by MS analysis, many studies now substantiate that ELISA can be applied to selectively detect nitrotyrosine within a sample (Baker, et al. 2000).

1.7 Nitration inhibitor

Through aging and disease, the concentration of $ONOO^-$ can be increased dramatically and can both alter and impair biological function via nitration reaction. It is important to maintain the protein structure by preventing nitration reaction using nitration inhibitors.

There are several nitration inhibitors such as glutathione (GSH) which acts by reacting the thiol group with peroxynitrite to prevent nitration (Sies, et al. 1997). Hydroxycinnamates acts to protect Tyr from nitration by preventing the electron transfer reaction (Pannala, et al. 1998), polyhydroxyphenols by scavenging hydroxyl radical ($^{\bullet}OH$) (Chung, et al. 1998), selenocystine, selenomethionine and ebselen by a catalytic cycle to reduce peroxynitrite to nitrite (NO_2^-) (Sies, et al. 1996), and ergothioneine (Ergo) by by scavenging $ONOO^-$ (Aruoma, et al. 1997). The study showed that Ergo is more effective as antioxidant activity towards peroxynitrite radical than other antioxidants for example; 80% higher than GSH or Trolox C and 25% higher than uric acids by protecting Tyr residues from peroxynitrite (Aruoma, et al. 1997; Franzoni, et al. 2006a).

1.8 Lactoferrin and health

1.8.1 The effect of peroxynitrite in eye

The presence of $ONOO^-$ in the eye is generated from over-production of $\cdot NO$ and $O_2^{\cdot -}$ in tissue and that was caused by physiological and pathological conditions (Allen, et al. 1998). For example, an *in vitro* study showed the effect of inflammation, which increased the production of nitric oxide synthase (NOS) in tear fluid and on ocular surface tissues, causing damage to the ocular surface. In that study the concentration of NOS in tears was 1.5-5 µM and 5-110 µM in aqueous humour (Park, et al. 2001). The oxidative stress markers nitrotyrosine, as a marker for nitric oxide, and malondialdehyde, as a marker for lipid peroxidation, were detected in human corneal disease and showed a significant relation of oxidative damage to corneal disease. In Figure 1 at *(Buddi, et al. 2002)* shows the possible pathways of oxidative stress markers which is produced by endothelial nitric oxide (eNOS) or inducible nitric oxide(iNOS)for protein nitration and reactive oxygen species for lipid peroxidation (Buddi, et al. 2002).

1.8.2 The effect of protein nitration in ocular surfaces

Ocular surfaces have been studied after being directly exposed to oxidative stress via environmental conditions and air pollution (Wakamatsu, et al. 2008). An association exists between traffic-borne air pollution and ocular diseases (Novaes, et al. 2007; Torricelli, et al. 2014). Increased NO_2 concentration from vehicle pollution is linked to an increase of the inflammatory response of ocular surfaces (Novaes, et al. 2010b). Also, oxidative stress affects the ocular health endogenously through diseases caused by inflammation (Bosch-Morell, et al. 2002; Chiou 2001). Protein tyrosine nitration occurs by tetranitromethane or peroxynitrite (Nakaki, et al. 1999). This

nitration happens by the addition of a nitro group in the phenolic ring of the tyrosine molecule. Protein tyrosine nitration produced NTyr, 6-nitrotryptophan, and 3,3'-dityrosine (Thiagarajan, et al. 2004). The NTyr is used a biomarker for several diseases such as asthma, hypertension, sickle cell disease and dry eye disease (Greenacre, et al. 2001). There is only one study that has been done for lactoferrin nitration. This study, by Teuwissen *et al*. showed changes in LF iron-binding properties during the nitration process (Teuwissen, et al. 1973).

1.8.3 Lactoferrin and disease

Lactoferrin associated with many diseases such as diabetes (Moreno-Navarrete, et al. 2009), Crohn's (Sipponen, et al. 2008), neurodegenerative diseases (Grau Armin, et al. 2001), and dry eye diseases (Ohashi, et al. 2003). Lactoferrin is important and widespread within mammalian bodily fluid, and our interest is to investigate it in relation to the ocular surface. The motivation of nitrated lactoferrin in our research relates to ocular disease due to the lack of study in this area. It is important to us to understand the role of lactoferrin in ocular surface and the related ocular diseases.

1.8.4 Lactoferrin role in tears

The tear film is a thin layer of fluid that covers and protects the ocular surface. Tears work as a carrier and excretory system for nutrients and metabolic products from corneal tissue (Tiffany 2003; Brock 1995). The ocular surfaces is covered in three layers: outer lipids (hydrophobic barrier), middle aqueous (physiological barrier such as electrolytes and proteins), and inner mucin (hydrophilic barrier) (Tiffany 2003). The thicknesses of the tear film ranges depend to each layer as the follows: 0.1–0.2 μm for

lipid, 7 to 8 μm for aqueous, and 30 μm for mucin layers (Johnson, et al. 2004; Walcott 1998).

The aqueous layer is an important film layer to the ocular health because it contains many components that protect the ocular surface. It contains electrolytes, vitamins, hormones, enzymes, immunoglobulins, and protein (Johnson, et al. 2004). Proteins in the tear are important to maintain ocular surface health and the changes in this protein composition will affect ocular health (Zhou, et al. 2006). Proteins in the tear are secreted mainly by the lacrimal gland (Prabha 2014). The tear has a high protein concentration of 8 μg/μL proteins and more than 60 proteins present, such as lacitin, proline rich proteins, lipocalin, lipophilin, lysozyme, and LF (de Souza, et al. 2006; Johnson, et al. 2004). LF has been shown to represent 25% of the tear protein concentration, making it a biomarker tear proteins for ocular diseases (Kijlstra, et al. 1983).

1.8.5 LF role in cornea

It has been determined that LF is present in human and murine eye tissues such as retina, iris, and cornea (Rageh, et al. 2016). LF works as a host defense protein due to multifunctional properties, such as its antibacterial and anti-inflammatory abilities, which plays an important role to protect ocular surface (Flanagan, et al. 2009).

1.8.6 The relation between ocular surface health and nitration

There are two possible ways for the nitration reaction to the human body: endogenous and exogenous. The endogenous pathway for nitration reaction via peroxynitrite that related to overproduction of nitric oxide ($\bullet NO$) and superoxide ($^{-}O_2$).

This increasing showed a relation to eye diseases such as utveitis and myopia (Chiou 2001). Also, review paper showed NO affect many part of the eye and caused diseases (Becquet, et al. 1997).

One exogenous pathway by which nitration reaction can occur is via reaction with reactive pollutant gases formed in urban atmospheres. The ocular surface can be directly exposed to gas-phase pollutants, which can then lead to certain medical conditions including various diseases. Previous studies have shown that long-term or acute exposure air pollution from traffic or industrial sources can cause ocular surface dysfunction and changes in tear film stability (Novaes, et al. 2010a; Torricelli, et al. 2013). Torricelli et al. (2011) presented a review discussing that the influence of long term exposure to outdoor air pollution such as nitrogen dioxide (NO_2), ozone (O_3), carbon monoxide (CO), and particulate matter ($PM_{2.5}$) can lead to ocular surface alterations (Torricelli, et al. 2011). One study showed that a healthy worker who is exposed to traffic air pollution that contains a high level of NO_2 (>100 $\mu g/m^3$ equivalent to 48 ppb) and $PM_{2.5}$ (40 $\mu g/m_3$) showed ocular surface irregularity and reduction in tear film osmolality (Torricelli, et al. 2014). All these studies tested the changes of the ocular surface using qualitative methods such as tear breakup time, the Schirmer test, and vital staining test. The investigation of the changes of the ocular surface components needs more consideration to understand the reason behind the observed irregularities.

1.9 Motivation

Protein nitration is a type of chemical modification that can be related to allergies, respiratory distress, and ocular disease in humans. Environmental exposure to air pollutants in urban areas can not only cause physical damage to non-living surfaces,

plants, and animals, but can also initiate damage to the ocular surface because it is in direct contact with reactive atmospheric species such as nitrogen oxide and ozone. The effects of this interaction are not known but could reasonably include changes in lactoferrin, an ocular protein whose reduced concentration correlates with many ocular diseases. The air pollution contains a mixture of chemical components that effect human health via protein modifications such as nitration and oxidation reactions. These modifications changed the natural characteristics of human tissue and caused diseases. There are many studies of air pollution and human diseases but few focuses on ocular surface disease. In order to promote this investigation, it is important to understand the connection between the ocular surface marker and the effects of modifications caused by air pollution. This research may help in the investigation and treatment of lactoferrin-related diseases such as dry eye diseases.

1.10 Hypotheses

Several linked hypotheses were investigated.

- The nitration modification can attenuate antibacterial activity of lactoferrin. Ergothioneine, an inhibitor of nitration, may be useful as a therapeutic treatment against NLF-related disease.
- Lactoferrin is an important protein in tear film function, and nitration of LF may actively It may be possible to develop a quantitative technique, such as sandwich ELISA, that is both sensitive and selective enough to quantify nitrated lactoferrin.
- A potential nitration inhibitor, ergothioneine, might also be effective in treatments of dry eye disease.

1.11 Objectives

To evaluate this modification, this study was designed to first investigate nitration reactions in the lab using two reactions as proxies of endogenous and exogenous models. Reaction products were identified and characterized using spectroscopic analysis. Next, a binding assay was developed in lab to quantify the nitration product. This assay is a novel and unique detection method which has eventual potential application in the clinical laboratory. Next, LF protein function was tested for biological changes using antibacterial and circular dichroism assays. These biochemical functions were used to evaluate the protein changes after nitration. Finally, an inhibitor molecule was applied to the nitration reaction to investigate the reduction of the nitration process. This investigation was used to work toward a possible anti-inflammatory treatment to protect the protein from the nitration affect.

Our research focused on the nitration role in lactoferrin and how that affects the bioactivities which can be useful in the clinical investigation for future research of ocular health in urban areas.

1.12 Research Aims

This dissertation describes three interrelated projects: Chapter 2 discusses the development of a novel sandwich ELISA to quantify nitrotyrosine in nitrated lactoferrin samples. Chapter 3 discusses changes in the antibacterial activity of nitrated lactoferrin. Chapter 4 discusses the effect of Ergo in protecting lactoferrin from the nitration process. The outcome of these studies hopes to provide value toward understanding the effects of protein nitration and its connection to maintaining health of ocular and other physiological systems.

Chapter two: Development of a sandwich ELISA with potential for selective quantification of human lactoferrin protein nitrated through disease or environmental exposure

Peer-reviewed and published in the following form, with only minor textual modification:

Anal Bioanal Chem. 2018 Feb;410(4):1389-1396. doi: 10.1007/s00216-017-0779-7.

Electronic publication date: December 6, 2017.

2.1 Abstract

Lactoferrin (LF) is an important multifunctional protein that comprises a large fraction of the protein mass in certain human fluids and tissues, and its concentration is often used to assess health and disease. LF can be nitrated by multiple routes, leading to changes in protein structure, and nitrated proteins can negatively impact physiological health via nitrosative stress. Despite an awareness of the detrimental effects of nitrated proteins and the importance of LF within the body, cost-effective methods for detecting and quantifying nitrated lactoferrin (NLF) are lacking. We developed a procedure to selectively quantify NLF using sandwich enzyme-linked immunosorbent assay (ELISA), utilizing a polyclonal anti-LF capture antibody paired with a monoclonal anti-nitrotyrosine detector antibody. The assay was applied to quantify NLF in samples of pure LF nitrated via two separate reactions at molar ratios of excess nitrating agent to the total number of tyrosine residues between 10/1 and 100/1. Tetranitromethane (TNM) was used as a laboratory surrogate for an environmental pathway selective for production of

3-nitrotyrosine, and sodium peroxynitrite ($ONOO^-$) was used as a surrogate for an endogenous nitration pathway. UV-vis spectroscopy (increased absorbance at 350 nm) and fluorescence spectroscopy (emission decreased by >96%) for each reaction indicates the production of NLF. A lower limit of NLF detection using the ELISA method introduced here was calculated to be 0.065 μg mL^{-1}, which will enable the detection of human-physiologically relevant concentrations of NLF. Our approach provides a relatively inexpensive and practical way to assess NLF in a variety of systems.

2.2 Introduction

Lactoferrin (LF) is an iron-binding protein that is present in many tissues and fluids of the human body and is critical to diverse physiological functions (Kanyshkova, et al. 2001). LF exists in various exocrine fluids such as tears, milk, and saliva (Vorland 1999; Kijlstra, et al. 1983) and possesses significant antifungal, antiviral, and antibacterial functions within the body (Jenssen, et al. 2009). Lactoferrin has a molecular weight of ca. 80 kDa and contains 703 amino acids, including 20 tyrosine residues and two globular lobes linked by an α-helix (Lönnerdal, et al. 1995). Each lobe contains two tyrosine residues at the center of its structure that participate with other amino acids as one iron binding site (Vorland 1999). The concentration of LF in human tissues has not been well-studied, but is critical for physiological function (González-Chávez, et al. 2009).

Chemical modification of proteins like LF can also play important roles in controlling protein function. Free radicals such as reactive oxygen species (ROS) and reactive nitrogen species (RNS) are broadly important within the human body

and as exogenous agents because they can lead to modifications that can affect protein function and harm the living system (Valko, et al. 2007). Specifically, the presence of nitrotyrosine-modified proteins is associated with many neurodegenerative, cardiovascular, respiratory, and ocular surface diseases (Yeo, et al. 2008). One mechanism by which tyrosine nitration may affect physiology is through protein denaturation leading to an irreversible loss of function (Gow, et al. 1996). Damage to tissue can also induce an increase in NO synthesis, releasing more peroxynitrite and leading to further increases in protein nitration (Pfeiffer, et al. 2001). Thus, 3-nitrotyrosine (NTyr) can be used as a biomarker for nitrosative stress diseases in body fluids such as blood, urine, and tears (Dalle-Donne, et al. 2005). Many ROS and RNS exist within the human body and contribute to the pathology of a variety of medical conditions. Peroxynitrite, in particular, has been shown to induce nitration of tyrosine (Tyr) residues as well as those of several other amino acids (Beckman 1996). One important pathway by which $ONOO^-$ induces tyrosine nitration involves an electron oxidation reaction of the phenolic ring, which forms an intermediate radical at the 3-position of the ring, followed by combination with NO_2 to generate NTyr, as summarized in Figure 2. 1 (Radi 2013).

Significant effort has gone into the investigation of ROS in the atmosphere and it is effects on human health. By comparison, relatively little study has been invested in what parallel role RNS may play in the same environmental systems (Wiseman, et al. 1996). One source of exogenous RNS is free radicals and reactive

gases in the air that are emitted, directly or indirectly, by combustion sources and are higher in polluted, urban areas (Reinmuth-Selzle, et al. 2017). Contact between adjuvants such as pollutant gases and proteins on the surfaces or fluids of the skin, eyes, mucous membranes, and lungs can provide an important pathway of chemical reactivity (Lakey, et al. 2016), and exposure to nitrogen oxide gases influences many cardiovascular, respiratory, and ocular surface diseases (Patel, et al. 1999). Investigating the amount of nitrated proteins in urban road dust indicates that proteins on the surface of pollen and other biological particles can be nitrated in urban air and thus could influence human health (Franze, et al. 2005).

In the atmosphere, tyrosine nitration is thought to proceed through a mechanism by which O_3 and NO_2 gases selectively produce a 3-NTyr product (Franze, et al. 2003; Reinmuth-Selzle, et al. 2014; Kampf, et al. 2015), whereas reaction with $ONOO^-$ can modify a wider set of amino acid residues, as discussed. Tetranitromethane (TNM) is frequently used in the laboratory as a surrogate for the heterogeneous O_3 and NO_2 mechanism, because it also selectively produces the 3-NTyr product (Franze, et al. 2005; Shuker, et al. 1993). Sokolovsky *et al.* illustrated the TNM mechanism that inserts a nitro group into the aromatic ring specifically at the ortho position to produce 3-NTyr as in Figure 2. 2 (Sokolovsky, et al. 1966). It is important to note that both Figure 1 and 2 lead to nitrated tyrosine residues, but that these can be at different sites within the protein.

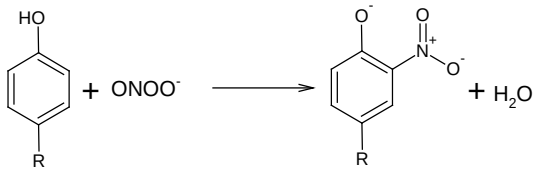

Figure 2. 1 Production of NTyr from Tyr reacting with peroxynitrite. Reaction product shown as one of several possibilities.

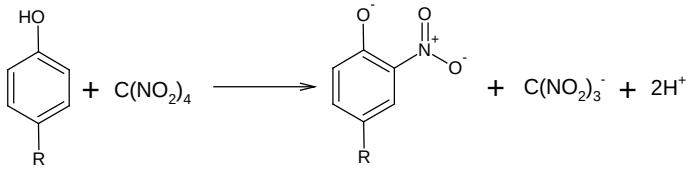

Figure 2. 2 Production of NTyr from Tyr reacting with tetranitromethane.

A number of laboratory techniques have been utilized to detect and quantify NTyr, especially for medically-relevant research endeavors (Crow, et al. 1995). Among those, tandem mass spectrometric (MS/MS) analysis is the most sensitive for detecting low concentrations of NTyr and has been used to investigate the relationship of nitrated proteins to many diseases, but requires very high up-front (ca. $300k to $1,000k) and maintenance costs (Yeo, et al. 2008; Reinmuth-Selzle, et al. 2014). To overcome some of the limitations presented by MS analysis, many studies now show that enzyme-linked immunosorbent assay (ELISA) can be applied to selectively detect and quantify low concentrations of nitrotyrosine within a sample (e. g.Baker, et al. 2009). ELISA has been used to quantify LF concentration in milk, plasma, and tear fluid (Kijlstra, et al. 1983) as well as NTyr in plasma and urine (Jamshad, et al. 1998). Only once has the detection of lactoferrin nitration been reported directly, however. Teuwissen *et al.* used a

combination of iron binding capacity and optical rotator dispersion to detect changing tyrosine properties upon nitration of LF (Teuwissen, et al. 1973).

Despite the importance of LF and nitrated proteins within the human system and as biomarkers for many diseases, very little has been reported on chemical modifications of LF. This is due in part to the challenges to inexpensively and selectively quantify nitrated lactoferrin (NLF). We summarize two independent methodologies to nitrate LF via aqueous reaction, utilizing TNM as a surrogate for exogenous atmospheric nitration and $ONOO^-$ as a model of endogenous physiological nitration pathway. Spectrophotometry was utilized as a method to show modifications to the protein. Further, we describe herein the development and optimization of a novel sandwich ELISA technique to selectively quantify NTyr in lactoferrin after nitration by each pathway. Using the reported ELISA protocol, we anticipate the ability to selectively quantify NLF at physiologically relevant concentrations, nitrated by either endogenous or exogenous pathways in human tissue and fluid samples, thus providing researchers without access to expensive instrumentation an accurate and effective way to measure NLF.

2.3 Experimental

2.3.1 Endogenous nitration of LF using sodium peroxynitrite

The peroxynitrite reaction was prepared following the method reported by Selzle *et al.* (Selzle, et al. 2013), replacing Bet v 1 with LF and adjusting for differences in the number of tyrosine residues between the two proteins. According to this procedure, 200 µL aliquots of 5.0 mg mL^{-1} LF in aqueous solution was

pipetted into 2.5 mL glass vials. PBS buffer, followed by NaONOO, was then added, and reaction solutions were stirred on ice for 2 hours. NaONOO was added in different amounts corresponding to peroxynitrite to tyrosine ($ONOO^-$/Tyr) molar ratios of 10/1, 20/1, 30/1, 40/1, 60/1, 80/1, and 100/1. PBS buffer was added to a total volume of 1000 µL for each solution at NLF concentration of 1.0 mg mL^{-1}. Previous work showed that concentrations of LF higher than this produced lower nitration reaction efficiency (Vincent, et al. 1970). Details regarding materials and reagents are listed in the supplemental material.

2.3.2 Exogenous nitration of LF using tetranitromethane

The tetranitromethane nitration reaction was prepared following the method reported by Teuwissen *et al.* (Teuwissen, et al. 1973). Similar to the above procedure, 200 µL aliquots of 5.0 mg mL^{-1} LF in aqueous solution was combined with Tris buffer, followed by 200 µL of ethanol and TNM, in 2.5 mL glass vials., TNM was added in amounts corresponding to tetranitromethane to tyrosine (TNM/Tyr) molar ratios between 10/1 and 100/1. Mixtures were stirred at room temperature (RT) for 4 hours. Tris buffer was added to a total volume of 1000 µL at NLF concentration of 1.0 mg mL^{-1}.

In all cases described below, NLF used as standard reference material for ELISA protocols was produced using the 40/1 molar ratio of TNM/Tyr reaction described here. Also in all cases, LF and NLF concentrations are reported as ±5%, which was limited by the precision of LF mass amount in the originally purchased vial.

2.3.3 Spectroscopic analysis

For all spectroscopic analyses, quartz cuvettes were used, and LF and NLF samples were diluted in PBS buffer. Dilution calculations were performed by taking the molecular mass of LF, irrespective of mass changes due to nitration.

UV-vis absorption spectroscopy was performed using a Cary BIO 100 spectrophotometer. Absorption spectra were acquired in 2 nm steps from 250 to 500 nm.

Fluorescence spectroscopy was conducted using a Varian Cary Eclipse Fluorescence G9800A spectrophotometer equipped with a xenon lamp as excitation source. The excitation wavelength was stepped every 2 nm, and fluorescence emission spectra were acquired from 200 to 500 nm at 2 nm resolution.

2.3.4 Direct ELISA for characterization of nitrotyrosine antibody

Direct ELISA was used to determine the optimal dilution factor of the detector antibody that was later used in the sandwich ELISA procedure. Nitrated bovine serum albumin (NBSA, 6/1 TNM/Tyr) was serially diluted into carbonate buffer producing five concentrations of NBSA. Microwells were coated in triplicate with each NBSA solution, and pure carbonate buffer was used as a blank. The plate was covered, sealed with sterile tape, and incubated at 4°C for 17 hours overnight. After incubation, the wells were washed in duplicate by adding 200 µL of PBST (PBS with 0.05% Tween). Each subsequent incubation step also followed a similar process of sealing, continuous shaking during the incubation period using a rocking platform (UltraRocker, BIO-RAD), and then

duplicate washing with PBST. After washing, wells were blocked with 200 µL of blocking buffer (5% BSA in PBS) and incubated at RT for 2 hours. After washing, mouse monoclonal to nitrotyrosine biotinylated antibody (anti-NTyr) was diluted in blocking buffer in four different dilution ratios between 1:100 and 1:1000). 50 µL of each dilution was added in triplicate and incubated for 1 hour at RT, thus utilizing 12 wells (four dilution ratios X triplicate measurements) for each NBSA concentration. Next, 50 µL of streptavidin-HRP (diluted 1:10,000 in blocking buffer) was added before incubation at RT for 1 hour. Each plate was developed by adding 100 µL of TMB substrate to each well and incubating at RT until the color turned blue (ca. 10 min). The substrate reaction was stopped after 10 minutes by adding 100 µL of 0.5 N aqueous sulfuric acid, prompting the solution to turn yellow. The optical absorbance of each well was measured using a microwell plate reader (Tecan Infinite, M1000 PRO). Following standard procedures (Rajasekariah, et al. 2003), the absorbance of the substrate background at 620 nm (blue) was subtracted from the absorbance at 450 nm (yellow) to produce the absorbance values reported on all plots.

2.3.5 Sandwich ELISA for quantification of NLF

For the sandwich ELISA procedure introduced here, goat polyclonal to lactoferrin non-conjugated antibody (anti-LF) was used as the capture antibody, and mouse monoclonal to nitrotyrosine biotinylated antibody (anti-NTyr) was used as the detector antibody (clone number CC.22.8C7.3). Details regarding the choice and dilution ratio of antibodies are outlined in the supplemental material (Section A. 6). Microwells were coated with 50 µL of diluted capture antibody and

incubated at 4°C overnight. The plate was then washed and blocked as described above. NLF was serially diluted into blocking buffer producing NLF solutions at eight concentrations. After a second washing step, 50 µL of each of the eight NLF solutions was added in triplicate to the plate and incubated at RT for 1 hour. Blocking buffer was used for blank measurements. 50 µL of the detector antibody, diluted in blocking buffer to a ratio of 1:100, was then added, and the plate was incubated with shaking at RT for 1 hour. Streptavidin-HRP and TMB were added following the ELISA protocol, as described above.

2.3.6 Data analysis

Data points are shown here as mean ± sample standard deviation (*s*). Statistical analysis was analyzed using Igor Pro 7 (Wavemetrics, Inc.; Oregon, USA). The experiments were carried out in triplicate and the results were subjected to t-tests to provide a measure of significance.

2.4 Results and Discussion

2.4.1 Detection of NLF using absorption spectroscopy

After nitration of LF via the two pathways (TNM and $ONOO^-$), nitration products were detected using UV-vis absorption spectroscopy. Figure 2. 3 shows absorption spectra of LF and NLF nitrated separately by $ONOO^-$ (NLF_{ONOO-}) and TNM (NLF_{TNM}) reactions. Absorption measurements at 280 nm are commonly used as a general tool for the detection of proteins that contain at least one of the three aromatic amino acids Phe, Tyr, or Trp. The spectrum of LF (Figure 2. 3, black trace) shows one band at 280 nm, which represents absorption by a

combination of these aromatic amino acids. The absorption spectrum of NLF_{TNM} (Figure 2. 3, red trace) shows a peak at 350 nm, consistent with the peak location of nitrated tyrosine (Riordan, et al. 1966). An additional product of the reaction is nitroformate, which also absorbs at 350 nm (Sokolovsky, et al. 1970). As a result, the reaction mixture was purified (see supplemental section A. 3), and the absorption spectra were compared before and after purification to verify the presence of NLF without interference. Both spectra show the peak at 350 nm, qualitatively verifying the presence of the product. Quantitative comparison is more complicated due to uncertainties in concentration introduced by dilution during purification.

The absorption spectrum of NLF_{ONOO^-} (Figure 2. 3, blue trace) shows a NLF peak at 350 nm as well as a double-humped peak at 280 from unreacted Phe, Tyr, and Trp in the protein. The NLF_{ONOO^-} product was not purified before spectroscopic analysis, because secondary reaction products and degradation by-products of $ONOO^-$ do not overlap with the 350 nm peak (Jankowski, et al. 1999). As a result, the quantity of NLF_{ONOO-} product is unambiguous here. In the case of the $ONOO^-$ reaction, modification of the protein is not limited to tyrosine, and the absorption spectrum of the nitrated product can be broadened by nitration of Phe, Tyr, and Trp residues (ter Steege, et al. 1998). Further, the relative tyrosine nitration yield from $ONOO^-$ is reduced compared to the TNM reaction, because the ratio of $ONOO^-$ to the sum of all nitrate-able amino acids is lower than the ratio of TNM to Tyr (Ischiropoulos, et al. 1992).

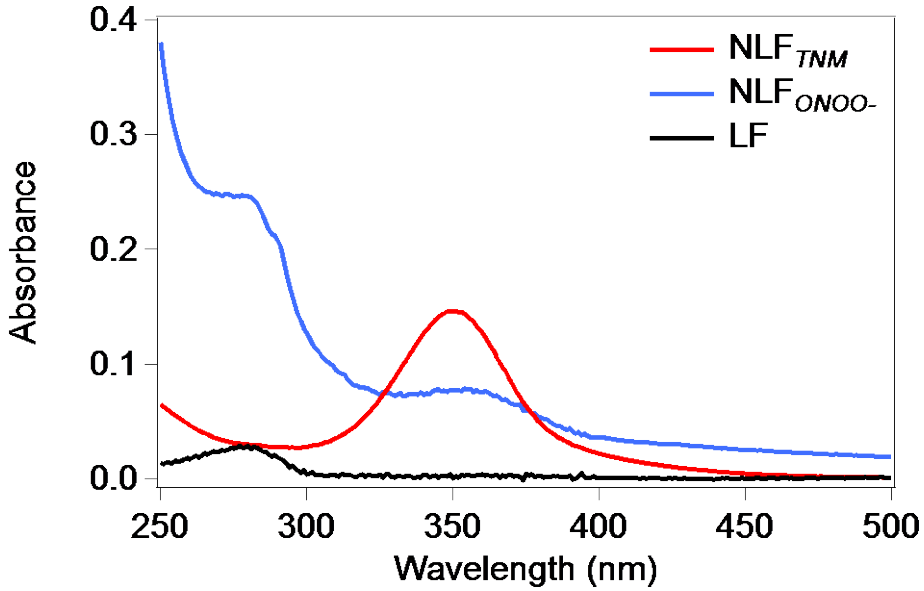

Figure 2. 3 Absorption spectra of lactoferrin and nitration products from two nitration reactions (1 mg mL-1 each). Each NLF product produced at 1/40 molar ratio of Tyr to respective nitrating reagent. NLFTNM product shown in purified form to remove interference from nitroformate by-product.

2.4.2 Detection of NLF using fluorescence spectroscopy

Fluorescence spectroscopy has also been frequently used to detect protein modifications, due to changes that can take place in protein molecular conformation (Kronman, et al. 1971). Tyr exhibits among the highest fluorescence quantum yield of all amino acids, and it is the primary source of fluorescence in proteins without Trp. When situated sufficiently close (ca. <5 nm) to Trp within a protein structure, however, Tyr experiences efficient resonance energy transfer to Trp and so is often not responsible for observed fluorescence (Lakowicz 2013; Pöhlker, et al. 2012). LF exhibits relatively strong fluorescence emission because it contains a large number of aromatic amino acids, including Phe (32), Tyr (20), and Trp (10) (Bläckberg, et al. 1980). Fluorescence from nitrated proteins has previously been shown to reduce total intensity from native proteins and can thus

be used as a quantitative measure of nitration (Crow, et al. 1996; De Filippis, et al. 2006).

Figure 2. 4 shows fluorescence excitation emission matrices for native LF as well as for NLF_{TNM} and NLF_{ONOO^-}. In the presence of nitrating agents, the addition of a nitro group (NO_2) onto Tyr decreases the pK_a of the hydroxyl group in the phenolic ring. As a result, the substitution of a large hydrophobic NO_2 group sterically hinders the tyrosine structure and can cause conformational changes to the protein (Radi 2013). This reduces the absorbance intensity due to the unmodified protein and also the intensity of the fluorescence emission.

LF shows strong emission centered at λ_{Em} 330 nm for two excitation bands at λ_{Ex} 224 and 280 nm due to a large number of Tyr and Trp residues, consistent with previous studies (Meyer, et al. 2015). Both nitrated products show dramatically decreased emission intensity (Figure 2. 4 d; NLF_{TNM}, 98% decrease and NLF_{ONOO^-}, 96% decrease) due to the addition of NO_2 groups to LF, qualitatively matching observations for nitrotyrosine reported by Crow *et al.* (Crow, et al. 1996). The emission intensity of NLF_{TNM} is reduced by a greater factor than NLF_{ONOO^-}, again because $ONOO^-$ nitrates more broadly than TNM.

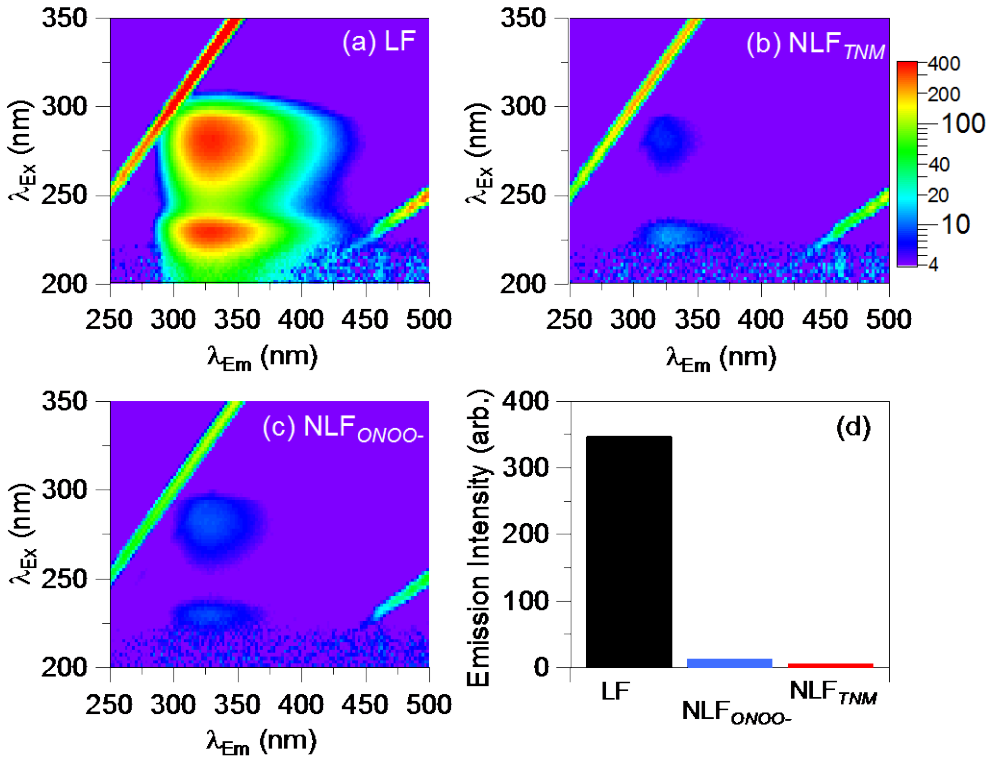

Figure 2. 4 Fluorescence EEMs for native LF (a), NLFTNM (b), and NLFONOO- (c). Diagonal lines indicate elastic scattering from excitation source. EEM color scale indicates emission intensity, in logarithmically scaled arbitrary units (arb.). Peak emission intensity at λEX280 nm for each panel summarized in panel (d).

2.4.3 Design of sandwich ELISA assay for quantification of NLF

The sandwich ELISA developed here was designed to detect NTyr bound to LF protein in NLF samples. The assay first utilizes polyclonal anti-LF capture antibodies to bind LF proteins. This antibody recognizes a specific sequence of 13 amino acids in the LF protein (see supplemental Section A. 4) (abcam 2017). Second, monoclonal anti-NTyr detector antibodies are used to attach to specific NTyr residues bound on captured NLF proteins. For the capture process, polyclonal antibodies were used to enhance the probability of binding, given the many sites at which nitration could affect LF binding, whereas monoclonal

antibodies were used as detector antibodies to selectively enhance the assay's sensitivity (Fig. A. 2). The scheme is conceptually similar to the sandwich ELISA protocol introduced by Franze *et al.*, which detects NTyr in nitrated birch pollen protein (Nitro-(3)-Bet v 1) and used rabbit polyclonal anti-Bet v 1 protein as capture and mouse monoclonal anti-NTyr as detector antibodies (Franze, et al. 2003). The detector antibody chosen here has been used in many immunoassay applications (Ferrante, et al. 1997) because it has low cross-reactivity (Chou, et al. 1996) and high sensitivity (Aggarwal, et al. 2011). See supplemental Section A. 6 and Figures A. 1-A. 2 for additional details about assay development.

2.4.4 Development of sandwich ELISA

In order to develop the modified sandwich ELISA for detection of NLF, each of the two antibodies was tested separately using direct ELISA and combined into a single sandwich ELISA. As a first step, direct ELISA was used to determine the optimal buffer dilution ratio of NBSA antigen to the nitrotyrosine biotinylated antibody (analogous to supplemental Fig. A. 3, without the initial capture antibody step). Four dilutions ratios from 1:100 to 1:1000 were investigated. The 1:100 dilution exhibited the highest binding sensitivity, shown as the steepest slope in Figure 2. 5.

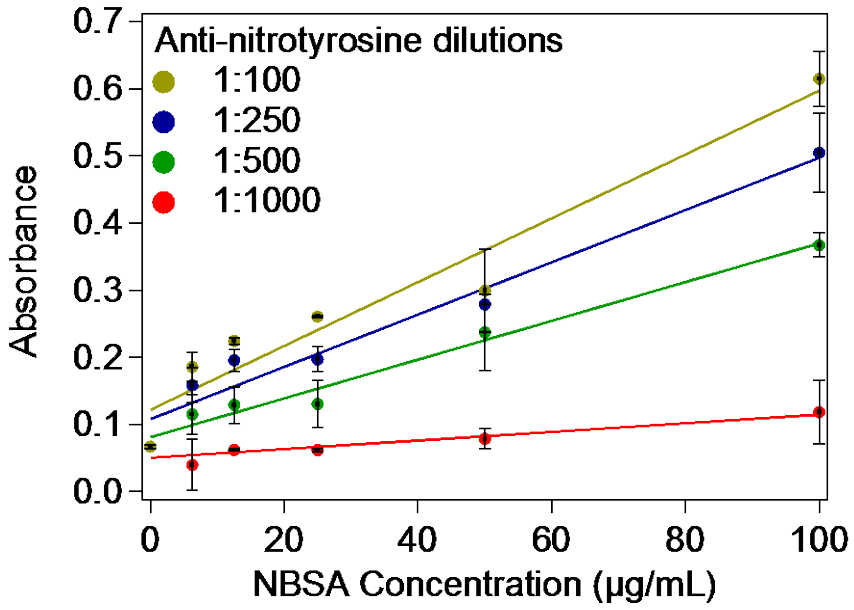

Figure 2. 5 Optimization of detector antibody using direct ELISA. The optical absorbance shows ELISA well absorbance at four dilution factors (anti-NTyr into blocking buffer). Data points are mean values ± s, n= 2. Traces are linear fits.

As a second step, the full sandwich ELISA was used to optimize the dilution of capture antibody (anti-LF). The 1:1000 (v/v) dilution of capture antibody was selected, because it exhibited binding sensitive similar to the 1:250 (v/v) dilution, but requires less antibody volume (Fig. A. 4). Using the higher dilution thus achieves sensitive detection at lower cost.

A calibration curve of optical absorption versus NLF concentration was developed as the final detection step of the sandwich ELISA (Figure 2. 6). A range of molar ratios between 10/1 and 100/1 were investigated (Fig. A.5-A.6), and the 40/1 molar ratio of TNM/Tyr was chosen as the protein standard. Sandwich ELISA results show a decrease in detected NLF concentration produced at nitration ratios higher than 40/1. The reason for this could be due to a reduction in antibody binding due to LF changes at capture antibody binding sites or as a result of

denaturation of LF protein. Results published by Teuwissen *et al. also* show NLF_{TNM} properties peaking at a 40/1 molar ratio (Teuwissen, et al. 1973).

The limit of detection (LOD) for the newly developed assay was calculated by two separate methods by measuring the mean + three times the sample standard deviation of a set of three absorbance measurements following sandwich ELISA. LOD_{LF} was calculated as 0.032 absorbance units (AU) by replacing native LF for NLF as the antigen in the assay, and LOD_{blank} was calculated as 0.022 AU by withholding any antigen from the assay. A minimum detectable NLF concentration of 0.065 µg mL^{-1} was calculated as $3\ s_{LF}/m$, where s_{LF} is the standard deviation of the blank measurement and m is the slope of NLF calibration curve. Using the responses from the sandwich ELISA (Figure 2. 6), t-tests showed the NLF measurement to be statistically different (p-value < 0.01) from the LF measurement at all antigen concentrations measured (minimum 0.18 µg mL^{-1}; see supplemental Table A.1).

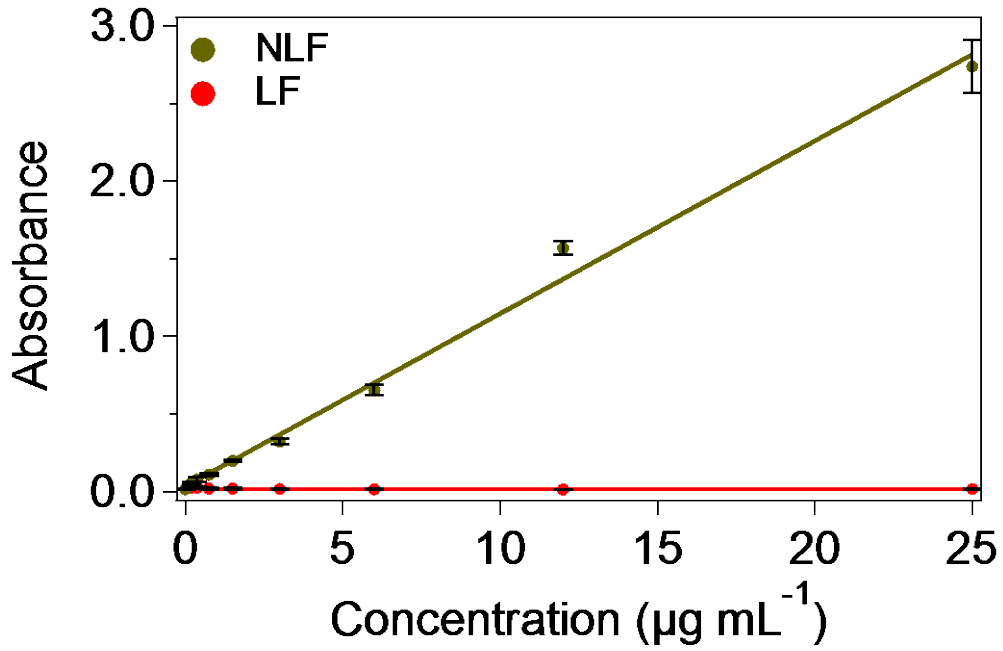

Figure 2. 6 Sandwich ELISA calibration curve.

for NLF (40/1 TNM/Tyr) and LF in several concentrations (0.18, 0.37, 0.75, 1.5, 3.0, 6.0, 12.0, and 25.0 µg mL^{-1}). Data points are mean values. Vertical error bars (black) shown as standard deviation s, n= 4. Linear fit for NLF, R^2 = 0.993.

To confirm the results from the new ELISA protocol, Figure 2.5 shows that the molecular absorbance of NLF (black traces) and responses from the sandwich ELISA (red bars) each increase with increasing molar ratio of TNM or $ONOO^-$ to Tyr. Supplemental Figure A.5 shows an extension of the ELISA response to higher ratios of nitrating agent.

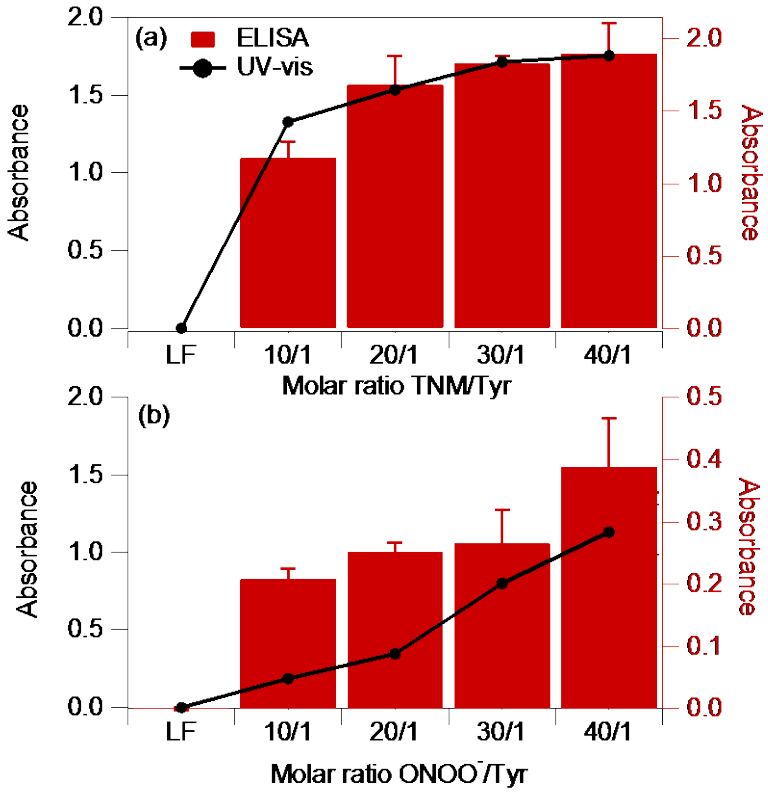

Figure 2. 7 UV-vis absorbance at 350 nm (black traces; left axes) and ELISA optical density at 450 nm (red bars; right axes) of NLF using two different nitration reagents; ONOO- (a) and TNM (b). Error bars on ELISA data represent standard deviation of measurements from individual wells (a) n = 6, (b) n = 3.

NLF samples produced using the TNM reaction were tested in both purified and non-purified forms, following procedures outlined above. Absorbance values and sandwich ELISA results show no statistical differences, and so all NLF_{TNM} data shown here (Figure 2. 6 and Figure 2. 7) are shown without any purification (see supplemental material and Fig. A. 7). The ability of the assay to work effectively without cleaning the product is important, because it shows that the ELISA protocol developed here can be applied broadly to samples extracted from tissues and fluids without need to perform additional cleaning steps that can increase analysis costs and quantitative uncertainty. In contrast to this, the

NLF_{ONOO^-} samples can degrade over time if produced via the reactions outlined above. NLF_{ONOO-} samples thus require purification before storage to limit agglomeration and protein changes induced by the presence of excess $ONOO^-$ (Estillore, et al. 2016).

2.5 Conclusions

NLF samples were synthesized using two different nitration reagents in varying ratios of molar excess. $ONOO^-$ was used as an endogenous model and TNM was used as an exogenous model. Both nitrated products were characterized by UV-vis and fluorescence spectroscopy, showing dramatic changes upon nitration. To quantify the concentration of NLF produced from each reaction, we developed a novel sandwich ELISA for the selective detection of NTyr bound within NLF antigens. We demonstrate a LOD_{LF} of 0.032 AU and a LOD_{blank} of 0.022 AU, translating to a lower limit of detectable NLF concentration of 0.065 µg mL^{-1}. An important feature of this sandwich ELISA protocol is that is does not require sample purification, meaning that quantitative uncertainty introduced from imprecise dilution through washing steps can be avoided. The NLF sandwich ELISA introduced here is a novel method that was demonstrated to be applicable to the quantification of nitrotyrosine in lactoferrin. LF is the most concentrated protein in human tears, representing up to 25% of protein mass, or approximately 2.2 mg mL^{-1} (Kijlstra, et al. 1983). The concentration of $ONOO^-$ generated in inflamed corneal tissue has been shown to be in the approximate range of 3-30 µM (Ashki, et al. 2014). NLF has never been quantified in tissue or fluid samples, but

if even 30 of every 10^6 LF molecules (30 ppm) were nitrated by $ONOO^-$, NLF concentrations would be above detection limits reported here. Thus, NLF is likely to be detectable by this procedure at physiologically relevant concentrations. As a result, this assay has important application to the investigation of NLF produced through inflammatory pathways in human tear, milk, and ocular tissues samples, and also through inflammation linked to traffic-borne air pollution.

Chapter three: Nitration reduces antibacterial activity of lactoferrin by changing its structural and functional properties

In preparation for submission for peer review.

3.1 Abstract

Protein nitration is an important protein modification that has been correlated with both disease and urban air pollution. Here we examine the antibacterial properties of lactoferrin (LF) protein, which plays an important role in the biological system as one of the most concentrated proteins in several human fluids and tissues. Peroxynitrite ($ONOO^-$) was used to induce nitration on LF as a mimic of physiologically relevant biochemical modification, producing nitrated lactoferrin (NLF). The reaction selectively generates nitrotyrosine residues, which are commonly used as biomarker molecules for a number of diseases. Our results show that nitration of LF at 10/1 and 40/1 molar ratios was sufficient to inhibit all of the antibacterial activity exhibited by native LF. Secondary structural changes in the LF protein were assessed using circular dichroism (CD) spectroscopy. Spectral changes upon nitration in both unligated and iron-bound cases show a significant reduction in alpha-helical properties, suggesting partial protein unfolding. Iron-binding capacity of LF also showed reduction after nitration using two separate assays. This study is the first to show inhibition of antibacterial properties of NLF, and the observations thus represent a possible link to pathways of biochemical modification that take place during diseases and due to environmental exposure. By understanding the critical role that

nitration could play in the immune defense system of the human eye, liver, and other organs, biochemical treatments may be explored that could reduce damage directly from nitration pathways, and also due to secondary bacterial infections.

3.2 Introduction

(Strøm, et al. 2002; Kang, et al. 1996b)(Nuijens, et al. 1996)(Ward, et al. 2002)LF is a member of the transferrin family of proteins that binds iron ions (Fe^{3+}) and regulates iron levels in the physiological system. Specifically, LF functions as an iron transporter and serves important bacteriostatic and anti-viral roles (Farnaud, et al. 2003). The protein structure consist of two iron binding sites, each of which can bind with an individual Fe^{3+} ion (Adlerova, et al. 2008). The iron binding site in each lobe consists of four amino acid residues: two tyrosine, one aspartic acid, and one histidine. Thus, the protein provides four ligands at each binding site: two phenolate oxygen atoms from Tyr, one carboxylate oxygen from Asp, and one imidazole nitrogen from His (Baker, et al. 1990).

LF is widely used as an antibacterial agent against both gram-positive (e.g. *Streptococcus faecalis*) and gram-negative bacteria (e.g. *Escherichia coli*), though gram-negative bacteria are more resistant than gram-positive bacteria due to the presence of outer membranes (Rt D. Ellison, et al. 1988). LF serves antibacterial functions by two separate mechanisms. As a bacteriostatic agent, LF serves to limit bacterial growth by binding Fe^{3+}, thereby reducing the concentration of available iron required for growth. As a bactericidal agent, LF can bind to the surface of bacterial cells, releasing lipopolysaccharide, which damages the bacterial membrane and can ultimately kill the

cell (Rt D. Ellison, et al. 1988). It is important to note that due to the iron-binding properties of LF, iron-bound LF shows no antibacterial activity (Dionysius, et al. 1993).

As a result of the interactions between the protein and either Fe^{3+} or the bacterial surface, chemical modifications at certain amino acid residues of the LF structure are likely to impact the protein's physiological functions. For example, modification of LF by replacing histidine with glutamic acid, cysteine, tyrosine, or methionine, was shown to reduce the iron-binding function of the protein (Nicholson, et al. 1997). Nitration of tyrosine resides bound within proteins has also been shown to be possible via several mechanisms and has been linked to a variety of deleterious health effects (Radi 2013). Peroxynitrite is one of the most effective endogenous protein nitrating agents, inducing changes in protein structure and function, and has been implicated as a stressor related e.g. to cardiovascular disease (Thiagarajan, et al. 2004; Saxena, et al. 2003). In particular, 3-nitrotyrosine has been used as a marker for inflammation and nitrosative stress (Eleuteri, et al. 2009) and is also selectively produced by reaction with certain environmental pollutants (Shiraiwa, et al. 2017; Franze, et al. 2005).

Despite the depth of literature that has focused on lactoferrin and the nitration of other human proteins, the effect of nitration on critical bioactivity functions of LF has not been studied. Here the study presents experimental results that show for the first time that peroxynitrite-induced nitration of LF reduces the antibacterial properties of the protein. This nitration presents an overview of changes in LF secondary structure as measured by circular dichroism (CD) spectroscopy and show a reduction in iron-binding capacity after

LF nitration. This study also suggests possible links between changes in the secondary protein structure and observations about reduced antibacterial activity.

3.3 Experimental

3.3.1 Materials

Human milk lactoferrin (LF; L0520), sodium phosphate dibasic (RES20908-A702X), potassium chloride (P9333), sodium chloride (S9625), potassium phosphate monobasic (P5655), Iron(III) chloride hexahydrate ($FeCl_3.6H_2O$; 236489), Nitrilotriacetic acid (NTA; N9877), Trizma base (Tris-HCl; T1503), Hydrochloric acid (H-7020), Tryptic Soya broth (TSB; 22092), Chloramphenicol antibiotic (CAM; C0378), and Tryptic Soya agar (TSA; 22091) were obtained from Sigma Aldrich (USA). Sodium peroxynitrite (NaONOO; 516620), Amicon Ultra-0.5 centrifugal filters (30 kDa, 0.5 mL volume; UFC503008), and Amicon Ultra-4 centrifugal filters (30 kDa, 4 mL size; UFC803024) were obtained from Calbiochem (USA). 100 mm x 15 mm petri dish with grip ring (sterile; 229692) were obtained from CELLTREAT (USA). Flat-bottom, 96-microwell plates (untreated; 333-8013-01F) and sterile sealing tape (ST-3095) were obtained from Life Science Products (USA). UV, 96-microwell plates with transparent flat bottom (3635) were obtained from CORNING (USA). Escherichia coli (*E. coli*; ATCC25922) were obtained from the American Type Culture Collection (USA).

Buffers and iron solution were prepared as follows: phosphate-buffered (PB; 0.1 mM sodium phosphate dibasic and 0.5 M sodium phosphate monobasic at pH 7.4), phosphate-buffered saline (PBS; 8.1 mM sodium phosphate dibasic, 0.8 mM sodium

phosphate monobasic, 1.3 mM potassium chloride, and 68.0 mM sodium chloride at pH 7.4), Tris-HCl buffer (Tris; 50 mM at pH 4.0, 150 mM sodium chloride ,20 mM sodium carbonate and 71.0 mM sodium bicarbonate at pH 7.4), ferric nitrilotriacetic acid ($Fe(NTA)_2$) solution ($FeCl_3.6H_2O$ 4.0 mM and NTA 8.0 mM and 1 N HCl add 2% to total solution volume at pH 4.0). Tryptic soya broth and tryptic soy agar were prepared following the manufacture instructions.

3.3.2 Nitration of lactoferrin by alkaline peroxynitrite (ONOO-)

Samples of nitrated lactoferrin were prepared for the iron-binding assays following the procedure described by Alhalwani *et al.* (Alhalwani, et al. 2018) Briefly, the reaction was prepared in 96-microwell UV-plates by adding 100 µL aliquots of 10.0 mg mL^{-1} (± 5%) human milk LF in aqueous solution into each well, then adding NaONOO to each well in two different amounts (5.66 and 22.73 µL) corresponding to peroxynitrite to tyrosine ($ONOO^-$/Tyr) molar ratios of 10/1 and 40/1. The volume of Tris-HCl buffer added to each solution was matched with the volume of NaONOO added in order to make a total volume of 200 µL and a NLF concentration of 5.0 mg mL^{-1} (± 5%). The microwell plate was set on ice for 120 min. The product of nitration reaction was purified using a micro-centrifugal filter device (0.5 mL) and rinsed twice with nanopure water.

Samples of NLF were prepared for the antibacterial assay, following above procedure, but replacing PBS buffer for Tris-HCl buffer. The buffer used for each assay was chosen to optimize assay results. Tris-HCl was chosen for the iron-binding tests to

properly dissolve Fe^{3+}, whereas PBS was used for the antibacterial assay as standard physiological buffer mimic that is non-toxic to the bacterial cells.

3.3.3 Broth antibiotic susceptibility assay to test antibacterial function

The protocol used here generally followed procedures outlined by Wiegand *et al.* for the minimum inhibitory concentration assay, with some modifications (Wiegand, et al. 2008). Briefly, *E. coli* was prepared by suspending the entire volume of the purchased bacterial powder in 5 mL of broth. After 24 hrs of incubation, 1 mL of this broth was mixed 1:1 with glycerol to produce the glycerol stock of *E. coli* that was stored up to long term for many years at ca. -80ºC. When ready, a 1 µL aliquot of the glycerol stock of bacteria was incubated in TSA plates at 37ºC for 24 hrs. Subsequently, three to five separate colonies from each plate were selected and transferred into 4 mL TSB and incubated at 37ºC for 24 hrs. After incubation, the 4 mL solutions of growth media were diluted to approximately 10% of the original concentration by adding 36 mL of TSB, subsequently referred to here as *E. coli* broth stock. 200 µL aliquots of broth stock were then placed into each microwell. Five separate sample types were prepared: assay blank using TSB and no bacteria, positive control with bacteria in 30 µg mL^{-1} CAM, and, bacteria in 1 mg mL^{-1} concentrations, separately, of LF, 10/1 NLF, and 40/1 NLF. 5 µL of *E. coli* broth stock was added to each well and incubated at 37ºC overnight. Finally, the absorbance of each well was examined at a wavelength of 600 nm using a plate reader (Tecan Infinite, M1000 PRO) with 5.0 nm incident bandwidth.

3.3.4 Circular dichroism assay to determine the secondary structure

CD spectra were recorded using the Jasco Model J-810 spectro-polarimeter using: a 1.0 mm path length quartz cell for absorption in the far-UV region (190 – 250 nm), scan speed of 20 nm/min, bandwidth of 1.0 mm, digital integration time of 4 sec per nm, and data pitch 1 nm. LF and NLF samples were diluted in PB buffer for analysis. Dilution calculations were performed using the molecular mass of LF, irrespective of the minor change in mass due to nitration.

3.3.5 Preparation of iron-bound lactoferrin and detection of iron concentration

The iron-loading assay was prepared following procedures outlined by Hamilton *et al.* (Hamilton, et al. 2009). After nitration reaction samples were purified, each UV-microwell was coated with 200 µL of either LF, 10/1 NLF, or 40/1 NLF. To each well, 20 equivalents of $Fe(NTA)_2$ were added, and the absorbance was measured using the plate reader after 45 minutes of waiting at room temperature and then analyzed. The absorbance of each well was detected using the plate reader at wavelength 470 nm.

The ferrozine method was used to determine the iron uptake following a method reported by Stookey *et al.* (Stookey 1970). The protein concentration was measured using the Bradford assay. 100 µL samples consisting of 19.0 µM of each protein were diluted into nanopure water. A blank consisting of only water was also prepared. 10 µL of 3 M of trichloroacetic acid was added to each sample and centrifuged at 14000 g for 12 min. The supernatant from each sample was collected and mixed with 330 µL of

nanopure water, 20 µL of 10 mM ferrozine, and 20 µL of saturated sodium acetate. Each mixture was analyzed at absorbance 562 nm (ε 27.9 mM^{-1} cm^{-1}).

3.3.6 Data analysis

Igor Pro 7 software (Wavemetrics, Inc.; Oregon, USA) was used to analyze results. Bacterial cultures were grown in replicates three to five, each culture referred to as an individual experiment. All assay measurements were also performed at a minimum of triplicates of technical replicates, i.e. three wells individually prepared. For experiments involving bacterial cultures, values were first averaged from technical replicates and are represented here as averages of individually cultured experiments. Data shown represent mean ± standard deviation (*s*) of data values. Results were subjected to t-tests, including associated p-values calculated using the unpaired t-test function in Microsoft Excel (i.e. ttest (Series1, Series2, 1,2)).

The protein secondary structures of CD samples were analyzed using β-Structure Selection (Bestsel) software available as online freeware (Micsonai, et al. 2015).

3.4 Results

3.4.1 Broth antibacterial assay for LF

The broth antibacterial susceptibility assay has previously been used to measure the minimum inhibitory concentration by using a visible measure of bacterial growth to determine the lowest concentration at which an antimicrobial agent was effective against a certain bacterial species (Wiegand, et al. 2008). Here the broth type was modified and

the protocol was applied to quantify the inhibitory effect of LF and nitrated LF (NLF) against *E. coli* growth. Samples of *E. coli* were incubated separately under five conditions to first demonstrate the antibacterial activity of LF and to test the optimized assay conditions. Figure 3. 1 shows the relative density of bacterial cell number as the absorbance of the suspension measured at 600 nm. Growth inhibition is thus related by the reduction in absorbance compared to the negative control (*E. coli* only) samples. The blank (no *E. coli*) is defined as no growth. Chloramphenicol (CAM), used as strong antibiotic, shows near complete inhibition of growth, and LF shows partial inhibition at each protein concentration. Experimental concentrations of LF were chosen to match the approximate range present in ocular tear fluid in the normal eye (~2.0 mg mL^{-1}) and during ocular disease (<2.0 mg mL^{-1}) (Ballow, et al. 1987). Results confirm that the optimized assay shows increasing *E. coli* growth inhibition with increasing concentration of added LF, as was previously shown by Kutila et al. over a range 0.7 – 2.7 mg mL^{-1} (Kutila, et al. 2003).

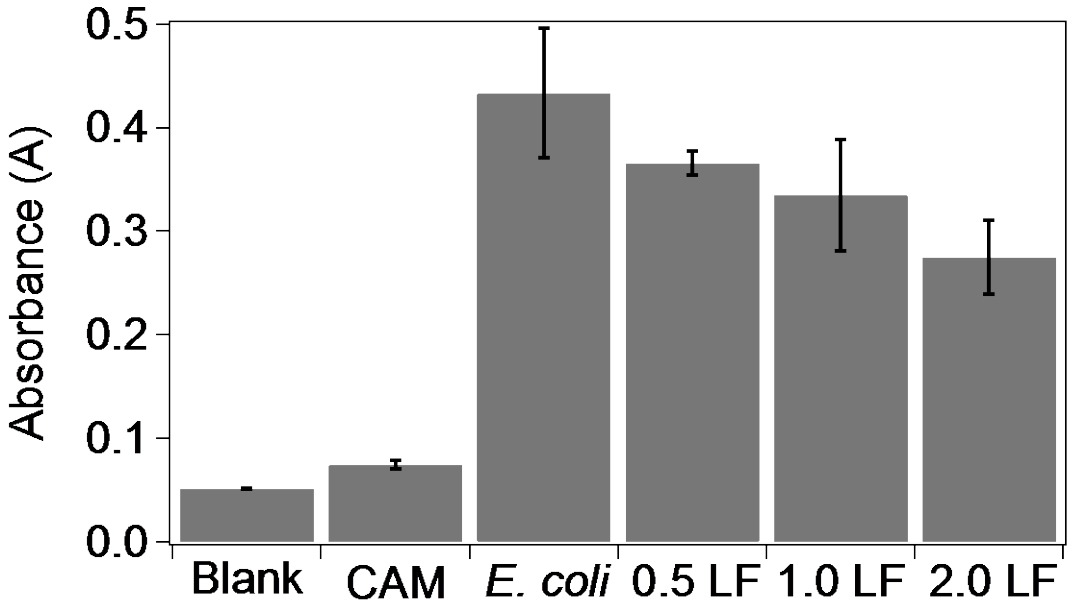

Figure 3. 1 Optimized antibacterial assay. Absorbance at 600 nm shown for blank (broth, no E. coli), CAM (positive control, strong inhibition), E. coli (negative control, no inhibition) tested against LF at three concentrations: 0.5, 1.0, and 2.0 mg mL^{-1}. Bars show mean values ± standard deviations of three individually cultured experiments. Absorbance values shown without blank subtraction.

3.4.2 Antibacterial activity of LF and NLF

The optimized broth antibacterial assay was subsequently used to determine the antibacterial activity of nitrated lactoferrin (10/1 and 40/1 molar ratios of nitrating agent to LF) compared to unmodified LF against *E. coli*.

Figure 3. 2 shows that LF inhibited *E. coli* growth by LF to be ca. 12%. In contrast, both concentrations of NLF show no inhibitory effect with respect to *E. coli*. Antibacterial inhibition tests show that 10/1 and 40/1 NLF exhibit p-values of <0.00005 and <0.005 when compared to cultures treated only with LF. Further, both NLF cultures show growth properties to be insignificantly different (*ns*) from *E. coli* cultures grown without any kind of LF or NLF treatment. These results suggest that modifying the LF through nitration at molar ratios of both 10/1 and 40/1 was sufficient to remove all of the antibacterial benefits presented by the unmodified protein.

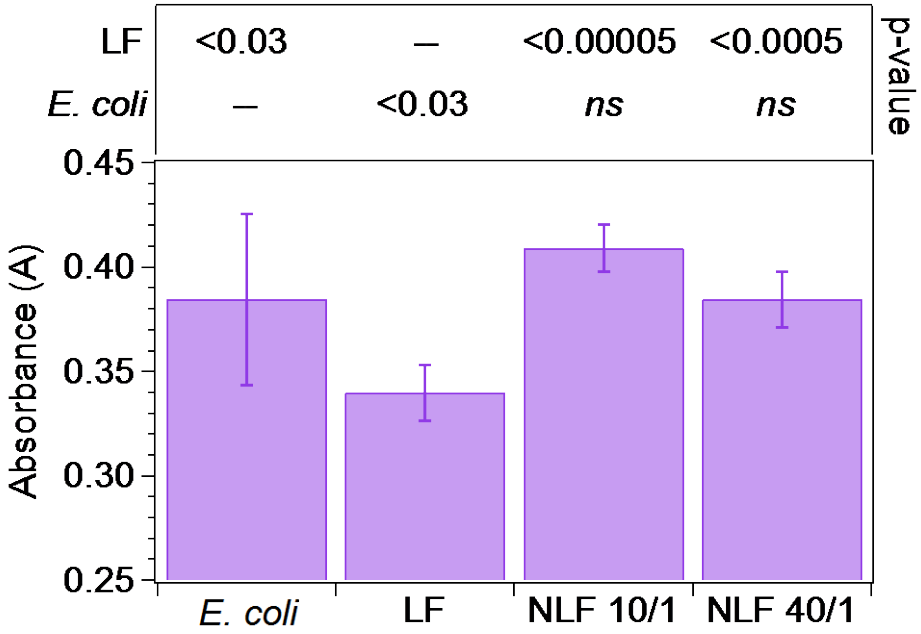

Figure 3. 2 Antibacterial activity of LF vs. NLF. Absorbance at 600 nm shown for blank-corrected absorbance values for E. coli grown against LF, 10/1 NLF, and 40/1 NLF (1.0 mg mL^{-1} each). Bars show mean values ± standard deviations of five individually cultured experiments. Absorbance value for each experiment averaged from measurements of four technical replicates. P-values show statistical significance of differences in inhibition with respect to LF and E. coli, respectively; ns - not statistically significant.

3.4.3 Secondary protein structures of LF and NLF

To investigate conformational changes in the secondary structure of LF before and after nitration, four samples of LF, with and without nitration and with and without bound Fe^{3+}, were analyzed using CD spectroscopy. The far-UV wavelength range (i.e. 190-250 nm) probed by CD spectroscopy reveals information about the folding properties of the protein through its secondary structure (Kelly, et al. 2005). Three CD spectra of each sample were averaged and are shown in Figure 3. 3.

The spectral minima for LF shifted approximately 10 nm to lower wavelength upon nitration (red → blue traces) for both the apolactoferrin (iron-free) and hololactoferrin (iron-bound) samples. The secondary structures associated with the protein samples were then analyzed using the Bestsel online software (Micsonai, et al. 2015). As expected from its crystal structure (Anderson, et al. 1989a), the measured CD spectrum of lactoferrin confirms it to be a well-folded protein of primarily alpha-helical character (Figure 3. 3). Iron binding was found to not significantly change the spectra in the cases of either LF or NLF.

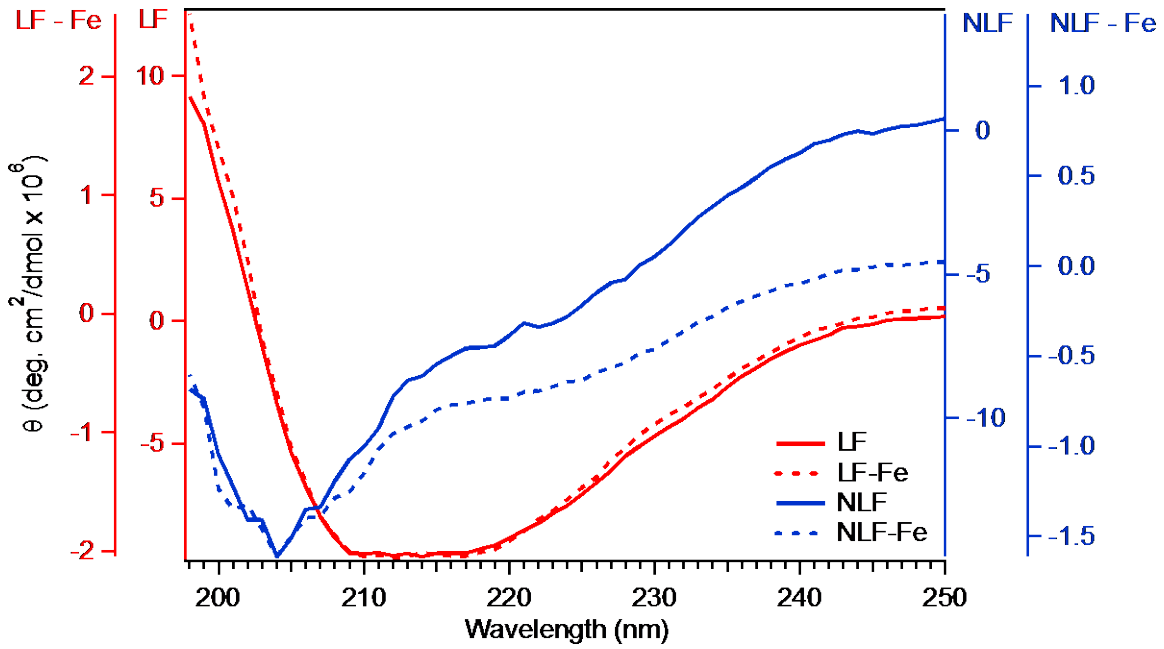

Figure 3. 3 Secondary protein structure via circular dichroism spectroscopy. CD spectra of LF (red solid trace), 10/1 NLF (blue solid trace), LF-Fe (red dashed trace), and 10/1 NLF-Fe (blue dashed trace) acquired between 190 and 250 nm. Spectra shown as averages of three readings. Y-scales independently scaled to highlight overlap of spectra.3.4.4 Iron-binding ability of LF and NLF

To examine the ability of the protein to bind iron, samples of LF and NLF were subjected to two iron-binding assays. In the case of NLF, Fe^{3+} was added to the samples after nitration reactions were complete. Results from both assays qualitatively show a reduction in the ability of LF to bind iron after nitration, with increasing effect from increased molar ratio of nitrating agent (Table 3. 1).

Table 3.1 Iron determination data. LF and NLF samples listed as blank-subtracted values. Relative reduction in iron capacity shown in parentheses for NLF samples with respect to LF.

Sample	Ferrozine Assay (µM)	Iron Loading Assay (A)
Blank	0.38	0.031
LF	25.5	0.072
NLF 10/1	22.0 (-13%)	0.010 (-74%)
NLF 40/1	19.1 (-24%)	-0.006 (-110%)

3.5 Discussion

The relationship between LF concentration and bacterial inhibition was shown here to exhibit approximately linear behavior (Figure 3. 1), consistent with observations shown by Ellison et al. (R. T. Ellison, et al. 1988). A reduction in the antibacterial activity of LF upon nitration had not been previously observed, however. Inhibition of the antibacterial activity is consistent with charge-related properties of the interaction between *E. coli* and LF. Gram-negative bacteria can generate inflammatory mediators such as LPS bound within the outer bacterial membrane, and these mediators can induce cytotoxicity in humans (Heumann, et al. 2002). LF proteins within human fluids act to protect against the toxic effects by binding to LPS and thus damaging the bacterial membrane (Lönnerdal, et al. 1995). The mechanism by which LF kills gram negative bacteria has previously been shown to proceed via binding of bacterial membrane porins

by cationic regions of LF concentrated at the N-terminus (Bellamy, et al. 1992; Erdei, et al. 1994). Nitration has been shown to add anionic nature to protein structure (Ignarro, et al. 1995). For example, the reaction of LF with $ONOO^-$ adds nitro groups (NO_2) to aromatic amino acid residues such as tyrosine (Alhalwani, et al. 2018), thereby increasing the anionic charge of the protein. The corresponding decrease in cationic surface properties of the protein would thus be expected to reduce the binding of LF to LPS, leading to a decrease in the antibacterial properties of LF qualitatively consistent with the results shown in Fig. 3. 2.

Separate from the ionic properties of LF that affect bactericidal activity, the secondary structure of native LF is critical to its antibacterial function (Japelj, et al. 2005). Teuwissen *et al.* showed that nitration of apolactoferrin using tetranitromethane (TNM) changed the tertiary protein structure sufficiently to reduce its ability to uptake iron (Teuwissen, et al. 1973). TNM is not a physiologically relevant nitrating agent, however, and so the extrapolation of effects within the body is not obvious. It was also previously shown that $ONOO^-$ present at physiologically relevant concentrations can efficiently nitrate LF (Alhalwani, et al. 2018). The secondary structure of LF has separately been investigated many times using CD spectroscopy (Kang, et al. 1996a), however, no previous reports had shown changes in LF structure associated with $ONOO^-$ nitration. Here we showed for the first time that LF nitration induced by $ONOO^-$ can cause significant changes to the protein structure (Fig. 3. 3). Quantification of structural properties using the Bestsel online software (Micsonai, et al. 2015) suggests that LF

undergoes a drop in both the alpha-helical and beta-parallel sheet character upon nitration. Similarly, LF nitrated after saturation with Fe^{3+} resulted in a drop in alpha-helical character by approximately half. Nitration of lactoferrin in both unligated and iron-bound cases thus causes significant changes in secondary structure that suggests partial protein unfolding. The LF nitrated without bound iron, however, shows relatively greater reduction in the alpha-helical spectral region than iron-bound LF. This may suggest that the bound Fe^{3+} stabilizes the protein and also protects against nitration of the two tyrosine residues in each binding site. These possibilities will need to be probed in a future study.

Our observations conceptually match results for a structurally similar protein alpha-Crystalline, shown to exhibit misfolding after nitration with $ONOO^-$ (Thiagarajan, et al. 2004). Several studies have shown that alpha-helical peptides from LF provide bactericidal activity against *E. coli. (Chapple, et al. 1998; Håversen, et al. 2000).* Elass *et al.* also showed that LPS in *E. coli* interacted with the alpha-helical region of LF peptides and caused membrane damage (Elass-Rochard, et al. 1995). Here we showed a reduction in the CD spectral band in alpha-helix regions (208 and 222 nm). Together, the complementary observations suggest that nitration within the alpha-helical structure of the LF protein is likely to partially explain the reduction in antibacterial activity for NLF.

A separate test of iron-binding ability for both LF and NLF samples showed a qualitative decrease in iron uptake after nitration. These tests will need to be duplicated at a broader range of protein concentrations, to establish a higher degree of statistical

significance, and to quantitatively calculate iron binding constants. The initial evidence shown, however, is suggestive that iron uptake by LF is diminished upon nitration.

The observations here are the first to show that NLF exhibits reduced antibacterial activity compared to native LF. These results have critical relevance to nitration pathways within the human body as a function of inflammation and environmental exposure. For example, $ONOO^-$ levels have been shown to increase dramatically during eye inflammation (Allen, et al. 1998), which suggests that proteins such as LF in ocular fluids are likely to exist in at least partially nitrated states. LF converted to NLF in these nitrosative environments are thus likely to increase the possibility of bacterial infection, which can dramatically exacerbate ocular stress. The exposure of proteins within ocular fluid and in mucous membranes of the lungs and nasal passages can also be exposed to nitration through interaction with urban pollutant gases such as NO_2 and O_3 (Shiraiwa, et al. 2012). Protein nitration reactions have been proposed to provide a mechanism by which allergic and toxic responses are increased. Our observations thus represent a possible link to biochemical modification pathway during diseases and due to environmental exposure.

3.6 Acknowledgments

The authors gratefully acknowledge funding support from a grant by the University of Denver Knoebel Institute for Healthy Aging. Amani Alhalwani acknowledges scholarship support from King Saud bin Abdulaziz University for Health Sciences. The authors are grateful to Shaun Bevers, who performed the CD analysis at

Biophysics Core Facilities at the University of Colorado, School of Medicine. The authors also acknowledge Scott Horowitz and John Latham for help interpreting experimental results.

Chapter four: Ergothioneine inhibits nitration of proteins and can enhance natural antibacterial activity

4.1 Abstract

Ergothioneine (Ergo) is a natural product compound with antioxidant activity. It is accumulated in high concentration in many mammalian tissues including the eye. Ergo decreases in concentration within aging adults and may correlate with the presence of aging-related disease (Cheah, et al. 2016). This study was to investigate the Ergo contribution to protecting several proteins from nitration effects. The nitration reactions were applied using $ONOO^-$ and TNM nitration agents with and without the presence of Ergo. The nitration products were analyzed using absorbance and fluorescence spectroscopy and were compared with respect to non-nitrated proteins. The quantification of the nitrotyrosine level was also detected via the ELISA technique. The antibacterial function of nitrated lactoferrin was tested by broth microplate antibacterial assays. Our results show that Ergo exhibits anti-peroxynitrite activity by reducing nitration, and Ergo exhibits anti-inflammatory activity by restoring the antibacterial activity. This investigation will play a role for Ergo in prevent oxidative and nitrosative ocular damage.

4.2 Introduction

There are many nitration inhibitors, including ergothioneine (Ergo). Ergo has other unique properties aside from nitration inhibition. Ergo has a relatively small

molecular weight of approximately 229 Da (Hartman 1990) , is a safe, natural product compound, is odorless, is colorless, does not autoxidize, has high solubility in aqueous solutions up to 0.9 M, is stable, and degrades slowly in the physiological system.

Ergo is synthesized in fungi and mycobacteria, but there is no evidence for presence of biosynthesis in mammals or higher plants (Melville, et al. 1954). It is accumulated in several parts of the human body in concentrations of 1.0-2.0 mM such as lens of the eye, the cornea, the liver, and in bone marrow (Melville, et al. 1954). The presence of a high level of Ergo in mammalian ocular tissue has previously been determined, suggesting that it accumulates after being eaten (Shires, et al. 1997).

Ergo has many functions (Cheah, et al. 2012); as an antioxidant, as an Ergo tumor necrosis factor (TNF-α), as a hydrogen peroxide (H_2O_2) inhibitor in alveolar epithelial cells (Rahman, et al. 2003). As an anti-peroxynitrite agent, Ergo inhibits peroxynitrite-dependent reactions and protects tyrosine from nitration (Aruoma, et al. 1997). As an anti-inflammatory, Ergo inhibits xanthine and hypoxanthine formation (Žitňanová, et al. 2004). The multifunctionality of Ergo shows the possibility for therapeutic usage in many diseases, such as cardiovascular diseases (Servillo, et al. 2017) and acute respiratory distress (Repine, et al. 2012). Ergo is a well-known anti-peroxynitrite, anti-oxidant, and anti-inflammatory substance (Franzoni, et al. 2006b; Cheah, et al. 2012). One of the main Ergo antioxidant mechanisms is the capture of free radicals such as hydroxyl radical, and peroxynitrite. To my knowledge there is no reported mechanism in arrow reaction for Ergo functions has been done.

The aim of this work is to investigate the nitration inhibition effect of Ergo using several nitrated proteins samples; bovine serum albumin, lactoferrin, and lamb cornea lysate. Described here are several techniques used to examine Ergo's inhibition activity, including ELISA and spectroscopy techniques. Also shown is the broth antibacterial assay used to examine LF's antibacterial activity.

4.3 Experimental

4.3.1 Materials

Ergothineine (Ergo, 26524) were obtained from OXIS international, Inc. Human milk lactoferrin (LF; L0520), bovine serum albumin (BSA; A7030), tetranitromethane (TNM; T25003), Tween®20 buffer (P1379), Trizma base (Tris-HCl; T1503), sulfuric acid (H_2SO_4; 320501), sodium phosphate dibasic (RES20908-A702X), potassium chloride (P9333), sodium chloride (S9625), potassium phosphate monobasic (P5655), sodium carbonate (S7795), sodium bicarbonate (S5761), glysrol (G9012), and ethanol (245119), 4-(2-Hydroxyethyl) piperazine-1-ethanesulfonic acid, N-(2-Hydroxyethyl) piperazine-N′-(2-ethanesulfonic acid) (HEPES; H3375), Triton X-100 (X100), ethylenediaminetetraacetic acid anhydrous, bioultra (EDTA), chloramphenicol antibiotic (CAM; C0378), Trizma base (Tris-HCl; T1503), Hydrochloric acid (H-7020), Tryptic Soya broth (TSB; 22092), and Tryptic Soya agar (TSA; 22091) and sodium chloride (S9625) were purchased from sigma-aldrish (USA).

HALT (tm) protease inhibitor (PI; QB203967A) from fisher scientific company (PA, USA). Sodium peroxynitrite (NaONOO; 516620), Amicon Ultra-0.5 centrifugal

filters (30 kDa, 0.5 mL size; UFC503008) and Amicon Ultra centrifugal filters (30 kDa, 4 mL size; UFC803024) were purchased from Calbiochem (USA).

The 1-step ultra 3,3',5,5'-tetramethylbenzidine substrate (TMB; 34028) and bicinchoninic acid assay (BCA; 23225) for total protein quantification were purchased from ThermoFisher Scientific (USA). Flat-bottom, 96-microwell plates (untreated; 333-8013-01F) and sterile sealing tape (ST-3095) were obtained from Life Science Products (USA). A biotinylated, mouse monoclonal to nitrotyrosine antibody (α-NTyr; ab24496), streptavidin horseradish peroxidase (HRP; ab7403), and non-conjugated goat polyclonal anti-human lactoferrin antibody (α-LF; ab77548) were obtained from Abcam (UK). 1.0 mL quartz cuvette with 10mm path length (MF-W-10-LID) was purchased from Science Outlet (USA).

Biotinylated, mouse monoclonal to nitrotyrosine antibody (α-NTyr; ab24496), non-conjugated goat polyclonal anti-human lactoferrin antibody (α-LF; ab77548), and streptavidin horseradish peroxidase (HRP; ab7403) were obtained from Abcam (UK). 100 mm x 15 mm petri dish with grip ring, sterile (229692) provided by CELLTREAT (USA). UV 96-microwell plate with a transparent flat bottom (3635) was purchased from CORNING (USA).

Escherichia coli (*E. coli*; ATCC25922) was purchased from the American Type Culture Collection, ATCC (USA). Lamb cornea (age: 3 months, male gender) was donated from local butcher store (Jerusalem Market, E. Illif Ave.), it was FDA approved for human consumption and handling.

Buffers used were: phosphate-buffered saline (PBS; 8.1 mM sodium phosphate dibasic, 0.8 mM sodium phosphate monobasic, 1.3 mM potassium chloride, and 68.0 mM sodium chloride at pH 7.4), Tris-HCl buffer (Tris; 0.1 mM at pH 8.0), carbonate buffer (29.0 mM sodium carbonate and 71.0 mM sodium bicarbonate at pH 9.6), tryptic soy broth, and tryptic Soy agar was prepared following the manufacture instructions, and extraction buffer (EB) solution (50.0 mM Tris-HCl, 10.0 mM HEPES, 150.0 mM NaCL, 5.0 mM EDTA, 0.5 % Triton at pH 7.7, and then fresh add 10 % protease inhibitor (PI) and Tris-HCl buffer (Tris; 50 mM at pH 8.0).

The volume of peroxynitrite used for production of NLF10/1 $_{ONOO-}$ sample discussed in Section 4.4.2 was 5.66 µL. Similarly, the volume of TNM used for production of NLF10/1$_{TNM}$ discussed in Section 4.4.2 was 0.29 µL. The volume of tetranitromethane used for production of NBSA6/1 discussed in Section 4.4.1 was 0.95 µL of 6/1. The volumes of (17.05 µL) peroxynitrite and (1.16 µL) tetranitromethane used for production of nitrated cornea lysate $_{ONOO-}$ and $_{TNM}$ samples. These values correspond to molar ratios of nitrating agent to tyrosine ($ONOO^-$/Tyr) or (TNM/Tyr).

Proteins samples were tested: (**1)** BSA, NBSA 6/1(TNM), NBSA6/1(TNM)-Ergo 0.1 and 1.0 mM, (**2)** LF, NLF10/1(TNM), NLF10/1(TNM)- Ergo 0.1 and 1.0 mM, (**3)** LF, NLF10/1($ONOO^-$), NLF10/1($ONOO^-$)-Ergo 0.1 and 1.0 mM,**(4)** cornea lysate, nitrated cornea lysate (TNM), and nitrated cornea lysate (TNM)- Ergo 5.0 mM, and (**5)** cornea lysate, nitrated cornea lysate ($ONOO^-$), and nitrated cornea lysate ($ONOO^-$)-Ergo 5.0 mM.

4.3.2 Protein nitration reaction

The nitration reactions protocol followed procedures outlined by Alhalwani *et al.* to produce nitrated BSA, nitrated LF, and nitrated cornea lysate using TNM or $ONOO^-$ (Alhalwani, et al. 2018). Briefly, TNM reaction occurs in a mixture of Tris-HCl buffer and 20% ethanol, followed by added TNM volume based in a preferred TNM/Tyr molar ratio and serried at RT for 3 hours. The $ONOO^-$ reaction occurs in PBS buffer at a preferred $ONOO^-$/Tyr molar ratio and serried in ice for 3 hours. Then, each nitration model (TNM or $ONOO^-$) has two nitration groups, one group with Ergo and another group without Ergo. Ergo was added to the protein before adding the nitration agents to work efficiently in protecting the protein from nitration modification. The nitration reaction for cornea lysate was performed by adding the same concentration of each nitration agent.

The nitration product was purified using Amicon centrifugal tube and the protein was quantified using BCA assay following the manufacturer's protocol. Instruments were used; UV-vis spectrophotometer (Cary BIO 100), fluorimeter (Carry eclipse), rocking platform (UltraRocker, BIO-RAD), and plate reader (Tecan Infinite, M1000 PRO).

4.3.3 Absorbance analysis

The UV-Vis analysis used wavelength range of 250-500 nm and 2 nm steps obtained the absorption spectra. The protein samples were analyzed at RT using a 100 mm quartz cuvette. The concentration of the samples was consistent and diluted in a

reaction buffer PBS or Tris-HCl. The dilution of protein samples was calculated based on the molecular mass of native protein, irrespective of mass changes due to nitration.

4.3.4 Fluorescence analysis

The fluorescence analysis used excitation wavelength at 280 nm which is related to higher fluorescence of tyrosine and tryptophan. The fluorescence detected in a 2 nm increment at RT using a 10.0 mm quartz cuvette. Sample concentrations were 0.2 mg/mL and diluted in a proper reaction buffer PBS or Tris-HCl. The result shows a correlation between excitation wavelength and the corresponding emission intensity. The fluorescence spectra were used to determine the difference between the chemical structure properties and the native, nitrated protein, and nitrated protein-Ergo.

4.3.5 (NTyr) Direct enzyme linked immunosorbent assay (ELISA) to determine nitrotyrosine level

To detect the differences in nitrotyrosine between protein samples, direct ELISA was used to quantify the nitrotyrosine residue in the following samples: NBSA 6/1(TNM), NBSA 6/1(TNM)- Ergo 0.1 and 1.0 mM, Cornea lysate, nitrated lysate(TNM)- Ergo 5.0 mM, and nitrated lysate($ONOO^-$)-Ergo 5.0 mM. BSA was used because it is a standard protein and has 21 tyrosine residues, which is similar to the 20 tyrosine residues in LF.

Here, samples were diluted into a carbonate buffer at concentration 5 μg mL^{-1}. The samples were coated in triplicate with each sample solution and added separately to three wells as a blank measurement. The plate was covered with tape and incubated at RT for 2 hours. Washing steps to each well was applied after the incubation using 200 μL of PBST (PBS with 0.05% Tween) followed by patting the plate with a laboratory wipe to take away the extra washing buffer, repeated twice. This step was repeated after each incubation step with the same process of covering and plate shaking while incubation time using a rocking platform and then washing steps using PBST.

After washing, the plate was blocked by the non-specific binding areas using 200 μL of blocking buffer (5% BSA in PBS). This was added to each well and incubated at RT for 2 hours. Following the washing step, mouse monoclonal to nitrotyrosine biotinylated antibody (α-NTyr) was diluted in blocking buffer in 1:500 dilution ratio and 50 μL of the dilution was added to each well and incubated at RT for 1 hour. After that, streptavidin-HRP diluted 1:10,000 in blocking buffer was added in 50 μL to each well and incubated at RT for 1 hour. The TMB substrate was added in 100 μL to each well and incubated at RT until the color developed from colorless to blue in about 10 minutes. The 0.5 N aqueous sulfuric acid was added in the top of the substrate and the color quickly changed to yellow.

The plate was measured using the optical absorbance of each well using a microwell plate reader. The measurement was based on standard procedures

(Rajasekariah, et al. 2003). The final absorbance is a value of the subtracted background wavelength 620 nm (blue) from the wavelength at 450 nm (yellow).

4.3.6 (LF- NTyr) Sandwich ELISA for quantify nitrotyrosine

The sandwich ELISA protocol was followed by Alhalwani *et al.*(Alhalwani, et al. 2018) which is a unique combination of antibodies which are that the captured antibody was goat polyclonal to lactoferrin non-conjugated antibody (α-LF), and the detector antibody was mouse monoclonal to nitrotyrosine biotinylated antibody (α-NTyr) to detect nitrotyrosine in LF molecules.

The microplate was coated with 50 µL of 1:1000 dilution ratio of captured antibody in carbonate buffer at at 4°C overnight. The plate was then washed and blocked as described above. After the washing step, 50µL of NLF10/1(TNM), NLF10/1(TNM)- Ergo (0.1 and 1.0 mM), NLF10/1($ONOO^-$), and NLF10/1($ONOO^-$)-Ergo (0.1 and 1.0 mM) that were diluted into the blocking buffer to produce NLF solutions of concentrations 5 µg mL^{-1} and added in triplicate to the plate and incubated at RT for 1 hour. Blocking buffer was used for blank measurements. The detector antibody diluted in blocking buffer was added in 50 µL of 1:100 dilution ratio and the plate was incubated with shaking at RT for 1 hour. The enzyme streptavidin-HRP and the substrate TMB were added following the ELISA protocol, as described above. The standard calibration curve was made according to the absorbance at each concentration of 40/1 molar ratio NLF.

4.3.7 Broth microplate antibacterial assay to detect the antibacterial activity

The assay was followed by broth microplate antibacterial assay in previous study (Jorgensen, et al. 2015; Balouiri, et al. 2016). *E. coli* broth stock was prepared from 1 µL of glycerol stock aliquot of *E. coli* was inculcated into TSA plates at 37 ºC for 24 hrs. Then, several (3-5) separate colonies were selected, transferred into 4 mL TSB, and incubated at 37 ºC for 24 hours. Finally, the 4 mL of *E. coli* in TSB was diluted 10% dilution by adding 36 mL of TSB to make *E. coli* broth stock.

In the microplate, TSB (200 µL) was added with the samples. All samples were prepared in TSB, (Blank) using TSB, (positive control) in CAM in 30 µg mL^{-1}, LF, Ergo, NLF ($ONOO^-$)10/1-Ergo 0.2, 1.0, 5.0 and 10.0 mM, and NLF ($ONOO^-$) 10/1, 20/1, 30/1, and 40/1 Ergo 5.0 mM all NLF's samples were in 1.0 mg mL^{-1}concentrations. In each well, 5 µL of *E. coli* broth stock was added and incubated overnight at 37 ºC. The microwell plates were examined at wavelength 600 nm using the plate reader.

4.3.8 Lamb cornea tissue dissection

The lamb cornea was extracted from the whole lamb eye using a surgical razor blade. Then, the cornea was cut into four pieces, weighted using an analytical scale, and followed by a snap freeze using liquid nitrogen. The cornea was placed in a cryogenic microtube and stored at -80°C until extraction occurs, see appendix B.

4.3.9 Protein extraction from lamb cornea

The cornea was washed using Tris-HCl buffer and placed into the extraction buffer 10% tissue mass per volume. The mixture was mixed in ice for 25 minutes and

sonicated at 8 powers for 2 minutes. Finally, the mixture was centrifuged at 1400 g for 30 minutes and the supernatant was collected and aliquot in cryogenic microtube and stored at -20°C until further analysis. The total protein in the lysate was detected using BCA assay following the manufacture protocol.

4.3.10 Statistical analysis

All data were analyzed using Igor Pro 7 software (Wavemetrics, Inc.; Oregon, USA). All ELISA and bacterial samples were run in triplicate, averaged, and represented mean ± standard deviation (*s*) of data values. Analyses of variance were subjected to t-tests, including associated p-values performed using GraphPad software.

4.4 Results and Discussion

4.4.1 Nitrated standard protein NBSA 6/1(TNM) used to characterize nitration inhibition via Ergo

The TNM nitration reaction was used to produce nitrated protein with the highest NTyr residues since the nitration reaction by TNM reagent mainly produce NTyr residues in the protein. An Ergo concentration of 1.0 mM was used as an effective inhibitory concentration against NTyr formation as has been shown in previously published reports (Aruoma, et al. 1997) Addionally, the NTyr formation was tested to detect the effective dose of inhibition using sandwich ELISA which confirm this concentration. The result of Sandwich ELISA shows the correlation between the reduction of NTyr formation and Ergo concentration which are Ergo 1.0, 5.0, and 10.0 mM; see Figure 4.1.

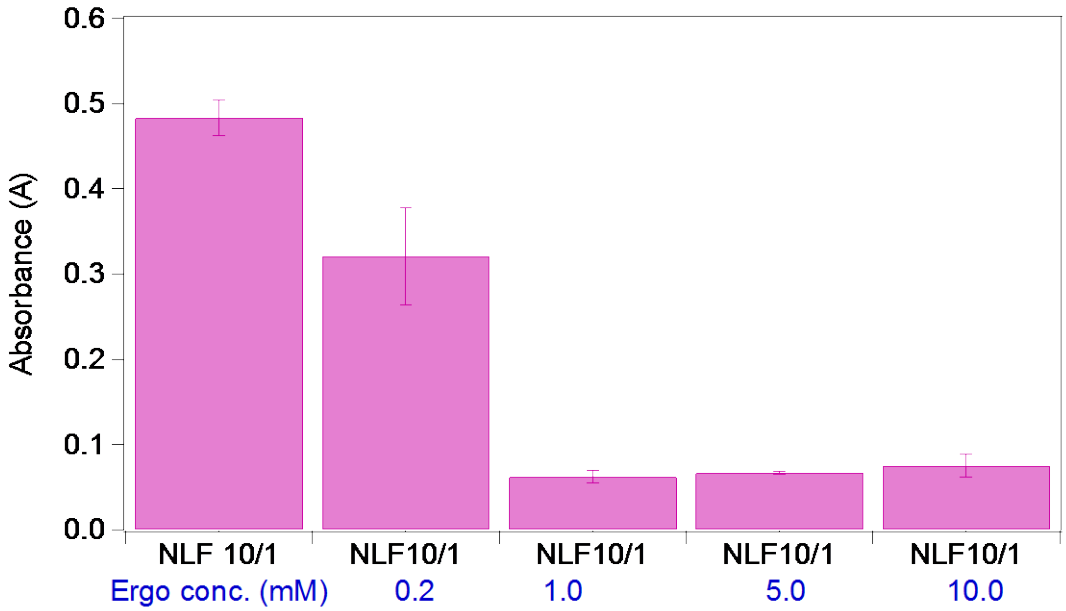

Figure 4. 1 Sandwich ELISA for NLF 10/1 and Ergo. The NLF 10/1 shows similar NTyr formation at Ergo 1mM and higher concentrations.

The NBSA 6/1(TNM) was used to test inhibitory effects of Ergo against nitration, (Figure 4. 2) using three analytical methods. Absorbance intensity at 350 nm obtains information about the nitration formation through the increase in nitrated product absorbance. The spectra of NBSA 6/1 (Figure 4. 2. A) showed higher absorbance intensity than NBSA with Ergo. The decrease in absorbance band indicates the inhibition effects of Ergo to nitration formation. Additionally, the fluorescence intensity at excitation 280 nm identifies the nitration formation by diminishing the intensity. The fluorescence spectra of NBSA 6/1 showed lower fluorescence intensity than NBSA with Ergo (Figure 4. 2. B). The increase in fluorescence band shows the inhibition effects by Ergo. Nitrotyrosine (NTyr) is a marker for the nitration formation and to determine the Ergo effects, the level of NTyr residue in the samples needs to be monitored. The direct

ELISA quantifies nitrotyrosine residues which indicate the nitration formation. The result of NBSA 6/1 (Figure 4. 2. C) detected higher NTyr concentration than NBSA with Ergo.

The three analyses each suggest that NBSA 6/1 has the highest nitration formation comparing to NBSA 6/1-Ergo 0.1 and 1.0 mM. These results together confirmed the inhibition effects of Ergo to the nitration. There was a direct correlation between the Ergo concentration and the nitration inhibition e.g. NBSA 6/1-Ergo1.0 mM had less nitration than NBSA 6/1-Ergo 0.1 mM. Our results are consistent with the study by Aruoma *et al.*(Aruoma, et al. 1997) that showed the association between the decrease in nitrotyrosine residues to the increase of the concentration of Ergo. Here, we used NBSA 6/1 as standard protein to help in adjusting the analysis for our target protein LF and cornea lysate.

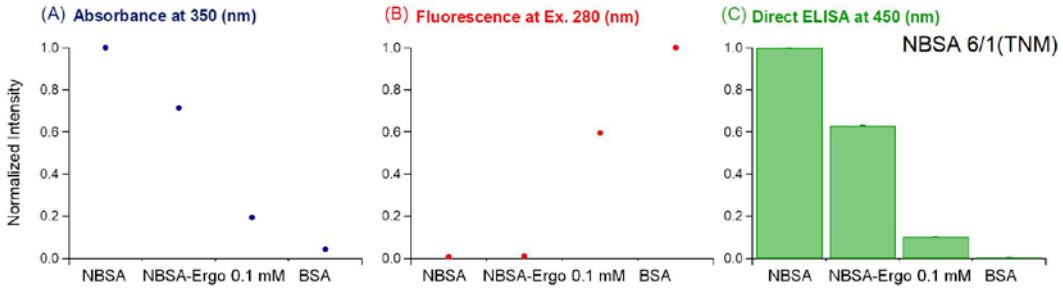

Figure 4. 2 The results of the effect of Ergo in NBSA 6/1. Three data sets presented are A: absorbance (blue mark), B: fluorescence (red mark), and C: direct ELISA n=3 (green mark) showed the nitration chemical properties with respect to Ergo effects. In each graph, the samples presented at x-axis were from right to left were NBSA 6/1(TNM), NBSA 6/1(TNM)- Ergo 0.1, and NBSA 6/1(TNM)- Ergo 1.0 mM.

4.4.2 Nitrated human protein NLF10/1 used to test Ergo inhibitory property

Herein, we nitrated lactoferrin using two models; TNM to produce mainly 3-nitrotyrosine (NTyr) and as nitration exogenesis model, and $ONOO^-$ to produce several nitrated amino acids and as nitration endogenous model. The NLF10/1 used as a positive

control for the nitration formation and to compare it with the samples of NLF10/1with Ergo.

The spectroscopic results (Figure 4. 3. A and B) showed an increase in absorbance intensity at 350 nm and a decrease in the fluorescence intensity at excitation 280 nm for NLF10/1 and these effects inverted after the addition of Ergo. The result of NLF10/1 with TNM was consistence to NLF10/1 with $ONOO^-$. The results of NLF and NBSA confirmed the Ergo inhibitory effects against protein nitration. In our previous study, we developed a specific sandwich ELISA that detects NTyr in nitrated lactoferrin samples (Alhalwani, et al. 2018), thus, the level of NTyr residues were determined using this sandwich ELISA. The sandwich ELISA quantifies nitrotyrosine residues (Figure 4. 3. C) which confirm the nitration formation. The NLF10/1 showed higher NTyr residues than NLF10/1 with Ergo.

The results of NLF10/1 with Ergo showed a decrease in NTyr residues with the increase of Ergo concentrations. This finding suggests that Ergo protects lactoferrin protein from nitration. By contrast, the link in both nitration agents $ONOO^-$ or TNM is to produce NO_2 in the reaction environment and cause protein nitration. We observed that NLF with $ONOO^-$ or TNM has similar inhibition response via Ergo. This observations lead to the possible Ergo inhibition mechanism by capturing an $\bullet NO_2$ molecule to prevent lactoferrin from the nitration process.

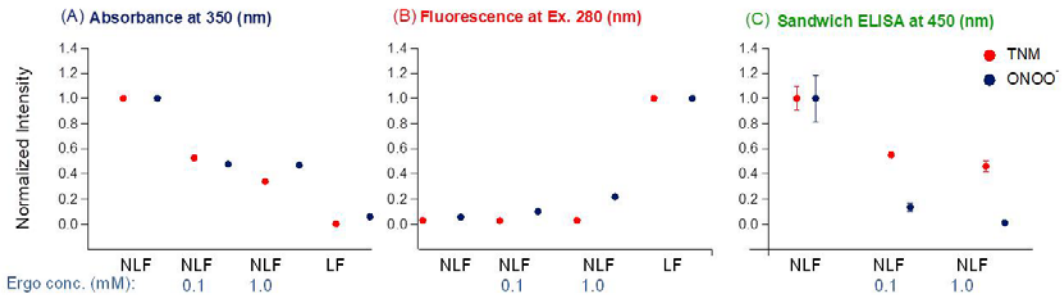

Figure 4. 3 The results of the affect of Ergo in NLF 10/1. A: absorbance in blue, B: fluorescence in red, and C: sandwich ELISA in green demonstrated the nitration chemical properties with respect Ergo effects. The circle presented NLF's (TNM) samples and the triangle presented NLF's ONOO- samples.

4.4.3 Nitrated cornea tissue proteins used to investigate Ergo inhibitory property

The goal of this part of the work is to investigate the changes associated with certain proteins due to nitration on an organ level. The inhibitory effects of Ergo will help us to understand the nitration of these proteins en route to understanding their potential importance in eye diseases and possibly toward finding a therapeutic target. Here, the cornea tissue was tested since it has been shown that LF presence in mammalian cornea and protein effects (Rageh, et al. 2016). The cornea lysate sample contains mixtures of proteins including lactoferrin and the nitration will produce multiple protein nitrations.

The Ergo concentration (5.0 mM) was higher than NBSA and NLF experiments to extend the highest level of protection, since the cornea lysate has many different proteins and the nitration formation level was unknown. The absorbance data (Figure 4. 4. A) showed decrease in intensity due to the reduction of nitration formation by Ergo, and the fluorescence data (Figure 4. 4. B) showed the increase in intensity via retraining the fluorescence chemical properties via Ergo. The direct ELISA (Figure 4. 4. C) quantified lower NTyr level in nitrated lysate with Ergo samples than nitrated lysate. The

inhibitory effects of Ergo in lysate samples were matched to the above results for NBSA and NLF which confirmed the anti-peroxynitrite activity of Ergo. This investigation verified the robust ability of Ergo effects to protect proteins from the nitration process.

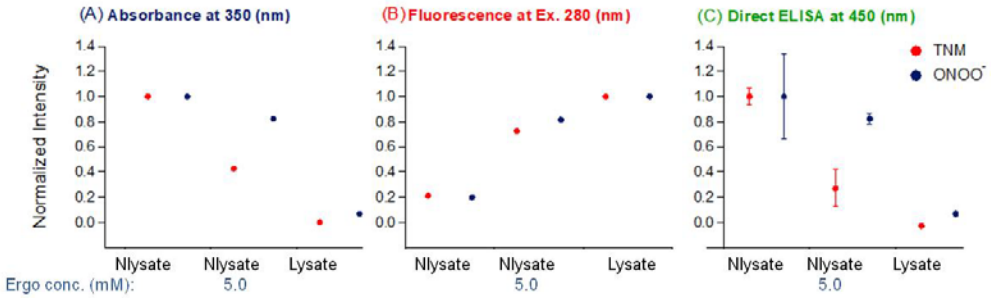

Figure 4. 4 The results of the affect of Ergo in N-lysate. A: Absorbance spectra in blue mark, B: fluorescence spectra in red mark, and C: direct ELISA spectra in green mark.

4.4.4 The antibacterial activity retrained for NLF after the addition of Ergo

LF plays an important role in the antimicrobial function via several mechanisms. In this study, the bacteria growth was monitored using visible absorbance at 600 nm. The protein nitration using $ONOO^-$ was tested for lactoferrin since it is related to the physiological nitration process and because Ergo has anti-peroxynitrite activity (Franzoni, et al. 2006b). The protein nitration using TNM was not suitable for antibacterial assay due to its toxicity. The antibacterial assay was tested for controls which are LF, Ergo 5.0 and 50.0 mM as result showed in Figure 4. 5. Also, Ergo results (Figure 4. 6. A and B) represented two different inhibitory models for Ergo to lactoferrin nitration.

First, (Figure 4. 6. A) showed the effects Ergo in different concentration to one molar ratio of nitrated lactoferrin. *E.coli* was tested against in several samples and showed no growth for the blank and CAM antibiotic, highest inhibition for LF (22%),

lower inhibition for NLF10/1 (12%) than NLF10/1-ERG 0.2 mM (-9 %), 1.0 mM (-2%), 5.0 mM (25%) and 10.0 mM (34%). The two concentrations NLF10/1-ERG 0.2 mM and 1.0 mM have a technical error and that explained the negative values. The *E.coli* linearly inhibited with the increase of Ergo concentration in nitrated lactoferrin samples which indicate antibacterial activity was protected during nitration by Ergo. P-values of *E. coli* against all samples were < 0.001 significantly different except NLF10/1-ERG 1.0 mM < 0.1 due to a technical error.

Second, (Figure 4. 6. B) showed the effects nitrated lactoferrin in different nitration molar to one concentration of Ergo 5.0 mM. *E.coli* was tested against many samples; LF (23%) highest growth, higher inhibition in NLF10/1-Ergo 5.0 mM (45%), NLF 20/1-Ergo 5.0 mM (32%), NLF30/1-Ergo 5.0 mM (21%) and NLF40/1-Ergo 5.0 mM (22%). P-values of *E. coli* against all samples were <0.001 significantly different. The Ergo 5 mM concentration in NLF10/1 inhibit the nitration and bacterial growth greater than the higher nitration molar NLF40/1. The presence of same Ergo concentration (5 mM) with a different NLF molar ratio showed a competitive reactivity of Ergo in protecting the protein from nitration, but generally, showed nitration inhibition. This confirmed the importance of the dose response of Ergo with respect to the level of protein nitration.

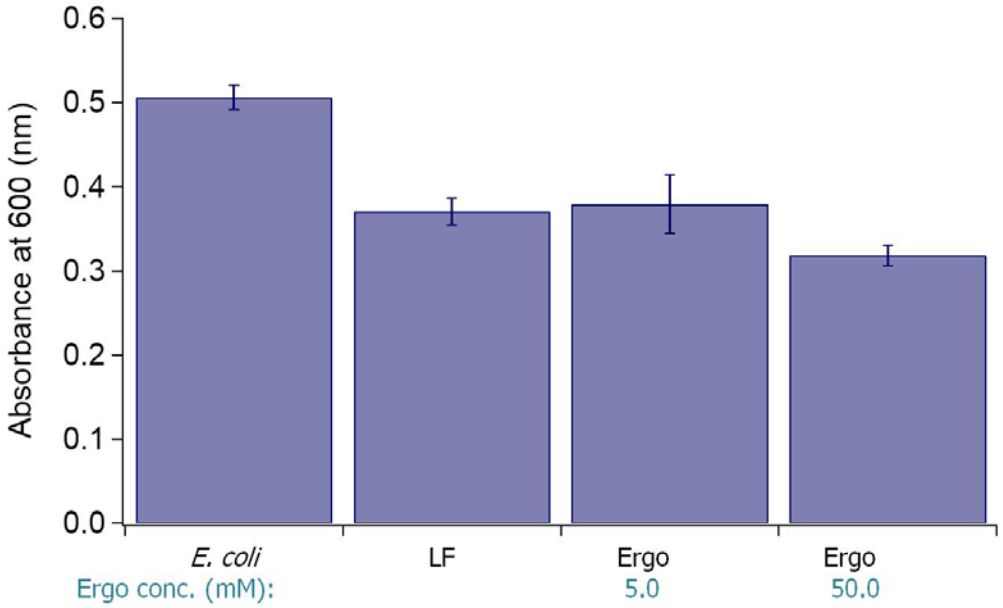

Figure 4. 5 Antibacterial activity of controls Ergo 5.0 mM has antibacterial activity similar to LF and Ergo 50.0 mM has the most antibacterial effect.

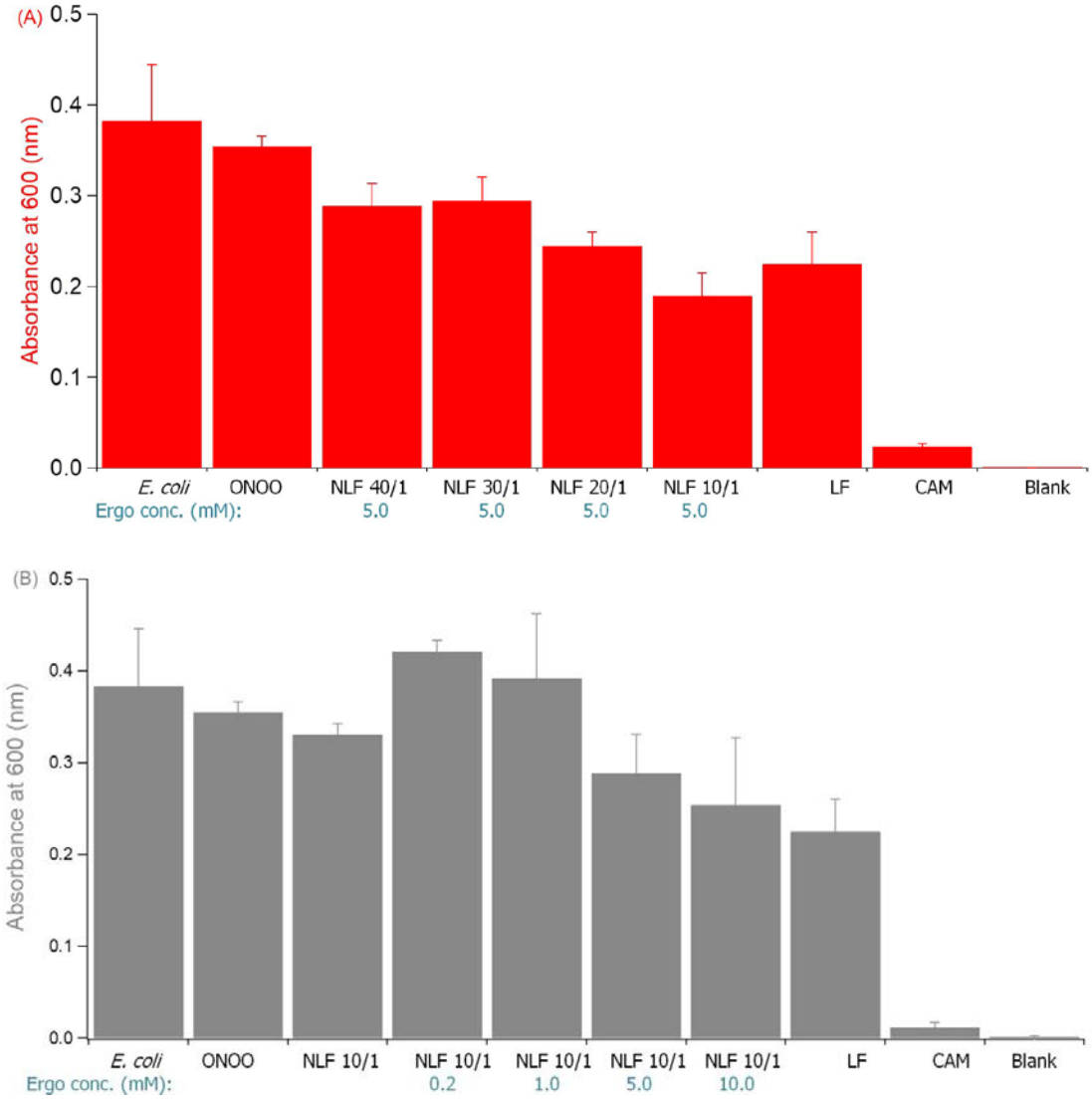

*Figure 4. 6 .Broth microplate antibacterial assay. Blank (broth, no **E. coli**), CAM (positive control, strong inhibition), **E. coli** (negative control, no inhibition) tested against A: LF and NLF at four molar concentrations 10/1, 20/1, 30/1, and 40/1 with same Ergo concentration 5.0 mM, and P-values of E. coli against LF (0.0001), NLF10/1-Ergo 5.0 mM (0.0001), NLF20/1-Ergo 5.0 mM (0.0001), NLF30/1-Ergo 5.0 mM (0.0008), and NLF40/1-Ergo 5.0 mM (0.0005). B: LF and NLF10/1 with four Ergo concentrations: 0.2, 1.0, 5.0, and 10.0 mM. Absorbance values shown without blank subtraction. Bars show mean values ± standard deviations of n=4. P-values of E. coli against LF (0.0001), NLF10/1 (0.0007), NLF10/1-Ergo 0.2 mM (0.0043), NLF10/1-Ergo 1.0 mM (0.81), NLF10/1-Ergo 5.0 mM (0.0047), and NLF10/1-Ergo 10.0 mM (0.031).*

4.5 Conclusion

The present work showed initial results regarding the inhibitory effect of Ergo in the nitration reaction for several physiological proteins. Our observation of qualitative and quantitative analysis showed an inhibitory effect of nitration through the addition of Ergo. Specifically, BSA protein nitration with Ergo was significant dropping at NBSA-Ergo 1.0 mM comparing by NBSA. Also, LF protein nitration with Ergo and cornea lysate nitration with Ergo showed decrease in nitration in the two nitration models ONOO and TNM with slight different in inhibition due to the mechanism of producing nitration from each model. Finally, the antibacterial activity results of Ergo-NLF showed an increase of antibacterial activity than NLF.

The results suggest a correlation between the decreases of the protein nitration level with the increase of Ergo concentration. This study demonstrated preliminary results for Ergo nitration inhibition in several nitrated proteins using quantitative and qualitative techniques, which could contribute to the potential treatment development for nitrosative and oxidative stress linked diseases.

Chapter five: Conclusion and future work

Protein nitration is a type of chemical modification that introduces nitro group into amino acid residues. The body can be exposed to nitration through various vectors, including via disease and air pollution. Certain proteins are highly affected by this nitration process, including lactoferrin. LF is widespread within bodily fluid and plays a role in health due to multitude of functions. Also, lactoferrin is used as a biomarker protein for several diseases. There is also a relationship between decreases in lactoferrin levels with many disease types, such as ocular disease.

The incidence of ocular surface disease are actively increasing as air pollution continues to rise. Clinical examinations of the ocular surface have shown links between reactive nitrogen species in air pollution and disease incidence, but the exact mechanism of this link is unknown. The studies presented here investigate lactoferrin nitration using a series of biochemical techniques. The observed chemical effect nitrogen species have on lactoferrin was then applied to biological samples with the intent of finding a therapeutic approach to preventing ocular disease caused by nitration.

Nitrotyrosine and lactoferrin, in tears, are both important biomarker targets for ocular disease. Biochemical studies on detecting the effect of nitration with respect to the decrease of lactoferrin in ocular disease are not well understood, so a method was developed which allows for simultaneous detection of both markers in a single assay. Fluorescence and absorbance spectrometric techniques were utilized to identify that

standards of lactoferrin, with different nitration molar ratios, reveal a linear dependence of binding between lactoferrin and nitrogen species. A unique, selective, and sensitive sandwich ELISA detection technique utilizing two antibodies, anti-lactoferrin and anti-nitrotyrosine was then developed to quantify the amounts of nitrotyrosine in nitrated lactoferrin samples. The sandwich ELISA method detecting nitrotyrosine bound to lactoferrin is important in better understanding the biological role of the decreasing lactoferrin levels in ocular disease.

Since lactoferrin is a host defense protein that protects the ocular surface, it's given that a loss of lactoferrin function is one potential link to ocular disease. Considering the knowledge that nitration is linked to other air pollution disease this study investigates potential effects that nitration of lactoferrin may have on its bioactivity. A broth antibacterial assay shows lactoferrin's antibacterial activity is diminished by nitration in a concentration dependent manner. This effect was explained using circular dichroism, in which spectra show conformational changes on lactoferrin due to nitration. These observations help elucidate the mechanism of how ocular disease can be linked to components of air pollution.

Given the negative effects nitration has on lactoferrin function a method of inhibiting this nitration has high therapeutic potential in ocular disease. Ergothioneine, a natural histidine mimic, is currently used as an anti-inflammatory, anti-oxidant, and anti-peroxynitrite agent. Because it is already utilized in other areas, ergothionene was chosen to pursue it as a target molecule to protect lactoferrin from nitration. To test its protection

potential, we utilized previously discussed spectroscopic, antibacterial and ELISA techniques, and our results universally show that ergothioneine blocks nitration of lactoferrin. These finding show excellent potential in utilizing ergothioneine to maintain health of ocular surface.

To better understand lactoferrin nitration within biological samples, I plan to utilize a quantitative sandwich ELISA technique on tear samples from patients with ocular surface disease. While tear analysis is one good way of investigating the effects of lactoferrin nitration in biological samples, more research is needed on lactoferrin nitration in living cells to evaluate whether they might exhibit altered function in *vivo*. To establish this, further research for the nitration reactions need to be explored for toxic effects with *in vivo* studies. Also, the quantification assay (ELISA) needs to be adjusted to the concentration range to quantify nitrotyrosine based on the matrix sample.

We gained insight on the mechanism of this altered function by observing the reduction in the antibacterial activity of nitrated lactoferrin, but future molecular structure investigations will lead to more understanding in the antibacterial mechanism. Also, the degree of nitration and the location of nitrotyrosine on lactoferrin will support the investigation of antibacterial mechanism.

Finally, ergothioneine is an excellent target molecule for inhibit protein nitration and help to maintain protein function, thus making it a robust treatment option with broad applications in ocular therapy. This project needs further investigation *in vivo,* in addition to concentration tests. The groundbreaking research detailed in this work may help in

experimental designs, clinical examination, and the therapeutic improvements intended to evaluate the role of protein nitration in ocular disease.

References

abcam. 2017. "Anti-Lactoferrin Antibody (Ab77548)." Accessed 26 Jun, 2017.

Adlerova, L., A. Bartoskova, and M. Faldyna. 2008. "Lactoferrin: A Review." *Veterinarni Medicina* 53, no. 9: 457-468.

Aggarwal, Saurabh, et al. 2011. "Attenuated Vasodilatation in Lambs with Endogenous and Exogenous Activation of Cgmp Signaling: Role of Protein Kinase G Nitration." *Journal of cellular physiology* 226, no. 12: 3104-3113.

Al-Garawi, Z. S., et al. 2017. "The Amyloid Architecture Provides a Scaffold for Enzyme-Like Catalysts." *Nanoscale* 9, no. 30: 10773-10783.

Alhalwani, A. Y., et al. 2018. "Development of a Sandwich Elisa with Potential for Selective Quantification of Human Lactoferrin Protein Nitrated through Disease or Environmental Exposure." *Anal Bioanal Chem* 410, no. 4 (Feb): 1389-1396. http://dx.doi.org/10.1007/s00216-017-0779-7.

Allen, Janice Benson, Teresa Keng, and Christopher Privalle. 1998. "Nitric Oxide and Peroxynitrite Production in Ocular Inflammation." *Environmental health perspectives* 106, no. Suppl 5: 1145.

Anderson, Bryan F., et al. 1989a. "Structure of Human Lactoferrin: Crystallographic Structure Analysis and Refinement at 2·8 Å Resolution." *Journal of Molecular Biology* 209, no. 4 (1989/10/20/): 711-734. http://dx.doi.org/https://doi.org/10.1016/0022-2836(89)90602-5.

---. 1989b. "Structure of Human Lactoferrin: Crystallographic Structure Analysis and Refinement at 2· 8 Å Resolution." *Journal of molecular biology* 209, no. 4: 711-734.

Andreadis, Athena A., et al. 2003. "Oxidative and Nitrosative Events in Asthma." *Free Radical Biology and Medicine* 35, no. 3: 213-225.

Aruoma, Okezie I., et al. 1997. "Antioxidant Action of Ergothioneine: Assessment of Its Ability to Scavenge Peroxynitrite." *Biochemical and biophysical research communications* 231, no. 2: 389-391.

Ashki, Negin, et al. 2014. "Peroxynitrite Upregulates Angiogenic Factors Vegf-a, Bfgf, and Hif-1α in Human Corneal Limbal Epithelial Cells." *Investigative Ophthalmology & Visual Science* 55, no. 3 (03/19
05/14/received

10/25/accepted): 1637-1646. http://dx.doi.org/10.1167/iovs.13-12410.

Aulak, Kulwant S., et al. 2004. "Dynamics of Protein Nitration in Cells and Mitochondria." *American Journal of Physiology-Heart and Circulatory Physiology* 286, no. 1: H30-H38.

Baggiolini, Mh, et al. 1970. "Association of Lactoferrin with Specific Granules in Rabbit Heterophil Leukocytes." *The Journal of experimental medicine* 131, no. 3: 559.

Baker, Heather M., and et al. 2000. Vol. 5: *JBIC Journal of Biological Inorganic Chemistry* 5.6

Baker, E. N., and H. M. Baker. 2005. "Molecular Structure, Binding Properties and Dynamics of Lactoferrin." *Cellular and molecular life sciences: CMLS* 62, no. 22: 2531-2539.

Baker, Edward N., et al. 1990. "Metal and Anion Binding Sites in Lactoferrin and Related Proteins." *Pure and Applied Chemistry* 62, no. 6: 1067-1070.

Baker, Edward N., and Heather M. Baker. 2009. "A Structural Framework for Understanding the Multifunctional Character of Lactoferrin." *Biochimie* 91, no. 1: 3-10.

Ballow, Mark, et al. 1987. "Tear Lactoferrin Levels in Patients with External Inflammatory Ocular Disease." *Investigative ophthalmology & visual science* 28, no. 3: 543-545.

Balouiri, Mounyr, Moulay Sadiki, and Saad Koraichi Ibnsouda. 2016. "Methods for in Vitro Evaluating Antimicrobial Activity: A Review." *Journal of Pharmaceutical Analysis* 6, no. 2 (2016/04/01/): 71-79. http://dx.doi.org/http://dx.doi.org/10.1016/j.jpha.2015.11.005.

Baveye, Sophie, et al. 1999. "Lactoferrin: A Multifunctional Glycoprotein Involved in the Modulation of the Inflammatory Process." *Clinical Chemistry and Laboratory Medicine* 37, no. 3: 281-286.

Beckman, Joseph S. 1996. "Oxidative Damage and Tyrosine Nitration from Peroxynitrite." *Chemical research in toxicology* 9, no. 5: 836-844.

Becquet, F., Y. Courtois, and O. Goureau. 1997. "Nitric Oxide in the Eye: Multifaceted Roles and Diverse Outcomes." *Survey of Ophthalmology* 42, no. 1 (1997/07/01/): 71-82. http://dx.doi.org/https://doi.org/10.1016/S0039-6257(97)84043-X.

Begara-Morales, Juan C., et al. 2013. "Protein Tyrosine Nitration in Pea Roots During Development and Senescence." *Journal of experimental botany* 64, no. 4: 1121-1134.

Bellamy, Wayne, et al. 1992. "Identification of the Bactericidal Domain of Lactoferrin." *Biochimica et Biophysica Acta (BBA) - Protein Structure and Molecular Enzymology* 1121, no. 1 (1992/05/22/): 130-136. http://dx.doi.org/https://doi.org/10.1016/0167-4838(92)90346-F.

Birgens, H. S., et al. 1983. "Receptor Binding of Lactoferrin by Human Monocytes." *Br J Haematol* 54, no. 3 (Jul): 383-91.

Bläckberg, Lars, and Olle Hernell. 1980. "Isolation of Lactoferrin from Human Whey by a Single Chromatographic Step." *FEBS Letters* 109, no. 2: 180-184. http://dx.doi.org/10.1016/0014-5793(80)81081-7.

Blanc, B., and H. Isliker. 1961. "Isolation and Characterization of the Red Siderophilic Protein from Maternal Milk: Lactotransferrin." *Bulletin de la Société de chimie biologique* 43: 929.

Bosch-Morell, Francisco, et al. 2002. "Role of Oxygen and Nitrogen Species in Experimental Uveitis: Anti-Inflammatory Activity of the Synthetic Antioxidant Ebselen." *Free Radical Biology and Medicine* 33, no. 5: 669-675.

Brock, Jeremy. 1995. "Lactoferrin: A Multifunctional Immunoregulatory Protein?" *Immunology Today* 16, no. 9 (1995/09/01/): 417-419. http://dx.doi.org/https://doi.org/10.1016/0167-5699(95)80016-6.

Buddi, Rajeev, et al. 2002. "Evidence of Oxidative Stress in Human Corneal Diseases." *Journal of Histochemistry & Cytochemistry* 50, no. 3: 341-351. http://jhc.sagepub.com/content/50/3/341.abstract.

Chapple, Daniel S., et al. 1998. "Structure-Function Relationship of Antibacterial Synthetic Peptides Homologous to a Helical Surface Region on Human Lactoferrin against Escherichia Coli Serotype O111." *Infection and immunity* 66, no. 6: 2434-2440.

Cheah, Irwin K., et al. 2016. "Ergothioneine Levels in an Elderly Population Decrease with Age and Incidence of Cognitive Decline; a Risk Factor for Neurodegeneration?" *Biochemical and Biophysical Research Communications* 478, no. 1 (2016/09/09/): 162-167. http://dx.doi.org/https://doi.org/10.1016/j.bbrc.2016.07.074.

Cheah, Irwin K., and Barry Halliwell. 2012. "Ergothioneine; Antioxidant Potential, Physiological Function and Role in Disease." *Biochimica et Biophysica Acta (BBA) - Molecular Basis of Disease* 1822, no. 5 (5//): 784-793. http://dx.doi.org/https://doi.org/10.1016/j.bbadis.2011.09.017.

Chiou, George C. Y. 2001. "Review: Effects of Nitric Oxide on Eye Diseases and Their Treatment." *Journal of ocular pharmacology and therapeutics* 17, no. 2: 189-198.

Chou, Samuel M., Helen S. Wang, and Kiyonobu Komai. 1996. "Colocalization of Nos and Sod1 in Neurofilament Accumulation within Motor Neurons of Amyotrophic Lateral Sclerosis: An Immunohistochemical Study." *Journal of chemical neuroanatomy* 10, no. 3: 249-258.

Chung, Hae Young, et al. 1998. "Peroxynitrite-Scavenging Activity of Green Tea Tannin." *Journal of Agricultural and Food Chemistry* 46, no. 11: 4484-4486.

Conneely, Orla M. 2001. "Antiinflammatory Activities of Lactoferrin." *Journal of the American College of Nutrition* 20, no. sup5 (2001/10/01): 389S-395S. http://dx.doi.org/10.1080/07315724.2001.10719173.

Crouch, S. P., K. J. Slater, and J. Fletcher. 1992. "Regulation of Cytokine Release from Mononuclear Cells by the Iron- Binding Protein Lactoferrin." *Blood* 80, no. 1: 235. http://www.bloodjournal.org/content/80/1/235.abstract.

Crow, J. P., and J. S. Beckman. 1995. "Quantitation of Protein Tyrosine, 3-Nitrotyrosine, and 3-Aminotyrosine Utilizing Hplc and Intrinsic Ultrviolet Absorbance." *Methods* 7, no. 1 (1995/02/01): 116-120. http://dx.doi.org/http://dx.doi.org/10.1006/meth.1995.1017.

Crow, John P., and Harry Ischiropoulos. 1996. "[17] Detection and Quantitation of Nitrotyrosine Residues in Proteins: In Vivo Marker of Peroxynitrite." *Methods in enzymology* 269: 185-194.

Dalle-Donne, Isabella, et al. 2006. "Protein Carbonylation, Cellular Dysfunction, and Disease Progression." *Journal of cellular and molecular medicine* 10, no. 2: 389-406.

Dalle-Donne, Isabella, et al. 2005. "Proteins as Biomarkers of Oxidative/Nitrosative Stress in Diseases: The Contribution of Redox Proteomics." *Mass spectrometry reviews* 24, no. 1: 55-99.

De Filippis, Vincenzo, Roberta Frasson, and Angelo Fontana. 2006. "3-Nitrotyrosine as a Spectroscopic Probe for Investigating Protein Protein Interactions." *Protein Science : A Publication of the Protein Society* 15, no. 5 (11/08/received 01/24/revised 01/24/accepted): 976-986. http://dx.doi.org/10.1110/ps.051957006.

De La Rica, Roberto, and Molly M. Stevens. 2012. "Plasmonic Elisa for the Ultrasensitive Detection of Disease Biomarkers with the Naked Eye." *Nature nanotechnology* 7, no. 12: 821-824.

de la Rosa, G., et al. 2008. "Lactoferrin Acts as an Alarmin to Promote the Recruitment and Activation of Apcs and Antigen-Specific Immune Responses." *J Immunol* 180, no. 10 (May 15): 6868-76.

de Souza, Gustavo A., Lyris M. F. de Godoy, and Matthias Mann. 2006. "Identification of 491 Proteins in the Tear Fluid Proteome Reveals a Large Number of Proteases and Protease Inhibitors." *Genome biology* 7, no. 8: R72.

Dionysius, David A., Paul A. Grieve, and Joanne M. Milne. 1993. "Forms of Lactoferrin: Their Antibacterial Effect on Enterotoxigenic Escherichia Coli." *Journal of Dairy Science* 76, no. 9 (1993/09/01/): 2597-2606. http://dx.doi.org/https://doi.org/10.3168/jds.S0022-0302(93)77594-3.

Elahi, Maqsood M., Yu Xiang Kong, and Bashir M. Matata. 2009. "Oxidative Stress as a Mediator of Cardiovascular Disease." *Oxidative Medicine and Cellular Longevity* 2, no. 5: 259-269.

Elass-Rochard, E., et al. 1995. "Lactoferrin-Lipopolysaccharide Interaction: Involvement of the 28-34 Loop Region of Human Lactoferrin in the High-Affinity Binding to Escherichia Coli 055b5 Lipopolysaccharide." *Biochemical Journal* 312, no. 3: 839-845.

Eleuteri, Ermanno, et al. 2009. "Increased Nitrotyrosine Plasma Levels in Relation to Systemic Markers of Inflammation and Myeloperoxidase in Chronic Heart Failure." *International Journal of Cardiology* 135, no. 3 (7/10/): 386-390. http://dx.doi.org/http://dx.doi.org/10.1016/j.ijcard.2008.11.013.

Ellison, R. T., T. J. Giehl, and F. M. LaForce. 1988. "Damage of the Outer Membrane of Enteric Gram-Negative Bacteria by Lactoferrin and Transferrin." *Infection and Immunity* 56, no. 11: 2774-2781. http://www.ncbi.nlm.nih.gov/pmc/articles/PMC259649/.

Ellison, Rt D., Theodore J. Giehl, and F. Marc LaForce. 1988. "Damage of the Outer Membrane of Enteric Gram-Negative Bacteria by Lactoferrin and Transferrin." *Infection and Immunity* 56, no. 11: 2774-2781.

Erdei, Janos, Arne Forsgren, and A. S. Naidu. 1994. "Lactoferrin Binds to Porins Ompf and Ompc in Escherichia Coli." *Infection and immunity* 62, no. 4: 1236-1240.

Estillore, Armando D., Jonathan V. Trueblood, and Vicki H. Grassian. 2016. "Atmospheric Chemistry of Bioaerosols: Heterogeneous and Multiphase Reactions with Atmospheric Oxidants and Other Trace Gases." *Chemical Science* 7, no. 11: 6604-6616.

Fahrbach, Kelly M., et al. 2013. "Differential Binding of Igg and Iga to Mucus of the Female Reproductive Tract." *PloS one* 8, no. 10: e76176.

Farnaud, Sebastien, and Robert W. Evans. 2003. "Lactoferrin—a Multifunctional Protein with Antimicrobial Properties." *Molecular immunology* 40, no. 7: 395-405.

Ferrante, Robert J., et al. 1997. "Increased 3-Nitrotyrosin e and Oxidative Damage in Mice with a Human Copper/Zinc Superoxide Dismutase Mutation." *Annals of neurology* 42, no. 3: 326-334.

Flanagan, J. L., and M. D. P. Willcox. 2009. "Role of Lactoferrin in the Tear Film." *Biochimie* 91, no. 1: 35-43.

Franze, Thomas, et al. 2003. "Enzyme Immunoassays for the Investigation of Protein Nitration by Air Pollutants." *Analyst* 128, no. 7: 824-831.

---. 2005. "Protein Nitration by Polluted Air." *Environmental science & technology* 39, no. 6: 1673-1678.

Franzoni, F., et al. 2006a. "An in Vitro Study on the Free Radical Scavenging Capacity of Ergothioneine: Comparison with Reduced Glutathione, Uric Acid and Trolox." *Biomedicine & pharmacotherapy* 60, no. 8: 453-457.

Franzoni, F., et al. 2006b. "An In vitro Study On the free Radical Scavenging Capacity Of ergothioneine: Comparison with Reduced Glutathione, Uric Acid And trolox." *Biomedicine & Pharmacotherapy* 60, no. 8 (2006/09/01/): 453-457. http://dx.doi.org/https://doi.org/10.1016/j.biopha.2006.07.015.

García-Montoya, Isui Abril, et al. 2012. "Lactoferrin a Multiple Bioactive Protein: An Overview." *Biochimica et Biophysica Acta (BBA) - General Subjects* 1820, no. 3

(2012/03/01/): 226-236. http://dx.doi.org/https://doi.org/10.1016/j.bbagen.2011.06.018.

Goldstein, Sara, and Gabor Merényi. 2008. "Chapter Four - the Chemistry of Peroxynitrite: Implications for Biological Activity." In *Methods in Enzymology*, edited by Robert K. Poole, vol 436, 49-61: Academic Press.

González-Chávez, Susana A., Sigifredo Arévalo-Gallegos, and Quintín Rascón-Cruz. 2009. "Lactoferrin: Structure, Function and Applications." *International journal of antimicrobial agents* 33, no. 4: 301-e1.

Good, Paul F., et al. 1998. "Protein Nitration in Parkinson'S Disease." *Journal of Neuropathology & Experimental Neurology* 57, no. 4: 338. http://jnen.oxfordjournals.org/content/57/4/338.abstract.

Gow, Andrew J., et al. 1996. "Effects of Peroxynitrite-Induced Protein Modifications on Tyrosine Phosphorylation and Degradation." *FEBS letters* 385, no. 1-2: 63-66.

Grau Armin, J., et al. 2001. "Assessment of Plasma Lactoferrin in Parkinson's Disease." *Movement Disorders* 16, no. 1: 131-134. Accessed 2018/04/13. http://dx.doi.org/10.1002/1531-8257(200101)16:1<131::AID-MDS1008>3.0.CO;2-O.

Greenacre, Stan A. B., and Harry Ischiropoulos. 2001. "Tyrosine Nitration: Localisation, Quantification, Consequences for Protein Function and Signal Transduction." *Free Radical Research* 34, no. 6 (2001/01/01): 541-581. http://dx.doi.org/10.1080/10715760100300471.

Hamilton, David H., et al. 2009. "Using Proteins in a Bioinorganic Laboratory Experiment: Iron Loading and Removal from Transferrin." *J. Chem. Educ* 86, no. 8: 969.

Hartman, Philip E. 1990. "[32] Ergothioneine as Antioxidant." In *Methods in Enzymology*, vol 186, 310-318: Academic Press.

Håversen, Liliana A., et al. 2000. "Human Lactoferrin and Peptides Derived from a Surface-Exposed Helical Region Reduce Experimental Escherichia Coli Urinary Tract Infection in Mice." *Infection and Immunity* 68, no. 10: 5816-5823.

Heumann, Didier, and Thierry Roger. 2002. "Initial Responses to Endotoxins and Gram-Negative Bacteria." *Clinica Chimica Acta* 323, no. 1 (2002/09/01/): 59-72. http://dx.doi.org/https://doi.org/10.1016/S0009-8981(02)00180-8.

Hinson, Jack A., et al. 2000. "Western Blot Analysis for Nitrotyrosine Protein Adducts in Livers of Saline-Treated and Acetaminophen-Treated Mice." *Toxicological sciences* 53, no. 2: 467-473.

Hutchens, T. William, Bo Lönnerdal, and Sylvia V. Rumball. 2012. *Lactoferrin: Structure and Function*. Vol. 357: Springer Science & Business Media.

Ignarro, Louis, and Ferid Murad. 1995. "Nitric Oxide: Biochemistry, Molecular Biology, and Therapeutic Implications."

Ischiropoulos, Harry. 1998. "Biological Tyrosine Nitration: A Pathophysiological Function of Nitric Oxide and Reactive Oxygen Species." *Archives of biochemistry and biophysics* 356, no. 1: 1-11.

Ischiropoulos, Harry, Ling Zhu, and Joseph S. Beckman. 1992. "Peroxynitrite Formation from Macrophage-Derived Nitric Oxide." *Archives of Biochemistry and Biophysics* 298, no. 2 (1992/11/01): 446-451. http://dx.doi.org/http://dx.doi.org/10.1016/0003-9861(92)90433-W.

Jamshad, Khan, et al. 1998. "3-Nitrotyrosine in the Proteins of Human Plasma Determined by an Elisa Method." *Biochemical Journal* 330, no. 2: 795-801.

Jankowski, Joseph J., David J. Kieber, and Kenneth Mopper. 1999. "Nitrate and Nitrite Ultraviolet Actinometers." *Photochemistry and Photobiology* 70, no. 3: 319-328.

Japelj, Boštjan, et al. 2005. "Structural Origin of Endotoxin Neutralization and Antimicrobial Activity of a Lactoferrin-Based Peptide." *Journal of Biological Chemistry* 280, no. 17: 16955-16961.

Jenssen, Håvard, and Robert E. W. Hancock. 2009. "Antimicrobial Properties of Lactoferrin." *Biochimie* 91, no. 1: 19-29.

Johnson, Michael E., and Paul J. Murphy. 2004. "Changes in the Tear Film and Ocular Surface from Dry Eye Syndrome." *Progress in Retinal and Eye Research* 23, no. 4 (7//): 449-474. http://dx.doi.org/http://dx.doi.org/10.1016/j.preteyeres.2004.04.003.

Jorgensen, James H., and John D. Turnidge. 2015. "Susceptibility Test Methods: Dilution and Disk Diffusion Methods." In *Manual of Clinical Microbiology, Eleventh Edition*, 1253-1273: American Society of Microbiology.

Kalmar, John R., and Roland R. Arnold. 1988. "Killing of Actinobacillus Actinomycetemcomitans by Human Lactoferrin." *Infection and immunity* 56, no. 10: 2552-2557.

Kampf, Christopher J., et al. 2015. "Protein Cross-Linking and Oligomerization through Dityrosine Formation Upon Exposure to Ozone." *Environmental science & technology* 49, no. 18: 10859-10866.

Kang, Joo Hyun, et al. 1996a. "Structure–Biological Activity Relationships of 11-Residue Highly Basic Peptide Segment of Bovine Lactoferrin." *Chemical Biology & Drug Design* 48, no. 4: 357-363.

---. 1996b. "Structure–Biological Activity Relationships of 11-Residue Highly Basic Peptide Segment of Bovine Lactoferrin." *International journal of peptide and protein research* 48, no. 4: 357-363.

Kanyshkova, T. G., V. N. Buneva, and G. A. Nevinsky. 2001. "Lactoferrin and Its Biological Functions." *Biochemistry (Moscow)* 66, no. 1: 1-7.

Kelly, S. M., T. J. Jess, and N. C. Price. 2005. "How to Study Proteins by Circular Dichroism." *Biochim Biophys Acta* 1751, no. 2 (Aug 10): 119-39. http://dx.doi.org/10.1016/j.bbapap.2005.06.005.

Kijlstra, A., S. H. Jeurissen, and K. M. Koning. 1983. "Lactoferrin Levels in Normal Human Tears." *British Journal of Ophthalmology* 67, no. 3: 199-202. http://dx.doi.org/10.1136/bjo.67.3.199.

Kim, J. C., et al. 2002. "The Role of Nitric Oxide in Ocular Surface Diseases." In *Lacrimal Gland, Tear Film, and Dry Eye Syndromes 3*, 687-695: Springer.

Krewulak, Karla D., and Hans J. Vogel. 2008. "Structural Biology of Bacterial Iron Uptake." *Biochimica et Biophysica Acta (BBA) - Biomembranes* 1778, no. 9 (9//): 1781-1804. http://dx.doi.org/http://dx.doi.org/10.1016/j.bbamem.2007.07.026.

Kronman, M. J., and L. G. Holmes. 1971. "The Fluorescence of Native, Denatured and Reduced-Denatured Proteins." *Photochemistry and Photobiology* 14, no. 2: 113-134.

Kutila, T., et al. 2003. "Antibacterial Effect of Bovine Lactoferrin against Udder Pathogens." *Acta Veterinaria Scandinavica* 44, no. 1 (2003/03/31): 35. http://dx.doi.org/10.1186/1751-0147-44-35.

Laemmli, Ulrich K. 1970. "Cleavage of Structural Proteins During the Assembly of the Head of Bacteriophage T4." *nature* 227, no. 5259: 680-685.

Lakey, Pascale S. J., et al. 2016. "Chemical Exposure-Response Relationship between Air Pollutants and Reactive Oxygen Species in the Human Respiratory Tract." *Scientific reports* 6: 32916.

Lakowicz, Joseph R. 2013. *Principles of Fluorescence Spectroscopy*: Springer Science & Business Media.

Latorre, Daniela, et al. 2010. "Reciprocal Interactions between Lactoferrin and Bacterial Endotoxins and Their Role in the Regulation of the Immune Response." *Toxins* 2, no. 1. http://dx.doi.org/10.3390/toxins2010054.

Lönnerdal, B., and S. Iyer. 1995. "Lactoferrin: Molecular Structure and Biological Function." *Annual review of nutrition* 15, no. 1: 93-110.

Lundblad, Roger L. 2018. *Chemical Reagents for Protein Modification: Volume I*: CRC press.

Masson, P. L., and J. F. Heremans. 1971. "Lactoferrin in Milk from Different Species." *Comparative Biochemistry and Physiology Part B: Comparative Biochemistry* 39, no. 1 (5/15/): 119-IN13. http://dx.doi.org/http://dx.doi.org/10.1016/0305-0491(71)90258-6.

Masson, P. L., J. F. Heremans, and C. H. Dive. 1966. "An Iron-Binding Protein Common to Many External Secretions." *Clinica Chimica Acta* 14, no. 6: 735-739.

Melville, Donald B., William H. Horner, and Rose Lubschez. 1954. "Tissue Ergothioneine." *Journal of Biological Chemistry* 206, no. 1: 221-228.

Metz-Boutigue, Marie- Hélène, et al. 1984. "Human Lactotransferrin: Amino Acid Sequence and Structural Comparisons with Other Transferrins." *European Journal of Biochemistry* 145, no. 3: 659-676.

Meyer, Arne, Christian Betzel, and Marc Pusey. 2015. "Latest Methods of Fluorescence-Based Protein Crystal Identification." *Acta Crystallographica Section F: Structural Biology Communications* 71, no. 2: 121-131.

Micsonai, A., et al. 2015. "Accurate Secondary Structure Prediction and Fold Recognition for Circular Dichroism Spectroscopy." *Proc Natl Acad Sci U S A* 112, no. 24 (Jun 16): E3095-103. http://dx.doi.org/10.1073/pnas.1500851112.

Moreno-Navarrete, J. M., et al. 2009. "Decreased Circulating Lactoferrin in Insulin Resistance and Altered Glucose Tolerance as a Possible Marker of Neutrophil Dysfunction in Type 2 Diabetes." *The Journal of Clinical Endocrinology & Metabolism* 94, no. 10: 4036-4044. http://dx.doi.org/10.1210/jc.2009-0215.

Nakaki, T., and T. Fujii. 1999. "Nitration Modifying Function of Proteins, Hormones and Neurotransmitters." *Jpn J Pharmacol* 79, no. 2 (Feb): 125-9.

Nicholson, Hale, et al. 1997. "Mutagenesis of the Histidine Ligand in Human Lactoferrin: Iron Binding Properties and Crystal Structure of the Histidine-253 → Methionine Mutant." *Biochemistry* 36, no. 2 (1997/01/01): 341-346. http://dx.doi.org/10.1021/bi961908y.

Novaes, Priscila, et al. 2007. "Ambient Levels of Air Pollution Induce Goblet-Cell Hyperplasia in Human Conjunctival Epithelium." *Environmental health perspectives* 115, no. 12: 1753.

Novaes, Priscila, et al. 2010a. "The Effects of Chronic Exposure to Traffic Derived Air Pollution on the Ocular Surface." *Environmental research* 110, no. 4: 372-374.

Novaes, Priscila, et al. 2010b. "The Effects of Chronic Exposure to Traffic Derived Air Pollution on the Ocular Surface." *Environmental Research* 110, no. 4 (5//): 372-374. http://dx.doi.org/http://dx.doi.org/10.1016/j.envres.2010.03.003.

Nuijens, Jan H., Patrick H. C. van Berkel, and Floyd L. Schanbacher. 1996. "Structure and Biological Actions of Lactoferrin." *Journal of Mammary Gland Biology and Neoplasia* 1, no. 3 (1996/07/01): 285-295. http://dx.doi.org/10.1007/BF02018081.

Ogino, Keiki, and Da-Hong Wang. 2007. "Biomarkers of Oxidative/Nitrosative Stress: An Approach to Disease Prevention." *Acta Medica Okayama* 61, no. 4: 181.

Ohashi, Yoshiki, et al. 2003. "Abnormal Protein Profiles in Tears with Dry Eye Syndrome." *American Journal of Ophthalmology* 136, no. 2 (8//): 291-299. http://dx.doi.org/http://dx.doi.org/10.1016/S0002-9394(03)00203-4.

Oram, J. D., and B. Reiter. 1968. "Inhibition of Bacteria by Lactoferrin and Other Iron-Chelating Agents." *Biochimica et Biophysica Acta (BBA)-General Subjects* 170, no. 2: 351-365.

Pan, Y., et al. 2007. "Comparison of the Effects of Acylation and Amidation on the Antimicrobial and Antiviral Properties of Lactoferrin." *Letters in applied microbiology* 44, no. 3: 229-234.

Pannala, Ananthsekher, et al. 1998. "Inhibition of Peroxynitrite Dependent Tyrosine Nitration by Hydroxycinnamates: Nitration or Electron Donation?" *Free Radical Biology and Medicine* 24, no. 4 (1998/03/01/): 594-606. http://dx.doi.org/https://doi.org/10.1016/S0891-5849(97)00321-3.

Park, Gun Sic, et al. 2001. "The Role of Nitric Oxide in Ocular Surface Diseases." *Korean Journal of Ophthalmology* 15, no. 2: 59-66.

Patel, Rakesh P., et al. 1999. "Biological Aspects of Reactive Nitrogen Species." *Biochimica et Biophysica Acta (BBA) - Bioenergetics* 1411, no. 2–3 (5/5/): 385-400. http://dx.doi.org/http://dx.doi.org/10.1016/S0005-2728(99)00028-6.

Pfeiffer, Silvia, et al. 2001. "Protein Tyrosine Nitration in Cytokine-Activated Murine Macrophages Involvement of a Peroxidase/Nitrite Pathway Rather Than Peroxynitrite." *Journal of Biological Chemistry* 276, no. 36: 34051-34058.

Pöhlker, C., J. A. Huffman, and U. Pöschl. 2012. "Autofluorescence of Atmospheric Bioaerosols–Fluorescent Biomolecules and Potential Interferences." *Atmospheric Measurement Techniques* 5, no. 1: 37-71.

Prabha, J. Lakshmi. 2014. "Tear Secretion-a Short Review."

Radi, Rafael. 2013. "Protein Tyrosine Nitration: Biochemical Mechanisms and Structural Basis of Its Functional Effects." *Accounts of chemical research* 46, no. 2 (11/16): 550-559. http://dx.doi.org/10.1021/ar300234c.

Rageh, Abrar A., et al. 2016. "Lactoferrin Expression in Human and Murine Ocular Tissue." *Current eye research* 41, no. 7: 883-889.

Rahman, Irfan, et al. 2003. "Ergothioneine Inhibits Oxidative Stress-and Tnf-A-Induced Nf-Kb Activation and Interleukin-8 Release in Alveolar Epithelial Cells." *Biochemical and biophysical research communications* 302, no. 4: 860-864.

Rajasekariah, G. H., et al. 2003. "Assessment of Assay Sensitivity and Precision in a Malaria Antibody Elisa." *J Immunoassay Immunochem* 24, no. 1: 89-112. http://dx.doi.org/10.1081/ias-120018471.

Reinmuth-Selzle, Kathrin, et al. 2014. "Nitration of the Birch Pollen Allergen Bet V 1.0101: Efficiency and Site-Selectivity of Liquid and Gaseous Nitrating Agents." *Journal of proteome research* 13, no. 3: 1570-1577.

Reinmuth-Selzle, Kathrin, et al. 2017. "Air Pollution and Climate Change Effects on Allergies in the Anthropocene: Abundance, Interaction, and Modification of

Allergens and Adjuvants." *Environmental Science & Technology* 51, no. 8: 4119-4141.

Repine, John E., and Nancy D. Elkins. 2012. "Effect of Ergothioneine on Acute Lung Injury and Inflammation in Cytokine Insufflated Rats." *Preventive Medicine* 54 (2012/05/01/): S79-S82. http://dx.doi.org/https://doi.org/10.1016/j.ypmed.2011.12.006.

Riordan, James F., Mordechai Sokolovsky, and Bert L. Vallee. 1966. "Tetranitromethane. A Reagent for the Nitration of Tyrosine and Tyrosyl Residues of Proteins1." *Journal of the American Chemical Society* 88, no. 17 (1966/09/01): 4104-4105. http://dx.doi.org/10.1021/ja00969a046.

Roşeanu, Anca, Maria Damian, and Robert W. Evans. 2010. "Mechanisms of the Antibacterial Activity of Lactoferrin and Lactoferrin-Derived Peptides." *Rom. J. Biochem* 47, no. 2: 203-209.

Saidel, L. J., A. R. Goldfarb, and S. Waldman. 1952. "The Absorption Spectra of Amino Acids in the Region Two Hundred to Two Hundred and Thirty Millimicrons." *J Biol Chem* 197, no. 1 (May): 285-91.

Savvides, Savvas N., et al. 2002. "Crystal Structure of the Antioxidant Enzyme Glutathione Reductase Inactivated by Peroxynitrite." *Journal of Biological Chemistry* 277, no. 4: 2779-2784.

Saxena, Rohit, et al. 2003. "Impact of Environmental Pollution on the Eye." *Acta Ophthalmologica Scandinavica* 81, no. 5: 491-494. http://dx.doi.org/10.1034/j.1600-0420.2003.00119.x.

Selzle, Kathrin, et al. 2013. "Determination of Nitration Degrees for the Birch Pollen Allergen Bet V 1." *Analytical and Bioanalytical Chemistry* 405, no. 27 (2013//): 8945-8949. http://dx.doi.org/10.1007/s00216-013-7324-0.

Servillo, Luigi, Nunzia D'Onofrio, and Maria Luisa Balestrieri. 2017. "Ergothioneine Antioxidant Function: From Chemistry to Cardiovascular Therapeutic Potential." *Journal of Cardiovascular Pharmacology* 69, no. 4. https://journals.lww.com/cardiovascularpharm/Fulltext/2017/04000/Ergothioneine_Antioxidant_Function___From.1.aspx.

Shimmura, Shigeto, et al. 1996. "Subthreshold Uv Radiation-Induced Peroxide Formation in Cultured Corneal Epithelial Cells: The Protective Effects of Lactoferrin." *Experimental eye research* 63, no. 5: 519-526.

Shiraiwa, M., K. Selzle, and U. Poschl. 2012. "Hazardous Components and Health Effects of Atmospheric Aerosol Particles: Reactive Oxygen Species, Soot, Polycyclic Aromatic Compounds and Allergenic Proteins." *Free Radic Res* 46, no. 8 (Aug): 927-39. http://dx.doi.org/10.3109/10715762.2012.663084.

Shiraiwa, Manabu, et al. 2017. "Aerosol Health Effects from Molecular to Global Scales." *Environmental Science & Technology* 51, no. 23 (2017/12/05): 13545-13567. http://dx.doi.org/10.1021/acs.est.7b04417.

Shires, Thomas K., et al. 1997. "Ergothioneine Distribution in Bovine and Porcine Ocular Tissues." *Comparative Biochemistry and Physiology Part C: Pharmacology, Toxicology and Endocrinology* 117, no. 1: 117-120.

Shuker, D. E., et al. 1993. "Urinary Markers for Measuring Exposure to Endogenous and Exogenous Alkylating Agents and Precursors." *Environmental Health Perspectives* 99: 33-37. http://www.ncbi.nlm.nih.gov/pmc/articles/PMC1567034/.

Sies, Helmut, and Hiroshi Masumoto. 1996. "Ebselen as a Glutathione Peroxidase Mimic and as a Scavenger of Peroxynitrite." In *Advances in Pharmacology*, vol 38, 229-246: Elsevier.

Sies, Helmut, et al. 1997. "Glutathione Peroxidase Protects against Peroxynitrite-Mediated Oxidations a New Function for Selenoproteins as Peroxynitrite Reductase." *Journal of Biological Chemistry* 272, no. 44: 27812-27817.

Sipponen, Taina, et al. 2008. "Crohn's Disease Activity Assessed by Fecal Calprotectin and Lactoferrin: Correlation with Crohn's Disease Activity Index and Endoscopic Findings." *Inflammatory bowel diseases* 14, no. 1: 40-46.

Sokolovsky, Mordechai, Miriam Fuchs, and James F. Riordan. 1970. "Reaction of Tetranitromethane with Tryptophan and Related Compounds." *FEBS letters* 7, no. 2: 167-170.

Sokolovsky, Mordechai, James F. Riordan, and Bert L. Vallee. 1966. "Tetranitromethane. A Reagent for the Nitration of Tyrosyl Residues in Proteins." *Biochemistry* 5, no. 11: 3582-3589.

Spitznagel, John K., et al. 1974. "Character of Azurophil and Specific Granules Purified from Human Polymorphonuclear Leukocytes." *Laboratory Investigation* 30, no. 6: 774-785.

Steijns, Jan M., and A. C. M. van Hooijdonk. 2000. "Occurrence, Structure, Biochemical Properties and Technological Characteristics of Lactoferrin." *British Journal of Nutrition* 84, no. S1: 11-17. http://dx.doi.org/10.1017/S0007114500002191.

Stookey, Lawrence L. 1970. "Ferrozine---a New Spectrophotometric Reagent for Iron." *Analytical chemistry* 42, no. 7: 779-781.

Strøm, Morten B., Øystein Rekdal, and John S. Svendsen. 2002. "Antimicrobial Activity of Short Arginine- and Tryptophan-Rich Peptides." *Journal of Peptide Science* 8, no. 8: 431-437. http://dx.doi.org/10.1002/psc.398.

ter Steege, Jessica C. A., et al. 1998. "Nitrotyrosine in Plasma of Celiac Disease Patients as Detected by a New Sandwich Elisa." *Free Radical Biology and Medicine* 25, no. 8: 953-963.

Teuwissen, Bruno, et al. 1973. "Metal-Combining Properties of Human Lactoferrin." *European Journal of Biochemistry* 35, no. 2: 366-371. http://dx.doi.org/10.1111/j.1432-1033.1973.tb02848.x.

Thiagarajan, Geetha, et al. 2004. "Peroxynitrite Reaction with Eye Lens Proteins: A-Crystallin Retains Its Activity Despite Modification." *Investigative Ophthalmology & Visual Science* 45, no. 7: 2115-2121. http://dx.doi.org/10.1167/iovs.03-0929.

Tiffany, J. M. 2003. "Tears in Health and Disease." *Eye (Lond)* 17, no. 8 (Nov): 923-6. http://dx.doi.org/10.1038/sj.eye.6700566.

Torricelli, André A. M., et al. 2013. "Correlation between Signs and Symptoms of Ocular Surface Dysfunction and Tear Osmolarity with Ambient Levels of Air Pollution in a Large Metropolitan Area." *Cornea* 32, no. 4: e11-e15.

Torricelli, André Augusto Miranda, et al. 2014. "Effects of Ambient Levels of Traffic-Derived Air Pollution on the Ocular Surface: Analysis of Symptoms, Conjunctival Goblet Cell Count and Mucin 5ac Gene Expression." *Environmental Research* 131 (5//): 59-63. http://dx.doi.org/http://dx.doi.org/10.1016/j.envres.2014.02.014.

Torricelli, André Augusto Miranda, et al. 2011. "Ocular Surface Adverse Effects of Ambient Levels of Air Pollution." *Arquivos Brasileiros de Oftalmologia* 74, no. 5: 377-381.

Tsang, Anthony H. K., and Kenny K. K. Chung. 2009. "Oxidative and Nitrosative Stress in Parkinson's Disease." *Biochimica et Biophysica Acta (BBA) - Molecular Basis*

of Disease 1792, no. 7 (7//): 643-650. http://dx.doi.org/http://dx.doi.org/10.1016/j.bbadis.2008.12.006.

Turko, Illarion V., and Ferid Murad. 2002. "Protein Nitration in Cardiovascular Diseases." *Pharmacological reviews* 54, no. 4: 619-634.

Uversky, Vladimir N., et al. 2005. "Effects of Nitration on the Structure and Aggregation of A-Synuclein." *Molecular Brain Research* 134, no. 1 (2005/03/24/): 84-102. http://dx.doi.org/https://doi.org/10.1016/j.molbrainres.2004.11.014.

Valenti, P., and Giovanni Antonini. 2005. *Lactoferrin: An Important Host Defence against Microbial and Viral Attack*. Vol. 62.

Valko, Marian, et al. 2007. "Free Radicals and Antioxidants in Normal Physiological Functions and Human Disease." *The International Journal of Biochemistry & Cell Biology* 39, no. 1 (//): 44-84. http://dx.doi.org/http://dx.doi.org/10.1016/j.biocel.2006.07.001.

Vincent, J. P., M. Lazdunski, and M. Delaage. 1970. "On the Use of Tetranitromethane as a Nitration Reagent. The Reaction of Phenol Side-Chains in Bovine and Porcine Trypsinogens and Trypsins." *Eur J Biochem* 12, no. 2 (Feb): 250-7.

Vorland, Lars H. 1999. "Lactoferrin: A Multifunctional Glycoprotein." *APMIS* 107, no. 7-12: 971-981. http://dx.doi.org/10.1111/j.1699-0463.1999.tb01499.x.

Wakamatsu, Tais Hitomi, Murat Dogru, and Kazuo Tsubota. 2008. "Tearful Relations: Oxidative Stress, Inflammation and Eye Diseases." *Arquivos brasileiros de oftalmologia* 71, no. 6: 72-79.

Walcott, Benjamin. 1998. "The Lacrimal Gland and Its Veil of Tears." *Physiology* 13, no. 2: 97. http://physiologyonline.physiology.org/content/13/2/97.abstract.

Ward, P. P., X. Zhou, and O. M. Conneely. 1996. "Cooperative Interactions between the Amino- and Carboxyl-Terminal Lobes Contribute to the Unique Iron-Binding Stability of Lactoferrin." *J Biol Chem* 271, no. 22 (May 31): 12790-4.

Ward, Pauline P., Sonia Uribe-Luna, and Orla M. Conneely. 2002. "Lactoferrin and Host Defense." *Biochemistry and Cell Biology* 80, no. 1: 95-102.

Wiegand, Irith, Kai Hilpert, and Robert E. W. Hancock. 2008. "Agar and Broth Dilution Methods to Determine the Minimal Inhibitory Concentration (Mic) of Antimicrobial Substances." *Nature protocols* 3, no. 2: 163.

Wiseman, Helen, and Barry Halliwell. 1996. "Damage to DNA by Reactive Oxygen and Nitrogen Species: Role in Inflammatory Disease and Progression to Cancer." *Biochemical Journal* 313, no. Pt 1: 17.

Yeo, Woon-Seok, et al. 2008. "Nitrosative Protein Tyrosine Modifications: Biochemistry and Functional Significance." *BMB reports* 41, no. 3: 194-203.

Zhou, Lei, et al. 2006. "Characterisation of Human Tear Proteins Using High-Resolution Mass Spectrometry." *ANNALS-ACADEMY OF MEDICINE SINGAPORE* 35, no. 6: 400.

Žitňanová, Ingrid, et al. 2004. "Uric Acid and Allantoin Levels in Down Syndrome: Antioxidant and Oxidative Stress Mechanisms?" *Clinica Chimica Acta* 341, no. 1-2: 139-146.

Appendix A: Supplementary material for chapter two

A.1 Materials and reagents

Human milk lactoferrin (LF; L0520), bovine serum albumin (BSA; A7030), tetranitromethane (TNM; T25003), Tween®20 buffer (P1379), Trizma base (Tris-HCl; T1503), sulfuric acid (H_2SO_4; 320501), sodium phosphate dibasic (RES20908-A702X), potassium chloride (P9333), sodium chloride (S9625), potassium phosphate monobasic (P5655), sodium carbonate (S7795), sodium bicarbonate (S5761), and ethanol (245119) were obtained from Sigma Aldrich (USA). Sodium peroxynitrite (NaONOO; 516620) and Amicon Ultra centrifugal filters (30 kDa, 4 mL size; UFC803024) were purchased from Calbiochem (USA). The 1-step ultra 3,3',5,5'-tetramethylbenzidine substrate (TMB; 34028) and bicinchoninic acid assay (BCA; 23225) for total protein quantification were purchased from ThermoFisher Scientific (USA). Flat-bottom, 96-microwell plates (untreated; 333-8013-01F) and sterile sealing tape (ST-3095) were obtained from Life Science Products (USA). A biotinylated, mouse monoclonal to nitrotyrosine antibody (anti-NTyr; ab24496, clone number CC22.8C7.3), streptavidin horseradish peroxidase (HRP; ab7403), and non-conjugated goat polyclonal anti-human lactoferrin antibody (anti-LF; ab77548) were obtained from Abcam (UK). 1.0 mL quartz cuvette with 10 mm path length (MF-W-10-LID) was purchased from Science Outlet (USA).

Buffers used were: phosphate-buffered saline (PBS; 8.1 mM sodium phosphate dibasic, 0.8 mM sodium phosphate monobasic, 1.3 mM potassium chloride, and

68.0 mM sodium chloride at pH 7.4), Tris-HCl buffer (Tris; 0.1 mM at pH 8.0), and carbonate buffer (29.0 mM sodium carbonate, 71.0 mM sodium bicarbonate at pH 9.6).

The volumes of peroxynitrite used for production of NLF_{ONOO^-} samples discussed in Section A. 2. 1 were 5.66, 11.36, 17.05, 22.73, 34.10, 45.46, and 56.67 µL. Similarly, the volumes of TNM used for production of NLF_{TNM} discussed in Section A. 2. 2 were 0.29, 0.58, 0.86, 1.16, 1.72, 2.32, and 2.89 µL. These values correspond to molar ratios of nitrating agent to tyrosine ($ONOO^-$/Tyr) or (TNM/Tyr) of 10/1, 20/1, 30/1, 40/1, 60/1, 80/1, and 100/1. The volumes of TNM used for production of NBSA discussed in Section A. 2. 4 and S.6.1 were 0.95 and 7.33 µL of 6/1 and 14/1.

A.2 Micropipette precision

The maximum precision reported for the variable volume, single channel micropipettes used (VWR; USA) is ± 1.5-0.3% for the 2-20 µL pipette (89079-964), ± 0.6-0.2% for the 20-200 µL pipette (89079-970), and ± 0.4-0.15% for the 100-1000 µL (89079-974). The 12-channel micropipette (4662030) has a maximum precision of ± 2.0-0.3% for the 30-300 µL purchased from (Thermo scientific, USA). The coefficient of variation for the small transfer pipette with variable volume 0.1-2.5 µL (704769; Transferpette-S, USA) is 0.7%, and 0.5% for the 0.5-10 µL volume pipette (704770).

A.3 Purification of nitration reaction products

After nitration reactions were completed, selected samples were analysed before and after purification. 1.0 mL of NLF was purified using an Amicon Ultra centrifugal filter with a 30 kDa cut-off membrane and rinsed twice with 1.0 mL PBS buffer. The total concentration of LF in each sample was determined using a bicinchoninic acid assay, following kit instructions. The absorbance of each solution was measured in triplicate, and the protein concentration of each solution was determined by comparing against an eight point calibration curve generated using BSA standard in a concentration range between 25 and 2000 μg mL^{-1}.

A.4 Sandwich ELISA for optimization of polyclonal to lactoferrin antibody

For the sandwich ELISA procedure, goat polyclonal to lactoferrin non-conjugated antibody was used as the capture antibody and mouse monoclonal to nitrotyrosine biotinylated antibody was used as the detector antibody. Capture antibody was diluted in carbonate buffer in several dilution ratios (1:250, 1:500, and 1:1000). Three microwells were coated with 50 μL of each capture antibody dilution, and the plate was incubated at 4°C for 17 hours. The plate was washed and blocked as described in Section A. 2. 6.

NLF (40/1 TNM/Tyr) was serially diluted into blocking buffer producing NLF solutions at seven concentrations (0.19, 0.39, 0.78, 1.56, 3.12, 6.25, and 12.5 μg mL^{-1}). Thus, each of seven concentrations of NLF was aliquoted into 9 wells (three capture antibody dilution ratios X triplicate measurements) for ELISA treatment. After incubation and washing, 50 μL of each NLF solution was added in triplicate to

wells processed with capture antibody in each of the three dilution ratios and incubated for 2 hour at RT. Blocking buffer was added separately to three wells as a blank measurement. After washing, 50 µL the detector antibody, diluted 1:100 in blocking buffer, was added to each well and incubated for at room temperature for 1 hour. The assay was analysed spectroscopically using the procedure detailed in Section A. 2. 6.

The polyclonal anti-LF capture antibody recognizes a specific peptide sequence (432-444: C-ENYKSQQSSDPDP) in the LF protein. The amino acid nomenclature used here: E (glutamic acid), N (asparagine), Y (tyrosine), K (lysine), S (serine), Q (glutamine), D (aspartic acid), P (proline).

A.5 Purification is not required before quantification

NLF produced using TNM also contains nitroformate as by-product, which has the same absorbance wavelength as NTyr (350 nm), which adds ambiguity to the interpretation of the NTyr spectral results. Figure A. 7 shows UV-vis absorbance and sandwich ELISA results for both purified and non-purified reaction products. Products before and after purification show similar trends. The absorbance intensity was slightly reduced after purification due to removing nitroformate by-product, but the sandwich ELISA result remain the same. We conclude that the purification process is not required for the sandwich ELISA process to achieve quantitative results.

A.6 Development and optimization of antibody usage

A.6.1 Anti-NTyr detector antibodies (polyclonal or monoclonal)

The initial step in the development of the NLF sandwich ELISA was to choose the anti-NTyr detector antibodies. We used direct ELISA to test nitrated bovine serum albumin (NBSA) using two different biotinylated nitrotyrosine antibodies: mouse monoclonal nitrotyrosine (ab24496) and goat polyclonal nitrotyrosine (ab27646). The monoclonal anti-NTyr antibody has increased specificity to binding at a specific epitope, compared to the polyclonal antibody that allows binding at multiple epitope, and thus allows sensitive quantification of antigens that contain the monoclonal epitope. NBSA was nitrated using two concentrations of excess nitrating agent (molar ratio of excess TNM to tyrosine of 6/1 and 14/1). The monoclonal anti-NTyr exhibited higher sensitivity than the polyclonal anti-NTyr to detect NBSA produced at both TNM concentrations, as shown in Figure A. 1.

A.6.2 Anti-LF capture antibody

The polyclonal antibody (ab77548) considered here for the capture portion of the assay contains a peptide sequence that includes only one tyrosine residue, which is included in the iron-binding site (Steijns, et al. 2000). Teuwissen et al. reported that iron binding of LF was not reduced after nitration, which suggests that the tyrosine residues involved in the iron binding region will not be nitrated and, by extension, will not affect the binding to this specific antibody (Teuwissen, et al. 1973). The antibody under consideration had previously shown a successful binding response for human samples

in immunoassays such as western blot, in human peripheral mononucleocytes, and using immunohistochemical assays for human tissues (Fahrbach, et al. 2013; de la Rosa, et al. 2008). Additionally, this capture antibody matches as a pair antibody to the anti-NTyr detector antibody previously chosen (Section A. 6. 1). Based on these piece of literature support, we tested the capture antibody via the ELISA. The results confirmed detection of NLF, supporting the assumptions stated above. A.6.3 Antibody sequence for the sandwich ELISA

The polyclonal anti-LF contains a pool of immunogenic antibodies for the specific peptide sequence listed above (Section A. 4). This allows the anti-LF antibody to recognize the specific peptide epitope in multiple arrangements, thus increasing the probability that binding occurs between anti-LF and LF.

Following the testing of the individual antibodies, the amplification of anti-LF was tested for use in the sandwich ELISA using combinations of four antibodies: [a] goat polyclonal capture anti-LF (ab77548), [b] rabbit polyclonal detector anti-LF (ab25811), [c] rabbit polyclonal capture anti-NTyr (ab42789), and [d] mouse monoclonal detector anti-Ntyr (ab24496). The following antibody combinations were tested:

(1) capture anti-LF [a] and detector anti-LF [b]

(2) capture anti-NTyr [c] and detector anti-NTyr [d]

(3) capture anti-LF [a] and detector anti-NTyr [d]

Combination 1 (Fig. A. 2, red bars) show detection of LF, as expected because of the two anti-LF antibodies, but very little in the NLF case. Combination 2 (brown

bars) shows detection of NLF, which is expected because the antigen was nitrated using excess nitrating agent. This combination did not show detectable signal with pure LF, which is expected given that the capture antibody is specific for NTyr. Combination 3 (blue bars) shows detection of NLF, but very little in the LF case. All three combinations show very little detection of the blank (blocking buffer incubated under otherwise identical conditions). Combinations 1 and 3 both utilize the same capture antibody (anti-LF). The fact that combination 3 shows efficient detection of NLF, but combination 1 does not, suggests that the capture binding of antigen to antibody is not inhibited by antigen nitration. This may imply that the detector antibody binding is inhibited by nitration. The anti-LF capture antibody binds whether LF is the antigen (red bars, center) or NLF is the antigen (blue bars, right). The anti-LF detector also to LF (red, center), but not to NLF (red, right). We conclude from this study that using the anti-LF as capture antibody presented minimal reduction in binding sensitivity and that Combination 3 was viable for further testing (see manuscript for subsequent details).

A.7 Supplemental Table and Figures

Table A.1 Statistical tests comparing detection of NLF vs. LF. NLF concentration at each point from manuscript Figure A. 4 (dark yellow points) compared against LF mean (red line, 0.0187 ± 0.005 AU).

NLF concentration $\mu g\ mL^{-1}$	**p-value**	**t-value**
0	0.26	1.15
0.1875	0.0001	11.7
0.375	0.0001	15.7
0.75	0.0001	28.8
1.5	0.0001	57.1
3	0.0001	76.6
6	0.0001	105
12	0.0001	215
25	0.0001	106

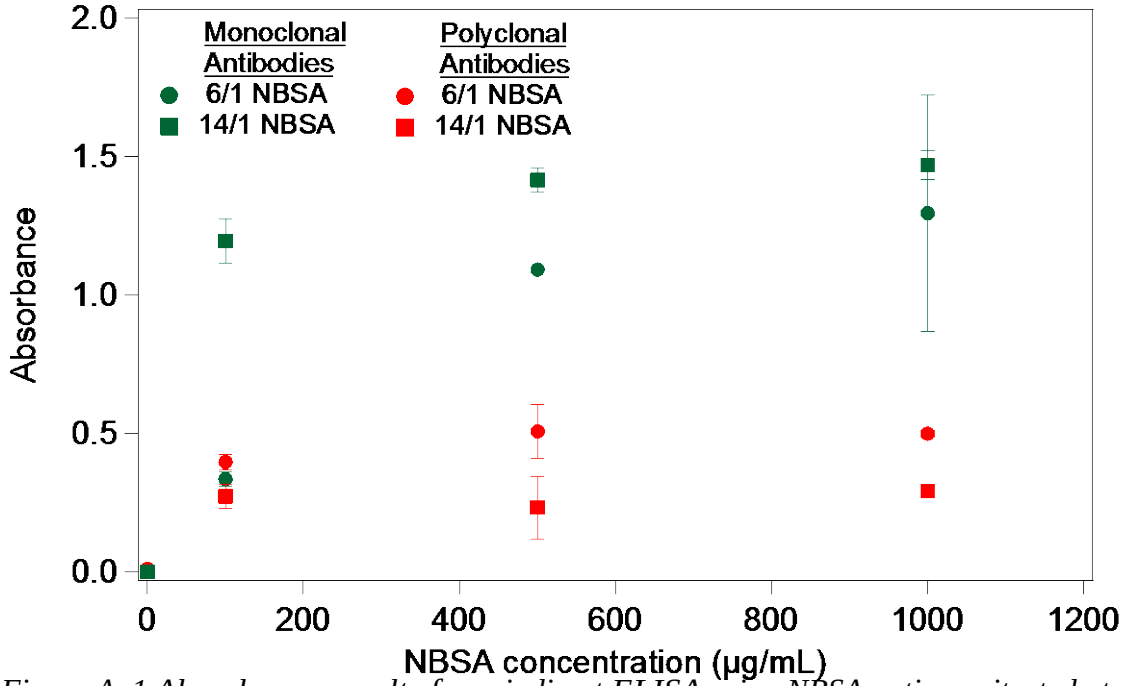

Figure A. 1 Absorbance results from indirect ELISA using NBSA antigen nitrated at two ratios of TNM to tyrosine (6/1 and 14/1). Marker color indicates NTyr antibody used for detection NBSA antigen diluted into blocking buffer. The green marks represented mouse monoclonal nitrotyrosine (ab24496) and the red marks represented goat polyclonal nitrotyrosine (ab27646).Data points are mean values, with error bars as standard deviation of absorbance measurements from individual wells (n = 2). In some case the uncertainty is smaller than the marker point and is not visible.

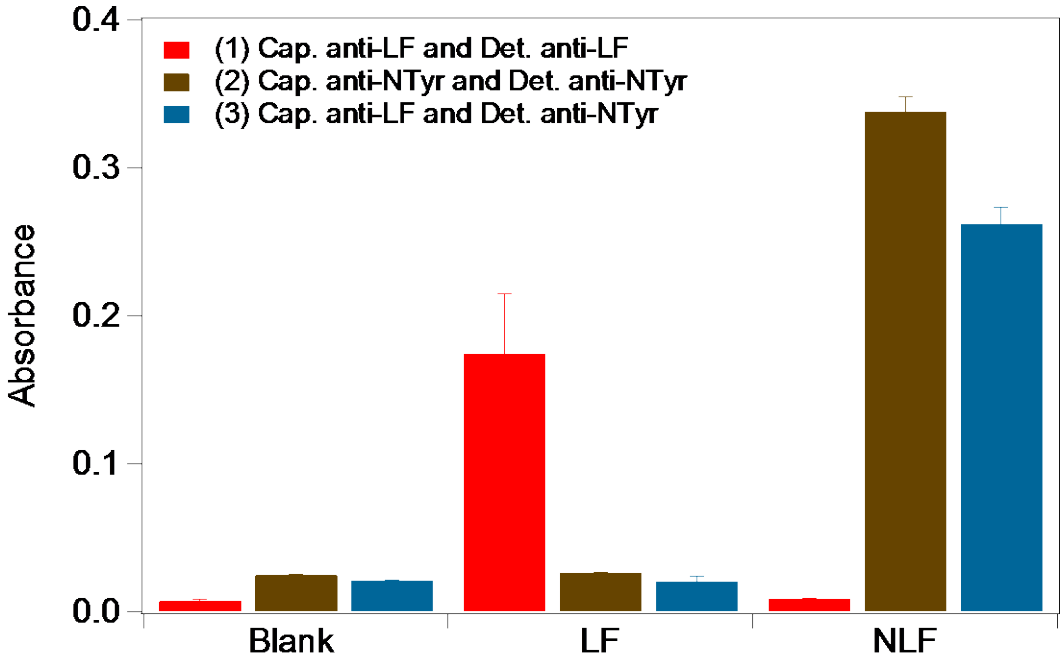

Figure A. 2 Absorbance results from sandwich ELISA testing efficacy of chosen antibodies: anti-LF capture (ab77548), anti-NTyr capture (ab42789, anti-LF detector (ab25811), and anti-NTyr detector (ab24496). Antigen selection shown on x-axis legend: Blank (PBS buffer), LF, and NLF (40/1 TNM/tyrosine). Each antigen used at 0.5 µg mL^{-1}. Order of antibody placement in ELISA indicated in legend. Bars are average values, with error bars as standard deviation of absorbance measurements from individual wells (n = 2).

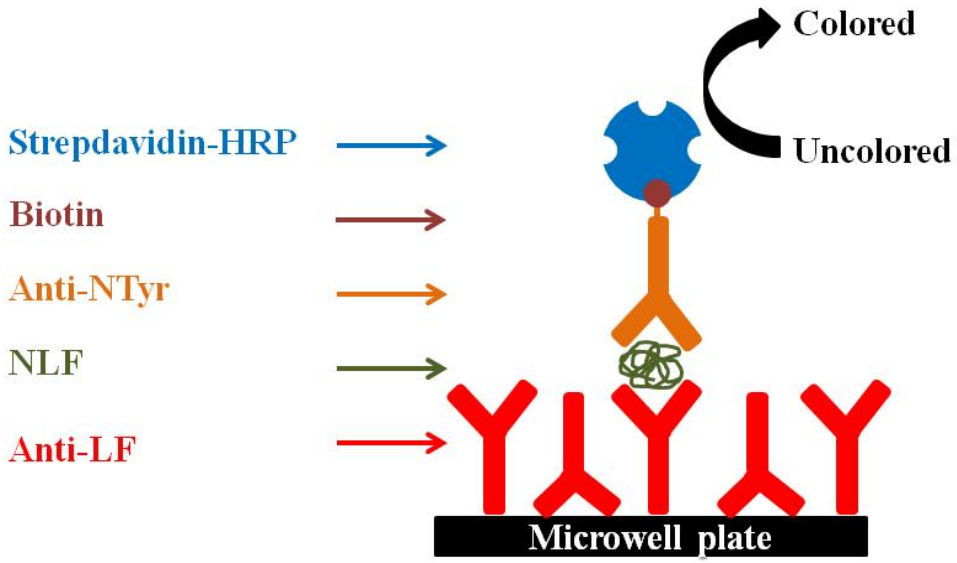

Figure A. 3 Conceptual model for the antibodies sequence of NLF sandwich ELISA. Shown from bottom to top: non-conjugated anti-lactoferrin (anti-LF) as capture antibody (randomly oriented), NLF as antigen, biotinylated anti-nitrotyrosine (anti-NTyr) as a detector antibody, and streptavidin conjugated to HRP. Figure adapted from de la Rica and Stevens (De La Rica, et al. 2012).

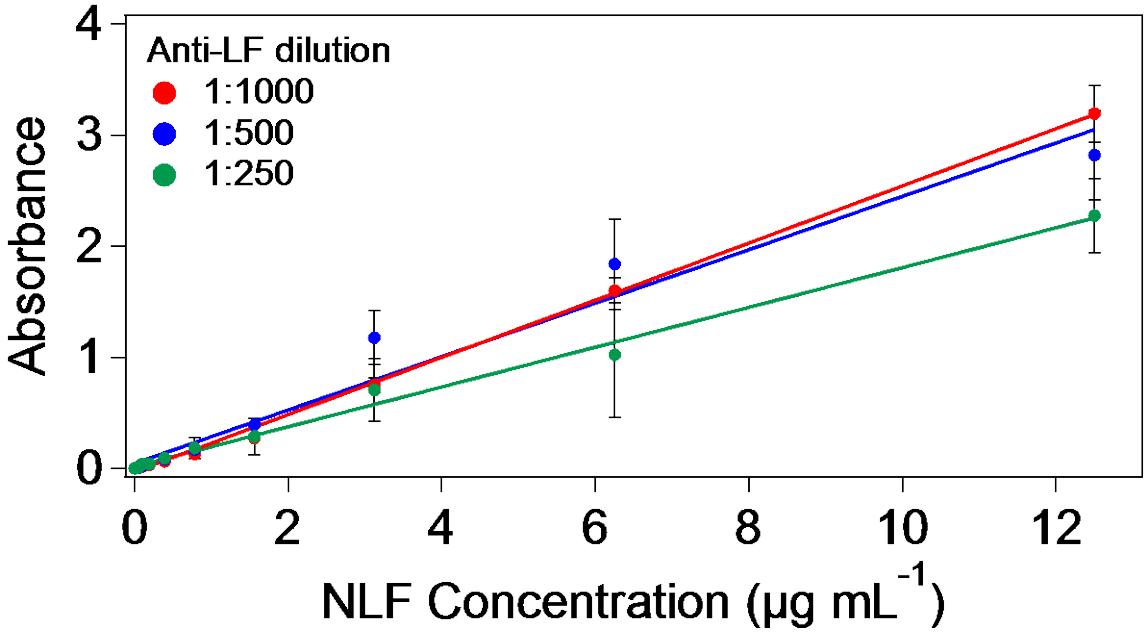

Figure A. 4 Dilution ratio plot for anti-lactoferrin and shows ELISA well absorbance at four dilution factors (anti-LF into blocking buffer). Data points are mean values ± s, n= 3. Traces are linear fits.

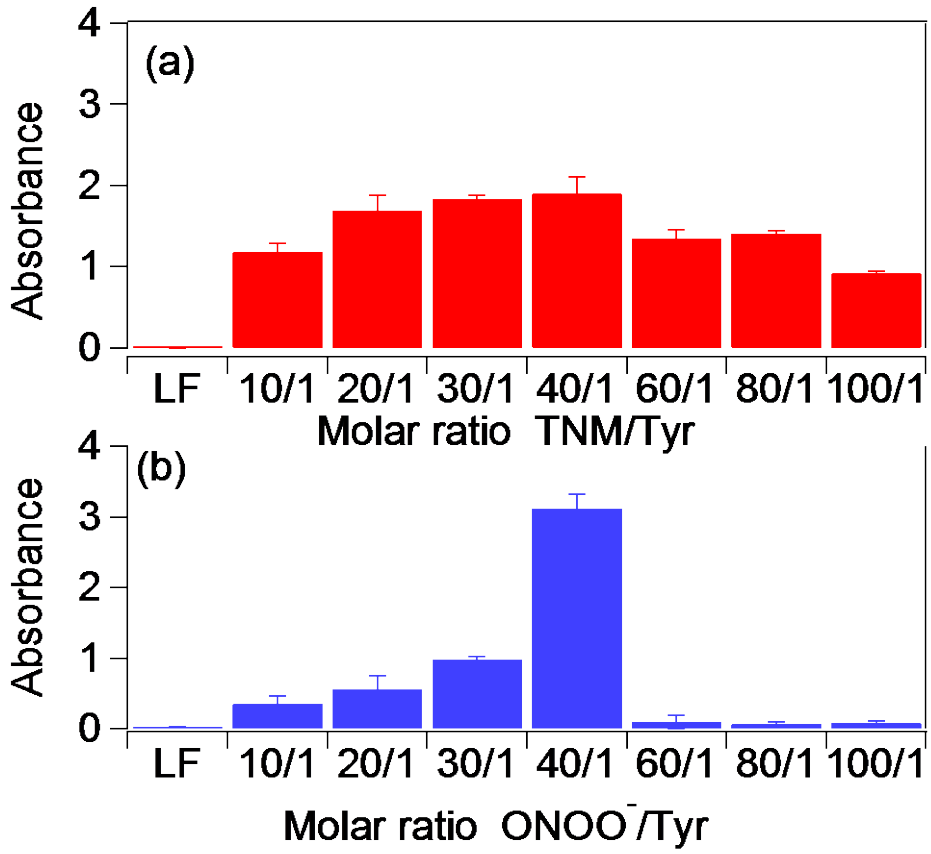

Figure A. 5 Sandwich ELISA of NLF_{TNM} (a) and NLF_{ONOO^-} (b). Error bars show standard deviation of absorbance measurements from individual wells.

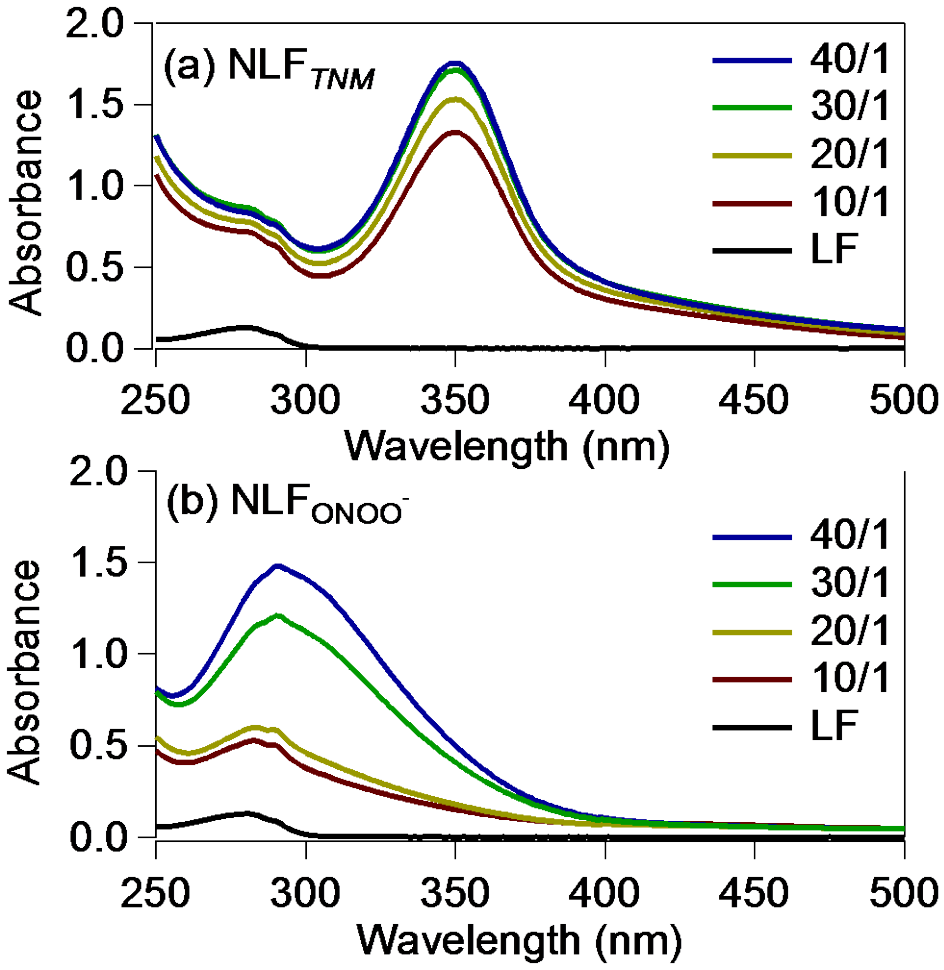

Figure A. 6 The absorbance of NLFTNM (a) and NLFONOO- (b). Legend value shows molar ratio of nitrating agent (TNM or ONOO-) to tyrosine.

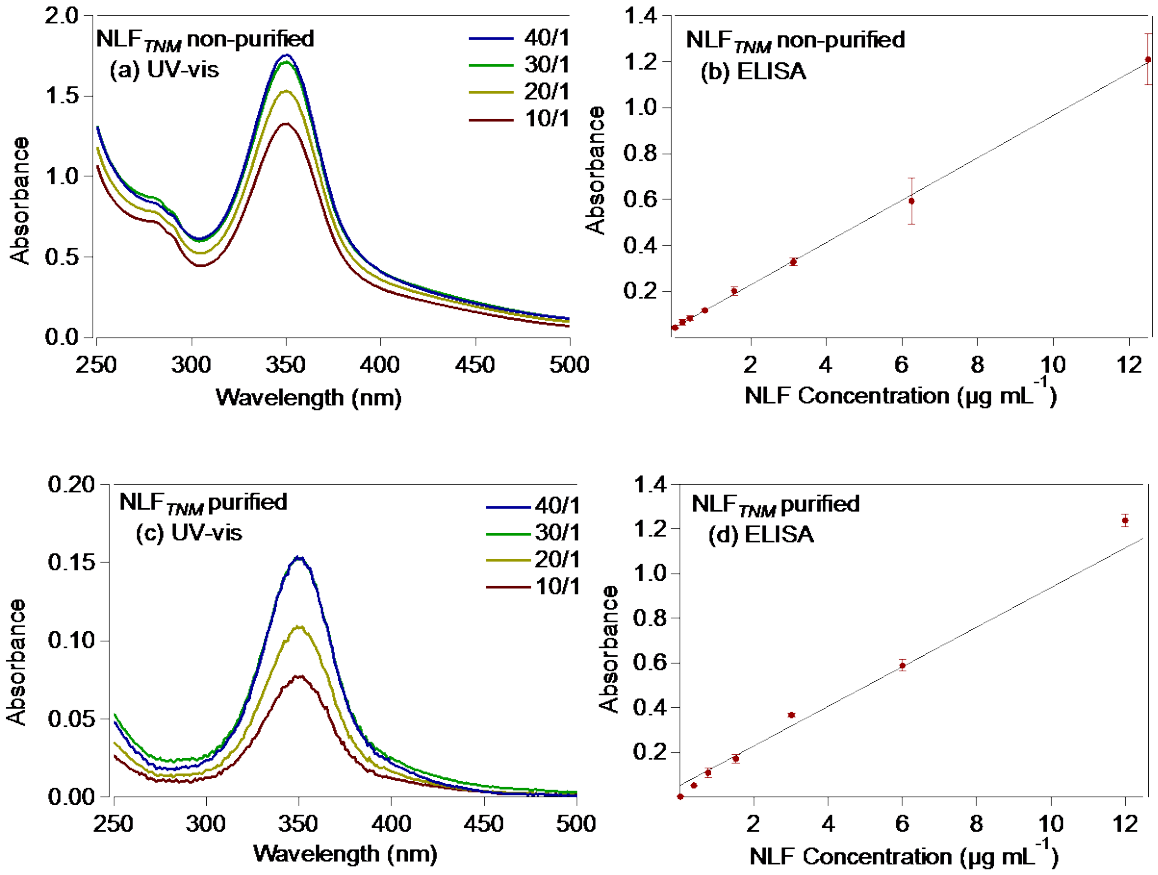

Figure A. 7 The absorbance of non-purified NLF_{TNM} (a-b: top panels) vs. purified NLF_{TNM} (c-d: bottom panels). Legend value on panels in left column (UV-vis results) shows molar ratio of TNM to tyrosine.

Appendix B: Extraction and quantification of LF from animal cornea

The following appendix includes preliminary research results toward quantify LF from animal tissue. A summary of the results and analysis are obtainable here as a documentation of my research in animal tissue which will help with future research.

B.1 Overview

Our project is investigating the effect of the nitration process that plays a role in diseases such as ocular disease. We will begin this study by performing in-vitro experiments on corneal lamb tissue which will help us investigate changes in the eye without requiring in-vivo experimentation.

The first experimental group will be the control group from which we will extract specific proteins (i.e. lactoferrin). To the second experimental group we will apply liquid-phase nitration reactions and extract the proteins to measure the extent of the nitration on the proteins. See chapter 3.

The goal of this project is to investigate the proteins changing due to nitration reaction on the cell level which will help us to understand the nitration of these proteins en route to understanding their potential importance in ocular diseases.

B.2 Materials and methods

Bovine cornea (age: 12-30 months, mixed gender) and rat cornea (age: 7-8 weeks, mixed gender) purchased from Pel-Freez Biological (AR, USA). Lamb cornea (age: 3 months, male gender) donated from local butcher store (Jerusalem Market, E. Illif Ave.), FDA approved for human consumption and handling. 4-(2-Hydroxyethyl) piperazine-1-

ethanesulfonic acid, N-(2-Hydroxyethyl)piperazine-N′-(2-ethanesulfonic acid) (HEPES; H3375), bicinchoninic acid Assay (BCA), Triton X-100 (X100), ethylenediaminetetraacetic acid anhydrous, bioultra (EDTA) , and sodium chloride (S9625) were purchased from sigma-aldrish (USA). HALT (tm) protease inhibitor (PI; QB203967A) from fisher scientific company (PA, USA).

Nitration reactions tetranitromethane (TNM), Sodium peroxynitrite ($ONOO^-$), Amicon Ultracentrifuges tube cutoff 30K, Carry Bio 100 UV-vis spectrometer, and Carry eclipse Fluorescence spectrometer .

The buffers used are: extraction buffer (EB) solution (50.0 mM Tris-HCl, 10.0 mM HEPES, 150.0 mM NaCL, 5.0 mM EDTA, 0.5 % Triton at pH 7.7, and then fresh add 10 % PI) and Tris-HCl buffer (Tris; 50 mM at pH 8.0).

Human milk lactoferrin (LF; L0520), bovine serum albumin (BSA; A7030), tetranitromethane (TNM; T25003), Tween®20 buffer (P1379), Trizma base (Tris-HCl; T1503), sulfuric acid (H_2SO_4; 320501), sodium phosphate dibasic (RES20908-A702X), potassium chloride (P9333), sodium chloride (S9625), potassium phosphate monobasic (P5655), sodium carbonate (S7795), sodium bicarbonate (S5761), Ammonium persulfate (APS; A3678), glycine (G8898), glycerol (G5516), acetic acid (320099), methanol (34860), Sodium dodecyl sulfate (SDS; L3771), and ethanol (245119) were obtained from Sigma Aldrich (USA). Sodium peroxynitrite (NaONOO; 516620), Amicon Ultra-0.5 centrifugal filters (30 kDa, 0.5 mL size; UFC503008), and Amicon Ultra centrifugal filters (30 kDa, 4 mL size; UFC803024) were purchased from Calbiochem (USA). The 1-step ultra

3,3',5,5'-tetramethylbenzidine substrate (TMB; 34028) and bicinchoninic acid assay (BCA; 23225) for total protein quantification were purchased from ThermoFisher Scientific (USA). Flat-bottom, 96-microwell plates (untreated; 333-8013-01F) and sterile sealing tape (ST-3095) were obtained from Life Science Products (USA). A biotinylated, mouse monoclonal to nitrotyrosine antibody (α-NTyr; ab24496), streptavidin horseradish peroxidase (HRP; ab7403), and non-conjugated goat polyclonal anti-human lactoferrin antibody (α-LF; ab77548) were obtained from Abcam (UK). 1.0 mL quartz cuvette with 10 mm path length (MF-W-10-LID) was purchased from Science Outlet (USA).

Iron(III) chloride hexahydrate ($FeCl_3.6H_2O$; 236489), Nitrilotriacetic acid (NTA; N9877), Trizma base (Tris-HCl; T1503), Hydrochloric acid (H-7020), Tryptic Soya broth (TSB; 22092), and Tryptic Soya agar (TSA; 22091) were obtained from Sigma Aldrich (USA). 100mmx15mm petri dish with grip ring, sterile (229692) providate from CELLTREAT (USA). Uv 96-microwell plates with transparent flat bottom (3635) was purshaced from CORNING (USA). Escherichia coli (E. coli; ATCC25922) was purchased from the American Type Culture Collection, ATCC (USA). Precision-plus protein dual color standard (ladder; 1610374), 30% acrylamdie 29:1 (1610156), Tetramethylethylenediamine (TEMED; 1610800), Precision Plus Dual Color Standards (1610374), and Coomassie blue R250 (1610436) BIO-RAD (USA). Buffers used were: phosphate-buffered saline (PBS; 8.1 mM sodium phosphate dibasic, 0.8 mM sodium phosphate monobasic, 1.3 mM potassium chloride, and 68.0 mM sodium chloride at pH 7.4), Tris-HCl buffer (Tris; 0.1 mM at pH 8.0), carbonate buffer (29.0 mM

sodium carbonate and 71.0 mM sodium bicarbonate at pH 9.6), loading buffer (200 mM tris-HCl pH 6.8, 400 mM dithiothreitol (DTT), 0.4% bromophenol blue, 40% glycerol and 8% SDS), running buffer (25 mM Tris-HCl, 192 mM glycine, and 0.1 % SDS), gel staining (coomassie blue R250 1%, acetic acid 10%, methanol 50%, and 40% water), gel destine buffer (50% methanol, 10% acetic acid, and 40% water), and Ferric nitrilotriacetate ($Fe(NTA)_2$) solution ($FeCl_3.6H_2O$ 4.0 mM and NTA 8.0 mM and 1 N HCl add 2% to total solution volume at pH 4.0), and the tryptic soya broth, and tryptic Soya agar was prepared following the manufacture instructions. SDS-PAGE gel containing 3.2 % stacking gel (30% Acrylamide 266.7 µL, Tris-HCL (1.5M) 312.5 µL, 10% SDS 25 µL, water 890.8 µL, APS 50 µL, and TEMED5 µL) and 10 % running buffer (30% Acrylamide 4166.7 µL, Tris-HCL (1M) 3125.0 µL, 10% SDS 125 µL, water 5070.8 µL, APS 125 µL, TEMED 12.5 µL).

B.3 Dissection of the cornea

B.3.1 Lamb cornea

The steps for lamb eye dissection to separate the cornea are as follows:

a. Washed the eye from the blood using water, washed first and Tris-HCl second and dried using the paper towel, see Figure B. 1.

Figure B. 1 The whole lamb eye after washed and dried.

b. The fatty tissue and muscles around the eye were removed using surgical scissors, see Figure B. 2.

Figure B. 2 Removing the fatty tissue and muscle around lamb eye.

c. The eye was silted using a surgical razor blade and then the point of the scissors was inserted into the slit and cut the eye sclera all the way around to get the eye into two halves. Each half of the eye was washed with Tris-HCl to remove the vitreous humor liquid that released after cutting the eye. The eye lens and iris were removed by the surgical forceps, see Figure B. 3.

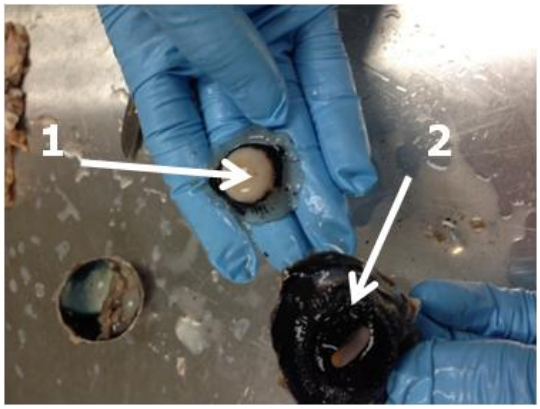

Figure B. 3 The lens (1) and iris with pupil (2) were separated from the front side of the lamb eye.

d. After detaching the lens and iris, the cornea was cut from the eye hemisphere using scalpel. The eye section and the tools used are shown in Figure B. 4 below.

Figure B. 4 The sections of the eye after dissection are; cornea (1), lens (2), iris (3), connective tissue around the cornea (4), half of the back side of the eye with the optic nerve, fatty tissue, and muscle around the eye (6), and the tools were used in the right side.

e. The lamb corneas were cut into four pieces and weighed, then snap frozen the tissue and stored it at -20 ºC until lysate extraction process.

B.4 Bovine and rat corneas

The bovine and rat corneas were purchased, as previously separated from the vendor and cut into four pieces using razor blade and weighed. Then snap frozen the tissue and stored at -20 ºC until lysate extraction process.

B.5 Tissue lysate from lamb, bovine, and rat

The cornea tissue was lysate using the follows protocol. The tissue was placed in the microtube and EB 10 % of tissue mass was added. Next, it was rotated at the cold room for 25 minutes and then sonicated at 8 powers for 2 minutes in ice. Finally, the mixture was centrifuged at 1400 g for 30 minutes in the cold room. The supernate was collected and aliquot in cryogenic microtube and store in -20 ºC until further analysis.

B.6 Qualitative analysis for tissue lysate using spectroscopy analysis

B.6.1 Quantification the total protein using BCA

The BCA used to quantify the total amount of the proteins from cornea lysate following the manufacture instruction.

B.6.2 Determination of protein using UV-vis and EEM

Quartz cuvette was used for spectroscopy analysis. Carry BIO 300 spectroscopy was used to detect the scan absorbance of protein at wavelength 230-500 nm. Carry eclipse spectrophotometer was used to detect EEM at excitation wavelength 200-500 nm and emission stop at 400 nm with 2 increments.

B.7 Quantitative analysis for LF from tissue lysate

B.7.1 Sandwich ELISA

Sandwich ELISA was used to quantify LF protein using the following protocol: The goat polyclonal to lactoferrin non-conjugated antibody (α-LF-n) was used as the capture antibody, and rabbit polyclonal to lactoferrin biotinylated antibody (α-LF-B) was used as the detector antibody. An optimal dilution ratio of 1:5000 capture antibody to carbonate buffer was followed from the abcam manufacturer recommendation. Microwells were coated with 50 µL of the diluted capture antibody and incubated at 4°C overnight. After incubation, the wells were washed by adding 200 µL of PBST (PBS with 0.05% Tween) to each well and tapping the plate upside down on a laboratory wipe to remove excess buffer, repeating twice. Each subsequent incubation step also followed a similar process of sealing, followed by continuous shaking during the incubation period using a rocking platform (UltraRocker, BIO-RAD), and then duplicate washing with PBST. LF was serially diluted into blocking buffer producing LF solutions at eight concentrations (0, 0.24, 0.48, 0.097, 1.95, and 3.90 ng mL^{-1}). After a second washing step, 50 µL of each of the five LF solutions were added in triplicate to the plate and incubated at room temperature for 1 hour. Blocking buffer was used for blank measurements. 50 µL of the detector antibody, diluted in blocking buffer to a ratio of 1:1000, was then added, and the plate was incubated with shaking at room temperature for 1 hour. Streptavidin-HRP and TMB were added following the ELISA protocol, as

described above. The standard calibration curve was made according to the absorbance at each concentration of LF.

B.7.2 Sodium dodecyl sulfate-polyacrylamide gel electrophoresis (SDS-PAGE) for molecular weight determination

LF (1 mg/mL), bovine, lamb, and rat cornea lysate in PBS were heated at 90°C for 8 min, containing loading buffer 1:1 dilution. The SDS-PAGE protocol followed by U. K. Laemmli, the mini gel performed on discontinuous buffer gel of - 3.2% stacking - 10% running polyacrylamide.(Laemmli 1970) The stacking 3.2% has large pore size which will increase the protein resolution before separating it onto running gel. The running gel 10% has good separation for the range of 80 kDa molecular weight protein.

B.8 Results and discussion

B.8.1 BCA assay

The cornea total proteins was detected and the result shows that the increased in total protein direct proption with the increase of the size of the cornea as shows in Figure B. 5, bovine cornea >lamb>rat.

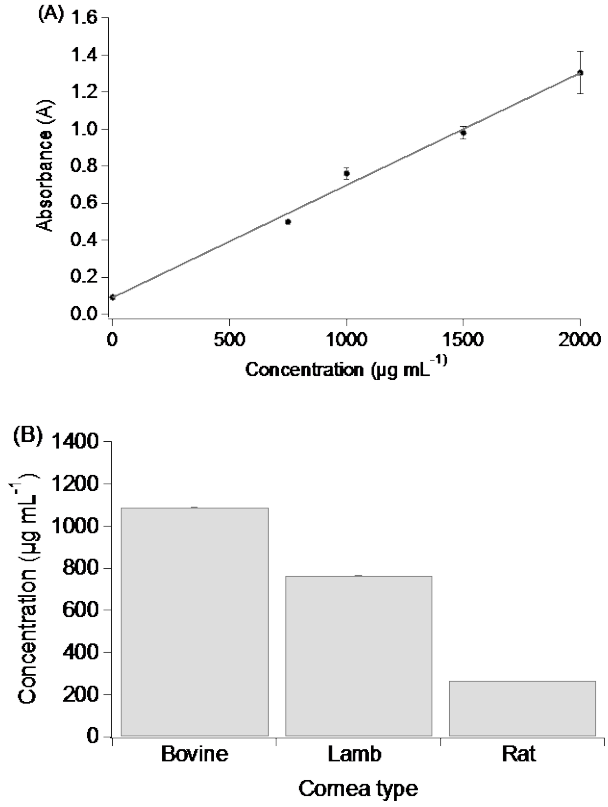

Figure B. 5 The BCA calibration curve (A) used to detect the total protein in animal cornea (B).

B.8.2 UV-vis

The absorbance at 280 nm was detected in all cornea lysate and LF spectra used for comparison. The absorbance intensity at 280 nm was increased with the increased in animal cornea size as shows in (Fig. B. 6. B-D).

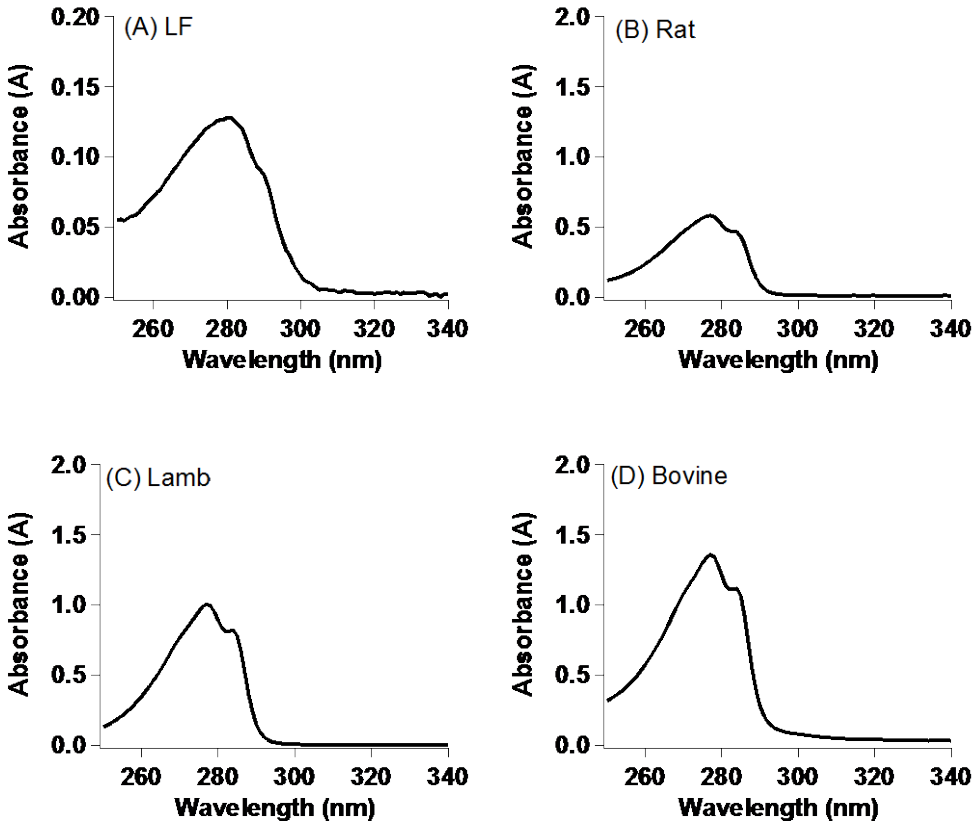

Figure B. 6 The absorbance spectra of LF 1mg/mL used as control (A), rat absorbance is 10 times higher than LF (B), lamb absorbance is 20 times higher than LF (C), and bovine absorbance is 30 times higher than LF (D).

B.8.3 EEM

The fluorescence spectra EEM used to detect multiple emission intensity for multiple excitation wavelength. The EEM of LF used as positive control, rat lysate, lamb lysate, and bovine lysate see (Fig. B.7. A-D).

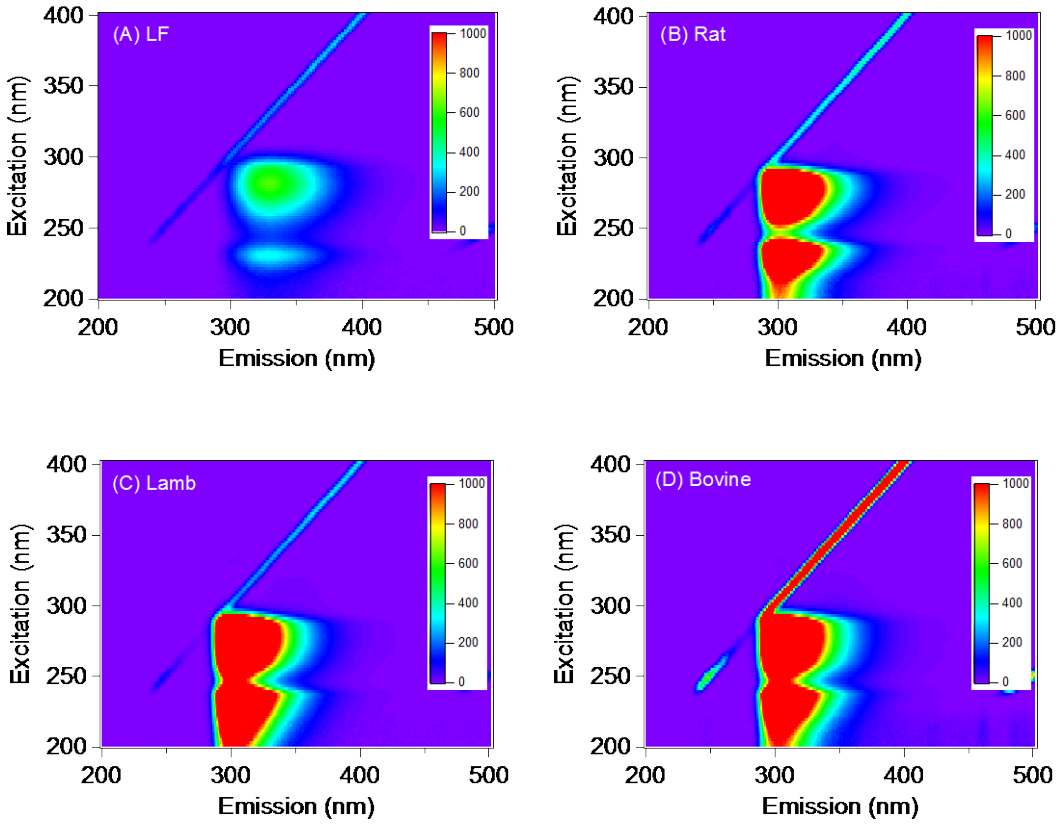

Figure B. 7 The EEM spectra of LF 1mg/mL (A), rat (B), lamb (C), and bovine (D).

B.8.4 SDS-PAGE

The routine SDS-PAGE protocol is a sensitive technique for the analysis of protein components of a matrix and was used with gel stained by coomassie blue and silver stain. The gel was scanned using an Epson scanner to provide the resultant image. Figure (B. 8. A) shows an example result where rat LF has a band lower than the bovine and lamb LF because of the low concentration. Also, we detected the relative intensity using imageJ programe to quantify the gel bands (see Figure B. 8. B).

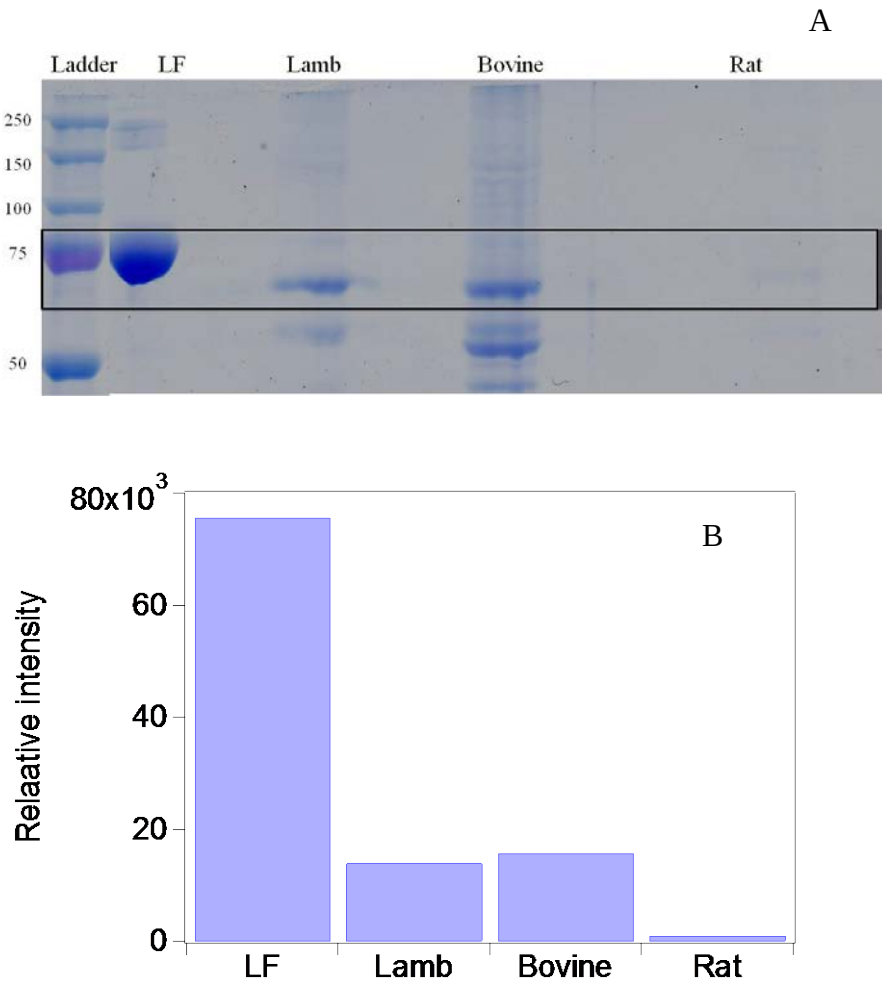

Figure B. 8 (A) SDS-PAGE with Coomassie blue stain, (B) the relative intensity of gel bands.

B.8.5 Sandwich LF ELISA

To detect LF concentration in animal cornea lysate, sandwich LF ELISA was used. The Figure B. 9 shows that the LF increase with the increasing of the cornea size.

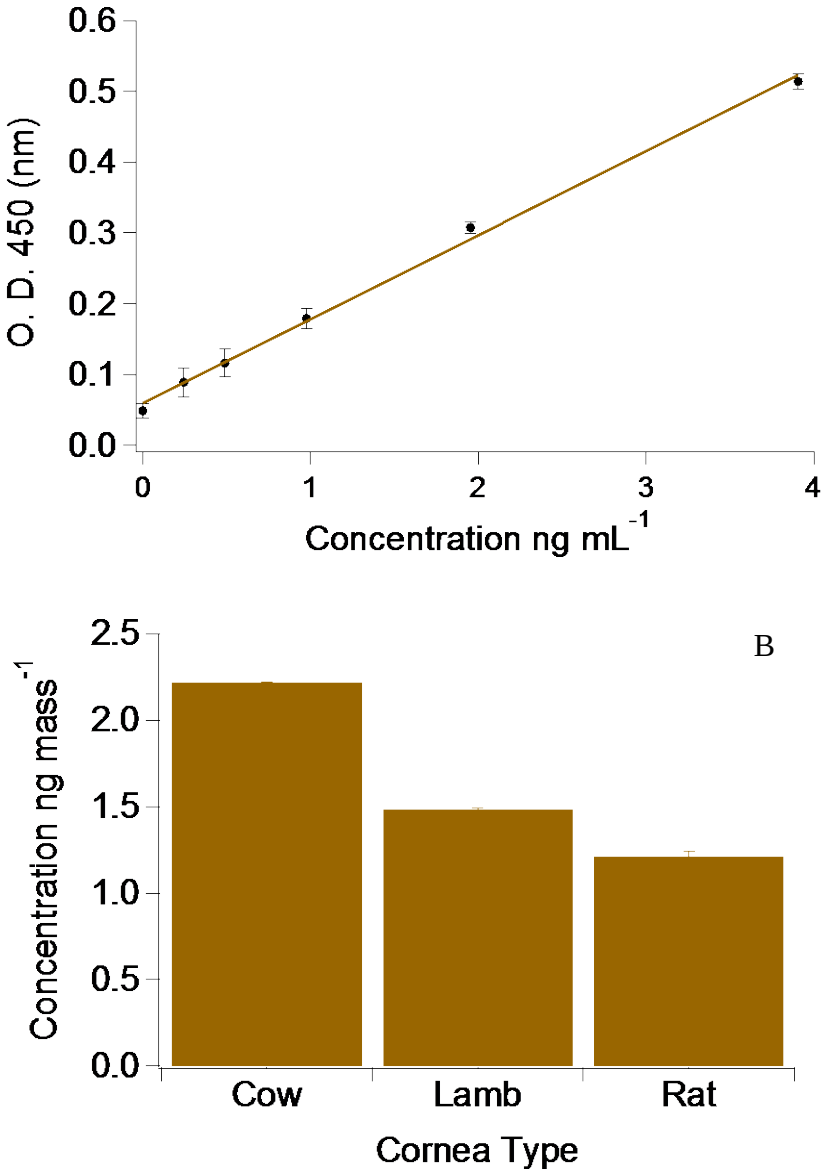

Figure B. 9 (A) Sandwich ELISA calibration curve of human milk LF, (B) the bar graph for quantify cornea concentration.

B.9 Summary

Sandwich ELISA was used to quantify LF in animal cornea. The LF concentration in animal cornea increased linear with the cornea size.

B.10 Acknowledgments

I would like to thanks Dr. Angela Hebel and Randall Mazzarino for all the help and support in lamb cornea dissection. Also, a great thanks to Larissa Ikenouye from Dr. Joseph Angleson lab's for the kind advice in the protein lysate process. Finally, a great thanks to Knoebel Center for the Study of Aging for the research grant and King Saud bin Abdulaziz University for Health Sciences for scholarship funds.

Appendix C: Ergo experimental plan

The following Figure C. 1 represented Ergo research plan for protein nitration.

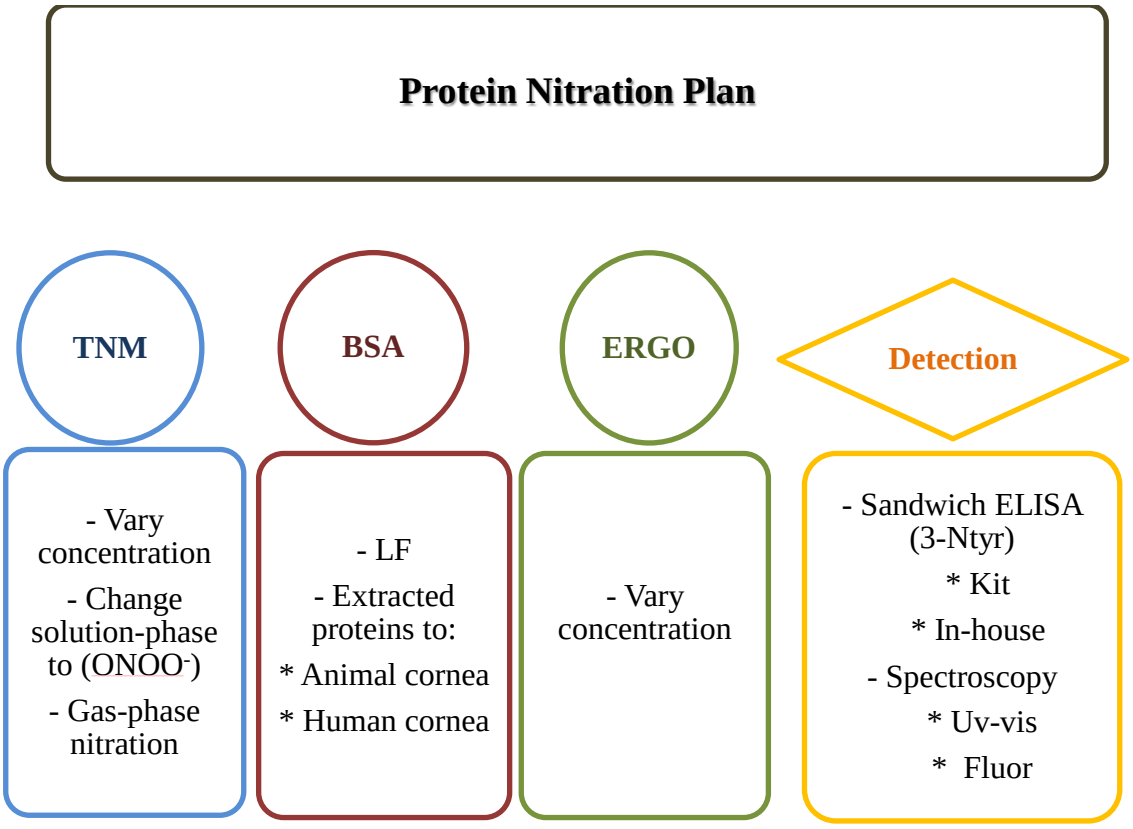

Figure C. 1 A diagram of Ergo research plan.

Appendix D: Kirby Bauer assay

D.1 Materials

Glycerol stock of Escherichia coli (ATCC25922) or Streptococcus faecalis (ATCC 19433) was inculcated into 4 mL Tryptic Soya agar (TSA) (Sigma Aldrich 22091) and incubated at 37ºC for 24 hrs. Then a few separate colonies 3-5 were selected and transferred into Tryptic Soya broth (TSB) (Sigma Aldrich 22092) and incubated at 37ºC for 24 hrs. Muller Hinton agar (MHA) (Sigma Aldrich M9552) was plated and storage in 4ºC until use. The plate has to incubate at 37ºC for 30 min before the assay. Then, 3 µL of the bacteria transferred directly into Muller Hinton agar plate and spread homogenously. The plate was dried for 3-5 minutes before the disc add. Blank disc (Remoel CT0998B) was loaded with 20 µL of the sample and placed into MHA plate and gentle press was applied to the disc before incubated at 37ºC for 24 hrs.

Test several growths Agar to improve the assay such as Tryptic Soya agar, Luria Broth Agar, and Muller Hinton agar. Then, many broths were tested in bacteria growth such as Tryptic Soya broth, Luria Broth, and Brain Heart broth. Test LF concentration 0.1-1 mg/mL in water and PBS.

Aim of Kirby Bauer (KB) study: To investigate antibacterial activity using zone of inhibition see the following scheme.

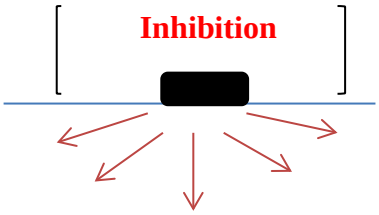

Zone of inhibition is the area around the disk that get affected by the antibiotic.

D.2 Methods

1 µL of glycerol stock aliquot of Escherichia coli (ATCC 25922) was inculcated Tryptic Soya agar (TSA) (Sigma Aldrich 22091) plate and incubated at 37ºC for 24 hrs. Then a few separate colonies 3-5 were selected and transferred into 4 mL Tryptic Soya broth (TSB) (Sigma Aldrich 22092) and incubated at 37ºC for 24 hrs. After incubation dilute this 4 mL into 50 mL TSB to make E.coli stock. The samples were placed into 96-microwell plate and 200 1 µL per well was used. All samples was prepared in TBS, (Blank) is TSB, (positive control) is chloramphenicol antibiotic in 60 µL mL^{-1}, LF and NLF was diluted it into 1mg mL^{-1}. Then 5 µL of E. coli stock was added to each well and incubated at 37ºC for overnight. Finally, microwell plate was detected by the plate reader (Tecan Infinite, M1000 PRO) at wavelength 600 nm.

D.3 Results

The agar plate showed the zone of inhibition of LF vs. NLF 10/1, NLF 20/1, NLF 30/1, NLF 40/1. The increase of nitration direct associated to the decrease of the zone of the inhibition, see Figure D. 1.

Figure D. 1 Three agar plates showed the antibacterial affect using zone of inhibition for LF vs. NLF 10/1, 20/1, 30/1, and 40/1.

Sample	10uL- E.coli	20uL- E.coli	5uL- E.coli
LF	Not clear	18 mm	17 mm
NLF 10/1	Not clear	15 mm	11 mm
NLF 20/1	Not clear	15 mm	10 mm
NLF 30/1	Not clear	14 mm	10 mm
NLF 40/1	Not clear	14 mm	8 mm

Appendix E: Buffer pH changed the nitration product yield

This study helped us to test the effect of the buffer pH in nitration reaction using TNM.

Figure E. 1 represents the absorbance spectra of BSA (TNM) nitration product using several buffers with different pH. The nitration reaction product increase with the increase of the buffer pH and the pH 12 buffer showed highest nitration peak at wavelength 350 nm. Also, no shift was observed in the nitration product peaks see Figure E. 1. Our concern was between Tris-HCl and PBS because they were the main buffers we used in TNM nitration reaction and both have similar nitration products.

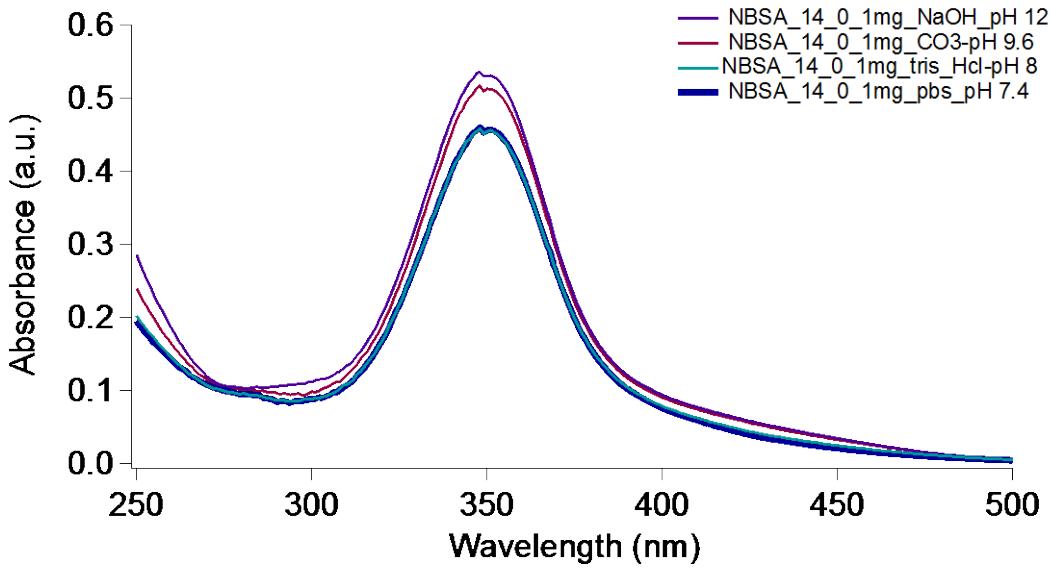

Figure E. 1 UV-Vis spectra of nitration reaction of BSA using TNM in several pH buffer

Appendix F: Comparison study of nitration reaction of aromatic amino acids using $ONOO^-$ and TNM

This study is a side project that helped to analyze the absorbance and EEM spectra for nitrated protein.

The following four set of Figures F. 1-4 showed the affect of nitration agents in free aromatic amino acid (Tryptophan, Tyrosine, Phenylalanine, and Histidine) and how that changes the optical properties. Our results matched the previous study by Mayer et al. for native amino acids for EEM analysis (Meyer, et al. 2015) and for absorbance from (Saidel, et al. 1952).

F.1 Tryptophan (Trp) and nitrated tryptophan (NTrp)

Trp as a native form has the highest absorbance and fluorescence intensity among aromatic amino acids. Figure F.1. A showed an absorbance band in 280 nm for Trp and two bands after nitration at 280 and 350 nm. Figure F.1 Figure F.1. B showed fluorescence intensity between 300-450 nm for Trp and it is reduced after nitration.

The nitration agents TNM and $ONOO^-$ have different amino acids mechanism in nitration but they all share producing nitrotyrosine. The TNM agent nitrated aromatic amino acids but produced mostly nitrotyrosine which explain the more reduction in EEM intensity than $ONOO^-$. Also, $ONOO^-$ has oxidation affect to cystine and methionine beside the nitration of Tryptophan, Tyrosine, Phenylalanine, and Histidine.

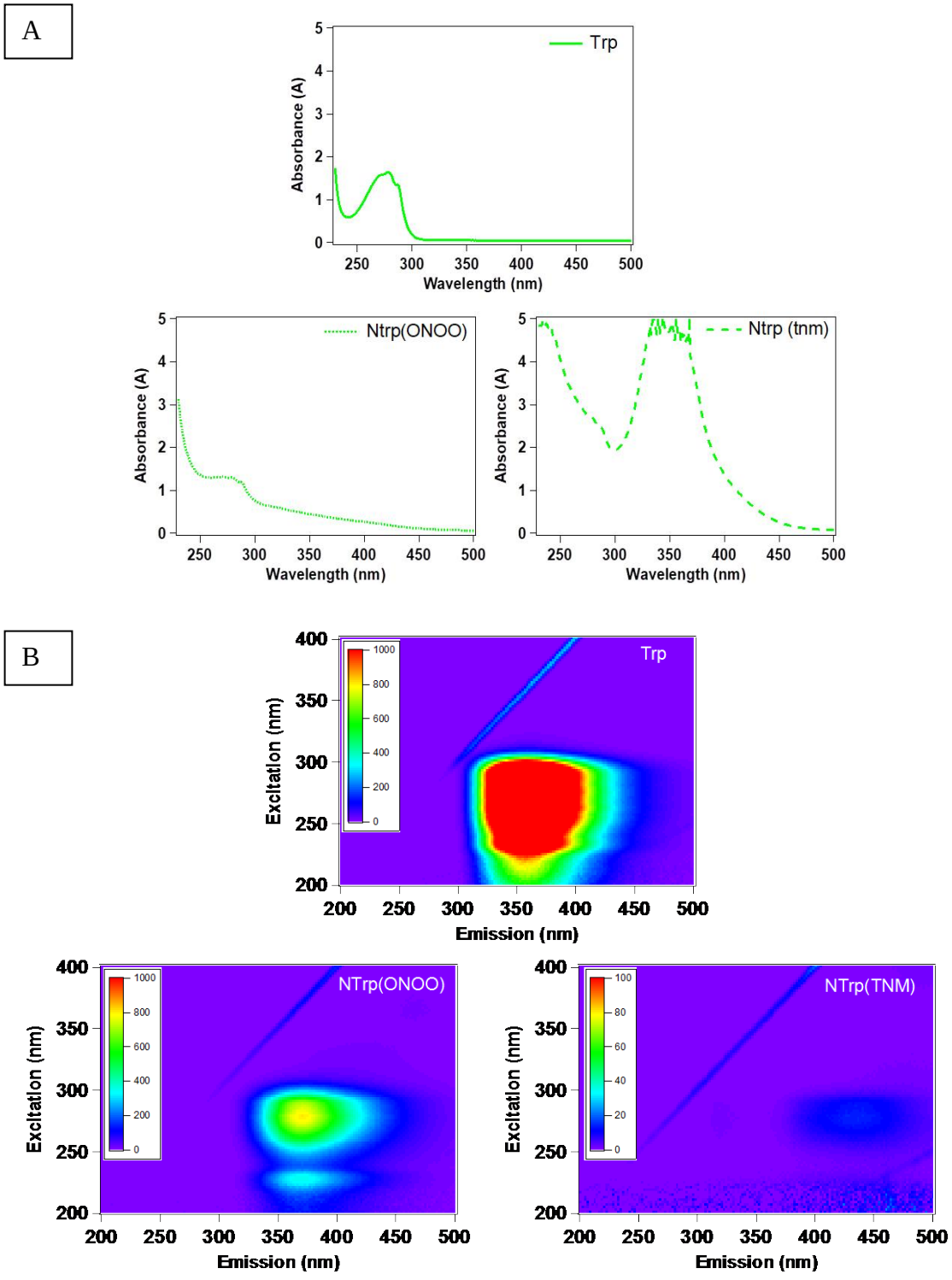

Figure F. 1 (A) Absorbance spectra for (B)EEM spectra for Tyr before (top) and after nitration (bottom).

F.2 Tyrosine (Tyr) and nitrated tyrosine (NTyr)

Tyr as a native form has the second highest absorbance and fluorescence intensity among aromatic amino acids. Figure F. 2. A showed absorbance band in 270 nm for Trp and two bands after nitration at 270 and 350 nm. Figure F. 2. B showed higher fluorescence intensity between 280-350 nm for Tyr and it is reduced after nitration. As mentioned above the nitration agents TNM and $ONOO^-$ have different amino acids mechanism in nitration, but they all share producing nitrotyrosine. The TNM agent produced mainly nitrotyrosine and nitrotryptophan which explain the greater reduction in EEM intensity than $ONOO^-$. Here $ONOO^-$ reduced the fluorescence intensity between 280-350 nm and generated a strong intensity between 380-500nm which related to dityrosine as a product of $ONOO^-$.(Goldstein, et al. 2008) Also, the fluorescence range matched to Al-Garawi et al fluorescence study for dityrosine.(Al-Garawi, et al. 2017).

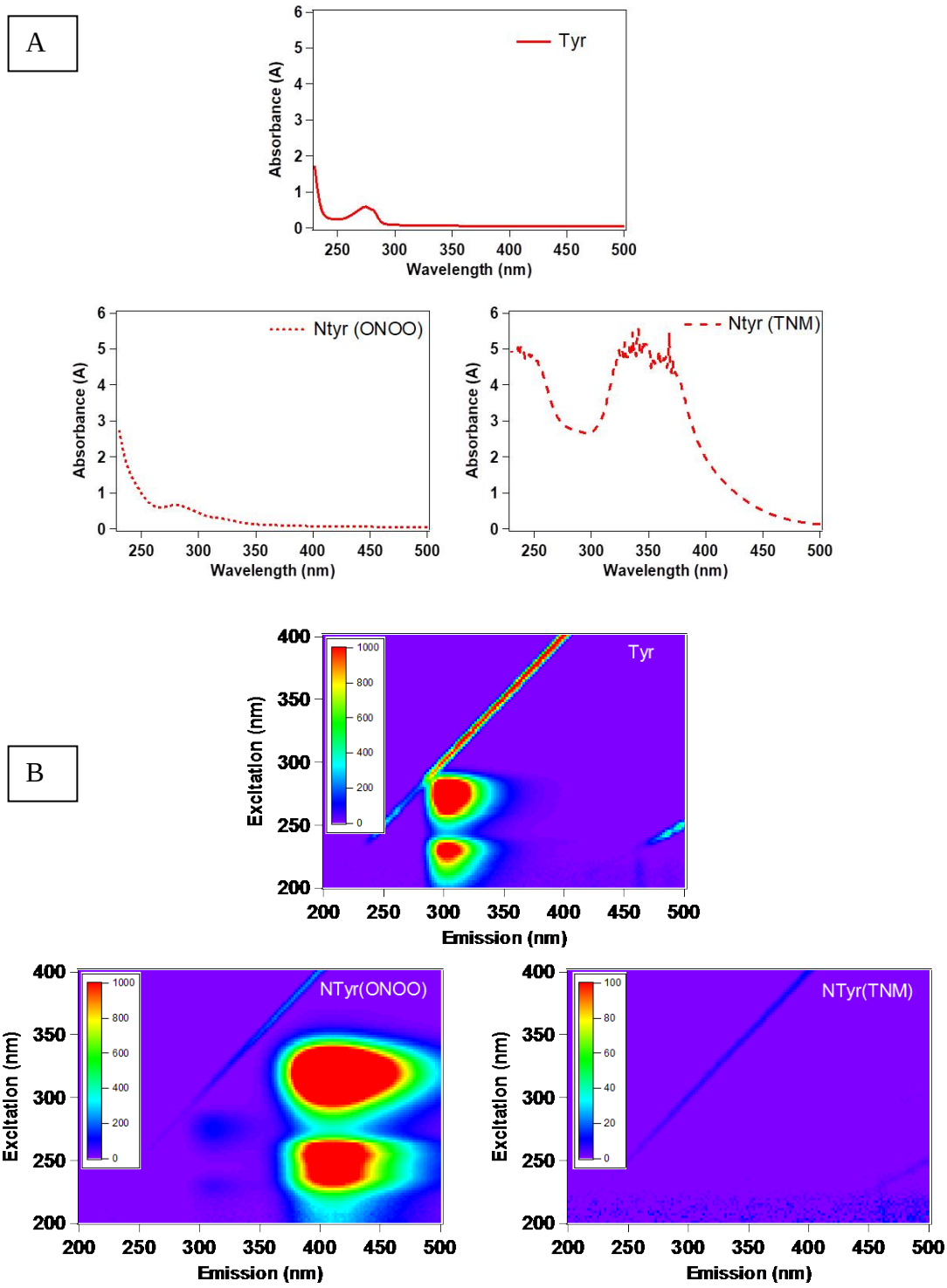

Figure F. 2 (A) Absorbance spectra and (B)EEM spectra for Trp before (top) and after nitration (bottom).

F.3 Phenylalanine (Phe) and nitrated Phenylalanine (NPhe)

Phe as a native form has the lowest absorbance and fluorescence intensity among aromatic amino acids. Figure F. 3. A showed absorbance band at 260 nm for Phe and two bands after nitration at 260 and 350 nm. Figure F. 1. B showed low fluorescence intensity between 280-300 nm and it is reduced after nitration. The nitration products have similar reduction after nitration as NTrp.

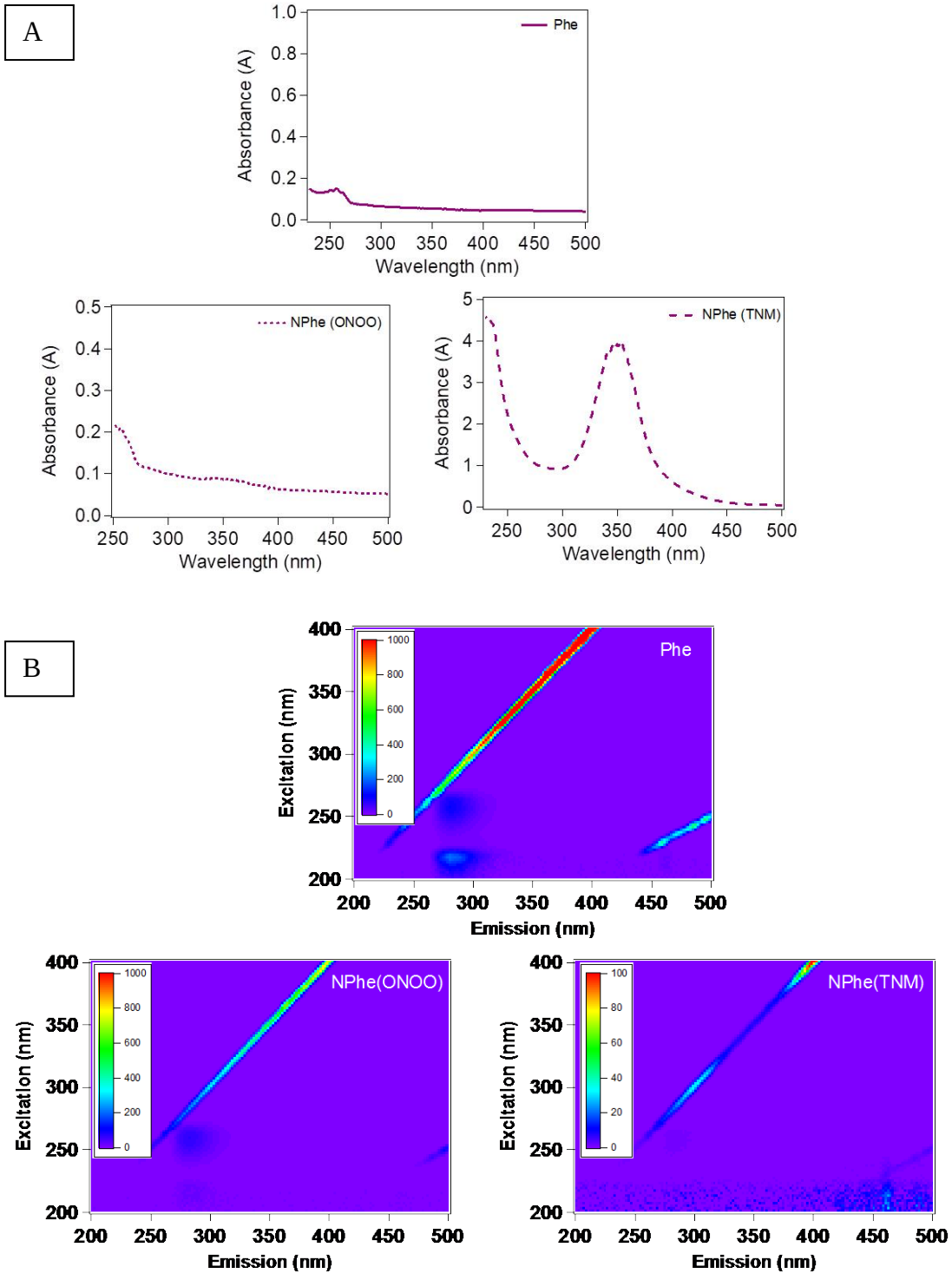

Figure F. 3 (A) Absorbance spectra and (B)EEM spectra for Phe before (top) and after nitration (bottom).

F.4 Histidine (His) and nitrated Histidine (NHis)

Figure F. 4. A showed His nitration band at 350 with $ONOO^-$ and no absorbance band with TNM. Figure F. 4. B His as a native form does not have fluorescence intensity and that matched to previous EEM study (Meyer, et al. 2015) which make it hard to detect the nitration fluorescence with $ONOO^-$.

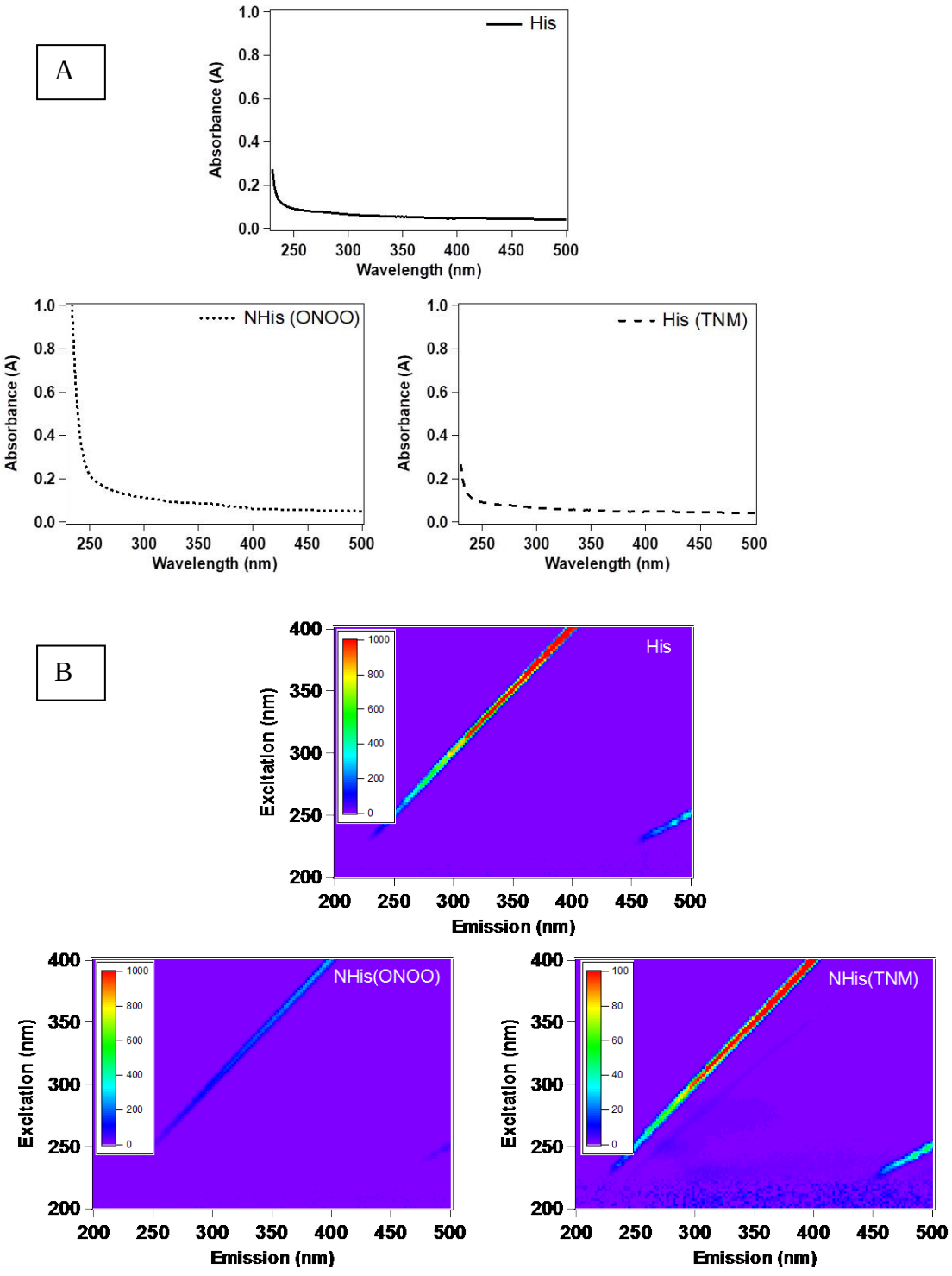

Figure F. 4 (A) Absorbance spectra and (B)EEM spectra for His before (top) and after nitration (bottom).

Appendix G: Infrared spectroscopic analysis for test functional groups of lactoferrin nitration

The following IR spectra used to investigate the fictional group of lactoferrin and nitrated lactoferrin.

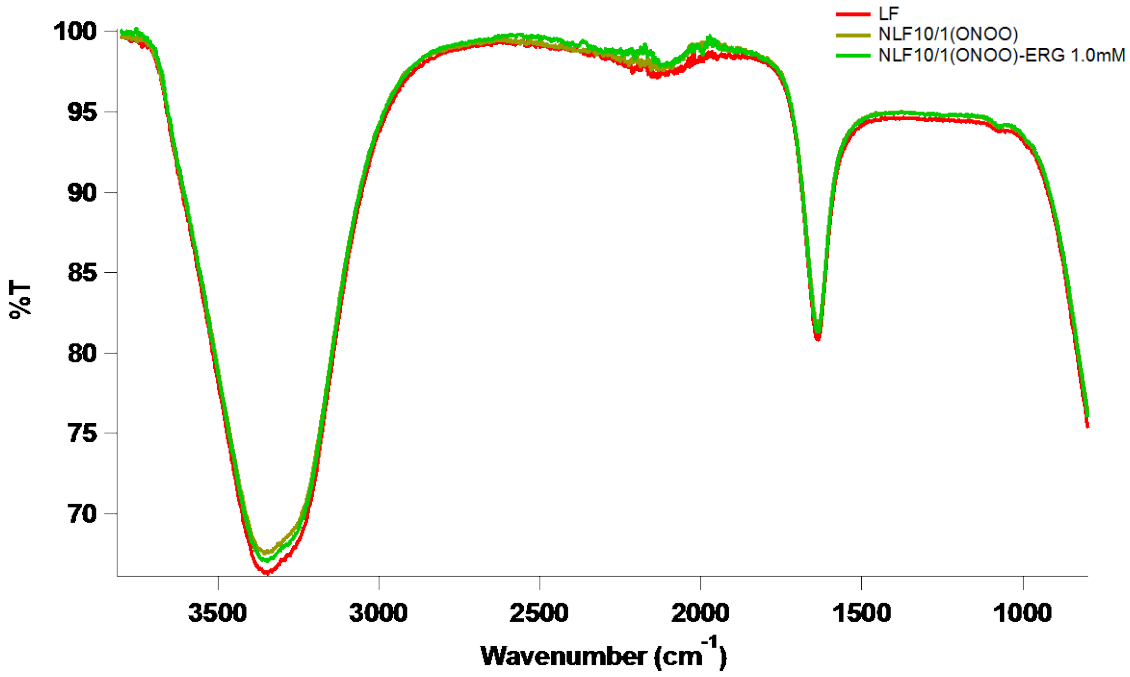

Figure G. 1 IR spectra LF vs. NLF10/1, and NLF10/1-Ergo 1.0 mM.

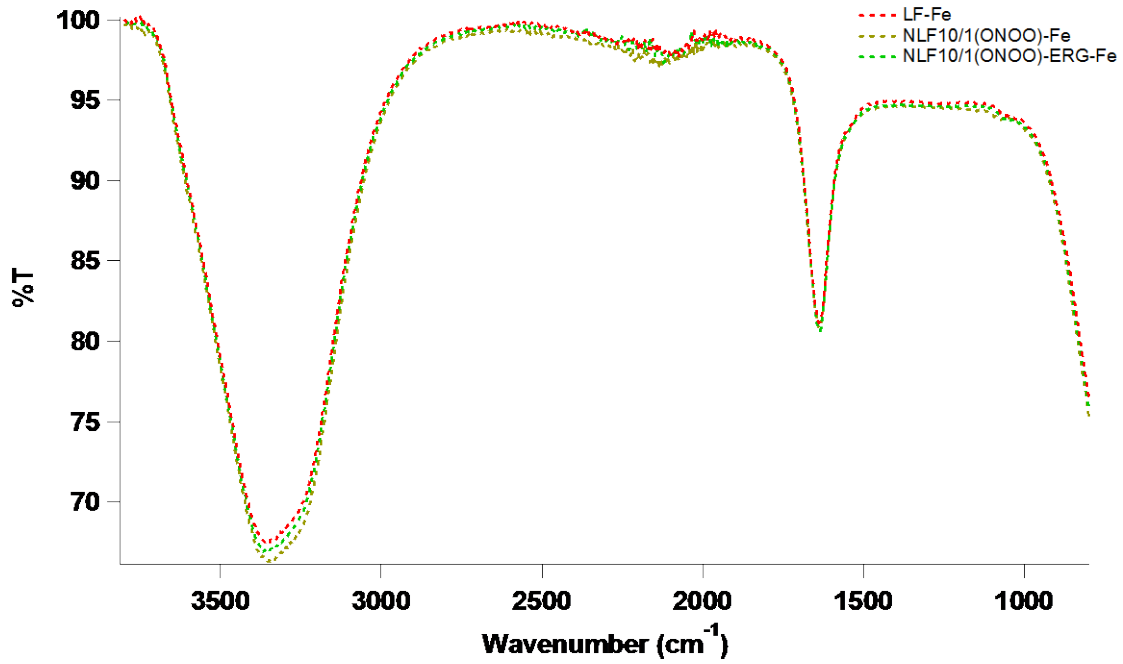

Figure G. 2 IR spectra LF-Fe vs. NLF10/1-Fe, and NLF10/1-Ergo 1.0 mM-Fe.

Figures G. 1 and 2 showed the functional groups that shows in the IR spectra for lactoferrin nitration samples 5mg/mL concentrations with and without Fe^{+3}. The spectra bands described as: amid I band 1700-1600 cm^{-1}, amid III band 1229-1301 cm^{-1} for CN stretching and NH bonding, amid B band 3300 cm^{-1} for NH stretching, amid B band 3300 cm^{-1}. The Tyr-OH band is in 1614-1621 cm^{-1} which showed decrease after nitration.

Appendix H: Iron binding analysis

H.1 Method: Iron titration to detect iron-binding capacity

The iron-binding assay was prepared following procedures outlined by Hamilton *et al.* (Hamilton, et al. 2009). After nitration reaction samples were purified, each UV-microwell was coated with 200 µL of either LF, NLF 10/1 NLF 40/1, NLF10/1-Ergo 0 .1, and NLF10/1- Ergo, 0.5 mM.. To each well, 1 equivalent of $Fe(NTA)_2$ was added, and the absorbance was measured using the plate reader after five minutes of waiting at room temperature. Another equivalent of iron was then added and the process was repeated until a total of nine equivalents had been analyzed. The absorbance of each well was detected using the plate reader at wavelength 470 nm.

H.2 Result: Iron-binding strength of LF and NLF

To determine the strength of the binding affinity from both unmodified and nitrated LF to Fe^{3+}, equivalents of $Fe(NTA)_2$ were titrated into solutions of LF, NLF 10/1 NLF 40/1, NLF10/1, NLF10/1- Ergo 0 .1,and NLF10/1- Ergo, 0.5 mM. Absorbance of the resultant solutions were measured at 470 nm (Fig. H. 2), where increasing absorbance indicates additional iron bound within the protein after addition to the ferric ion (Fe^{3+}), according to Figure H. 1.

$$Fe^{3+} + LF \leftrightarrows Fe^{3+}\text{-}LF + 2H^{+}$$

Figure H. 1: Addition of ferric ion to lactoferrin.

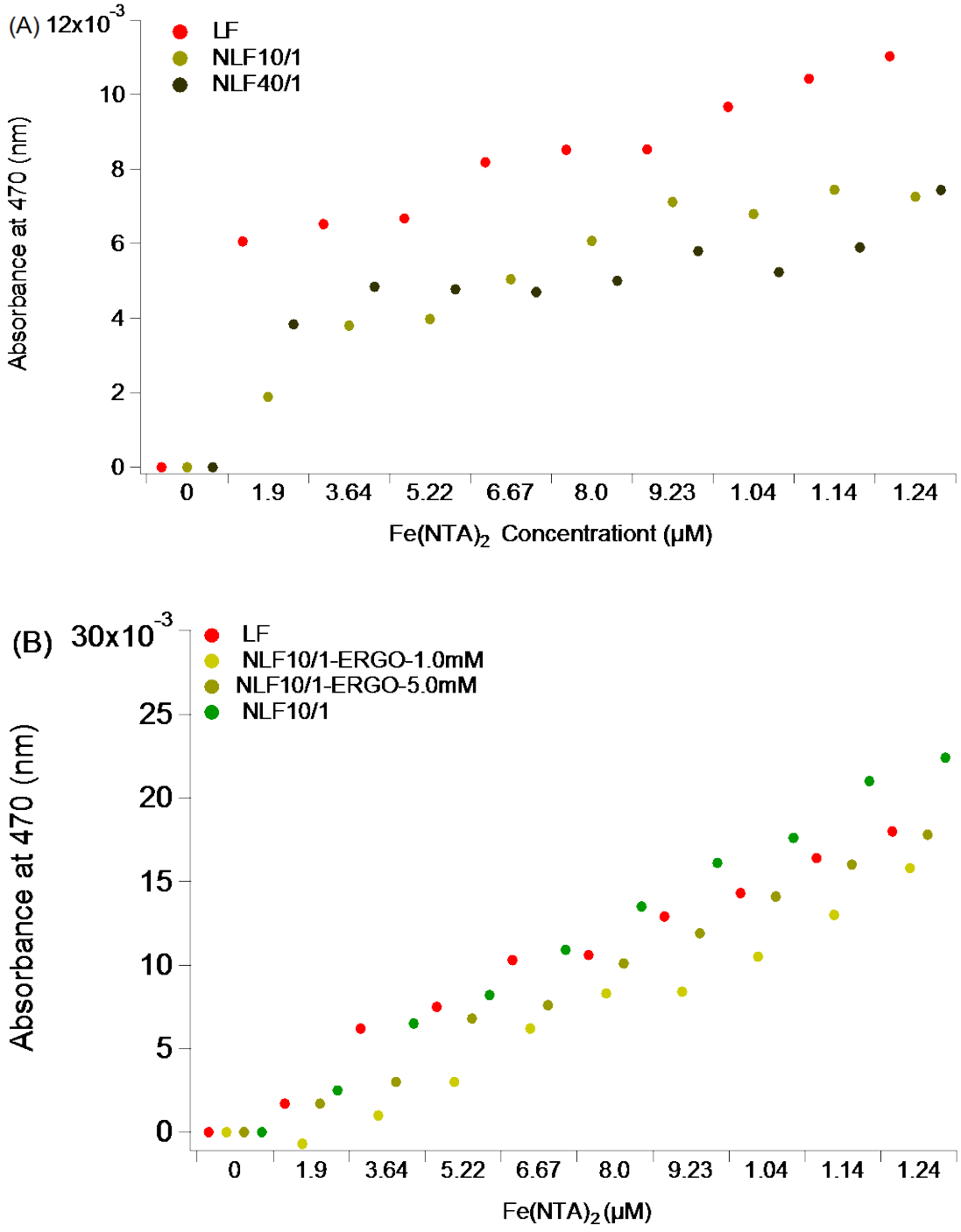

Figure H. 2 Identified iron binding activity of absorbance spectra of iron titration for LF, 10/1 NLF, an 40/1 NLF in spectra (A), , NLF10/1, NLF10/1- Ergo 0 .1,and NLF10/1-Ergo, 0.5 mM.in spectra (B), data points are mean values ±, (spectra A:n= 5 and spectra B:n=1).

The absorbance of iron binding represented in (Figure H. 2, graph A). The binding strength was tested for each sample using absorbance at wavelength 470 nm. There were no significant differences in iron binding for LF comparing to NLF 10/1 and 40/1. Same results for Ergo, there were no significant differences between NLF10/1, NLF10/1-0 Ergo.1, 0.5 mM and LF in (Figure H. 2, graph B). This finding suggested that the LF binding site was not affected by nitration.

Appendix I: Denaturing study of LF and NLF 40/1-(TNM) using guanidine in four different concentrations 0.25, 0.5, 1.0, and 2.0 M

The guanidine used to test the denaturing difference between LF and NLF 40/1. The denature effect of guanidine was examined using two techniques: EEM and SDS-PAGE.

I.1 SDS-PAGE

The SDS-PAGE (Figure I. 1) showed one strong band for LF-Guanidine 0.25, 0.5, 1.0, and 2.0 M at molecular weight 75kDa. There were two strong bands for NLF 40/1-Guanidine 0.25, 0.5, 1.0, and 2.0 M around 75 kDa and one at 50 kD. There is missing band for LF 0.5 guanidine due to technical error.

These bands indicate the structure change of NLF 40/1 from LF due to the different response with the denature agents.

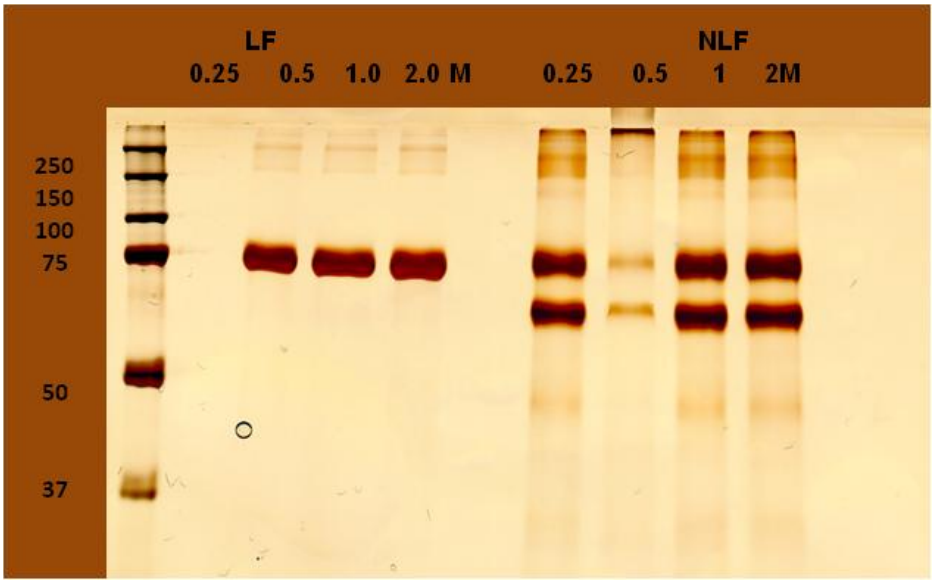

Figure I. 1 The SDS-PAGE stained with silver nitrate. The bands were presented ladder, LF-Guanidine 0.25, 0.5, 1.0, and 2.0 M , and NLF 40/1 Guanidine 0.25, 0.5, 1.0, and 2.0 M.

I.2 EEM

The guanidine fluorescence was tested as background for the detection and does not show fluorescence properties (Figure I. 2).

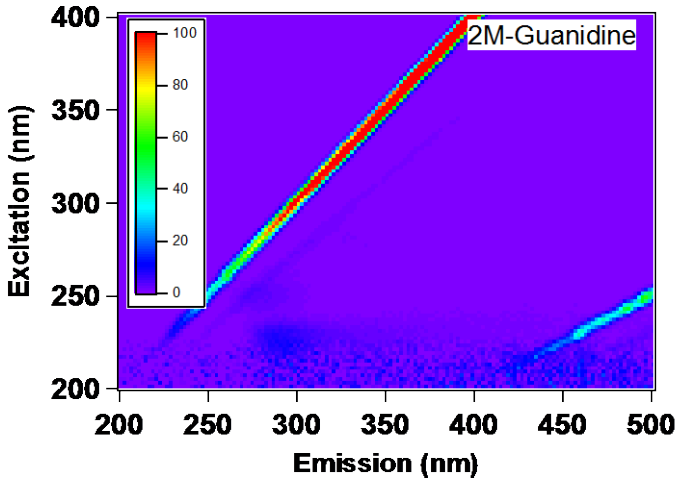

Figure I. 2 The EEM of guanidine 2.0 M.

The EEM for LF at wavelength range 300-350 nm showed decrease in fluorescence intensity with the increase of guanidine concentrations (Figure I.3)

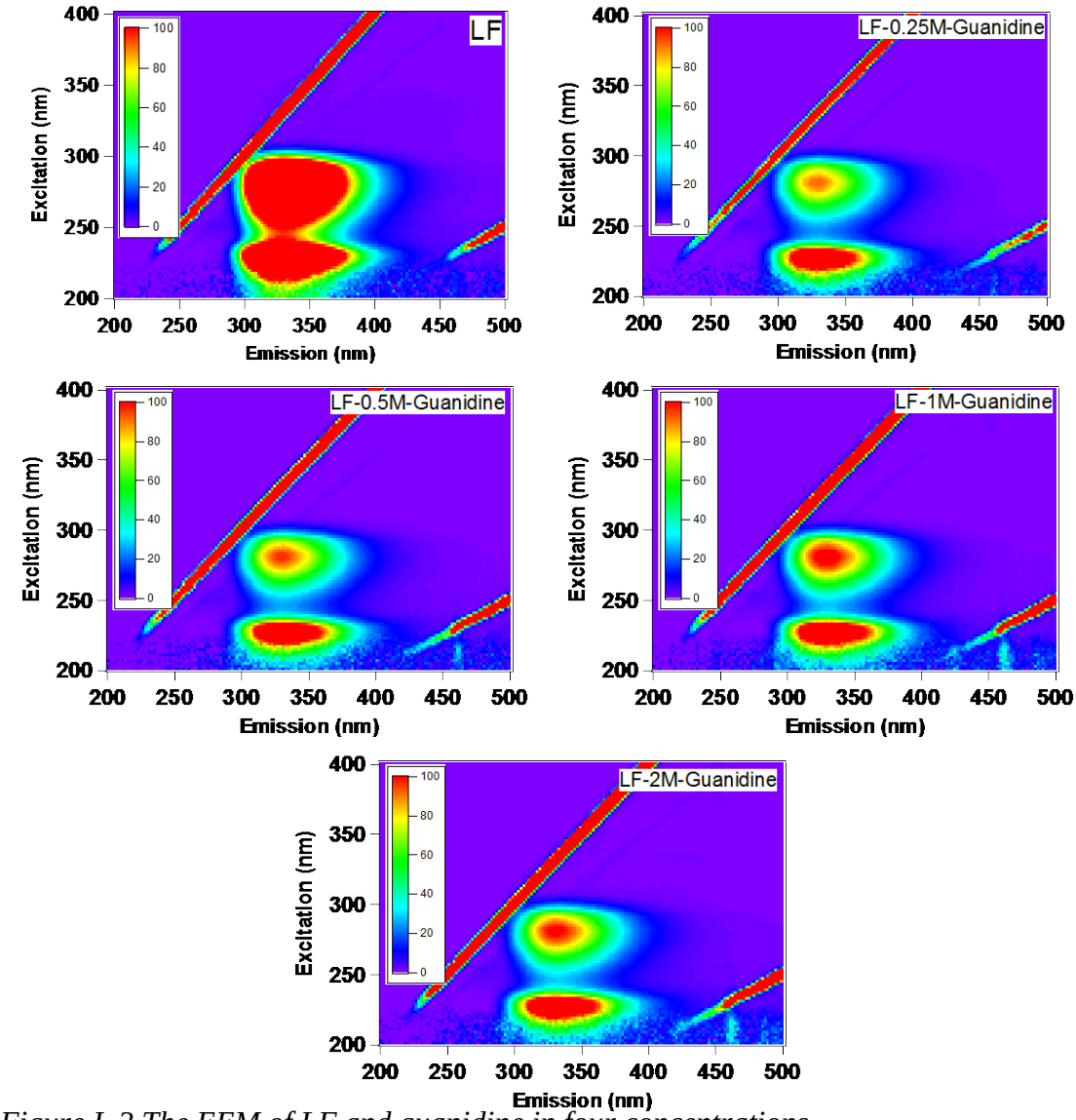

Figure I. 3 The EEM of LF and guanidine in four concentrations.

The EEM for NLF 40/1 at wavelength range 300-350 nm decrease as the guanidine concentration increase (Figure I. 4).

The behavior of LF comparing to LF 40/1 were different which indicate structure dysfunction of LF after nitration.

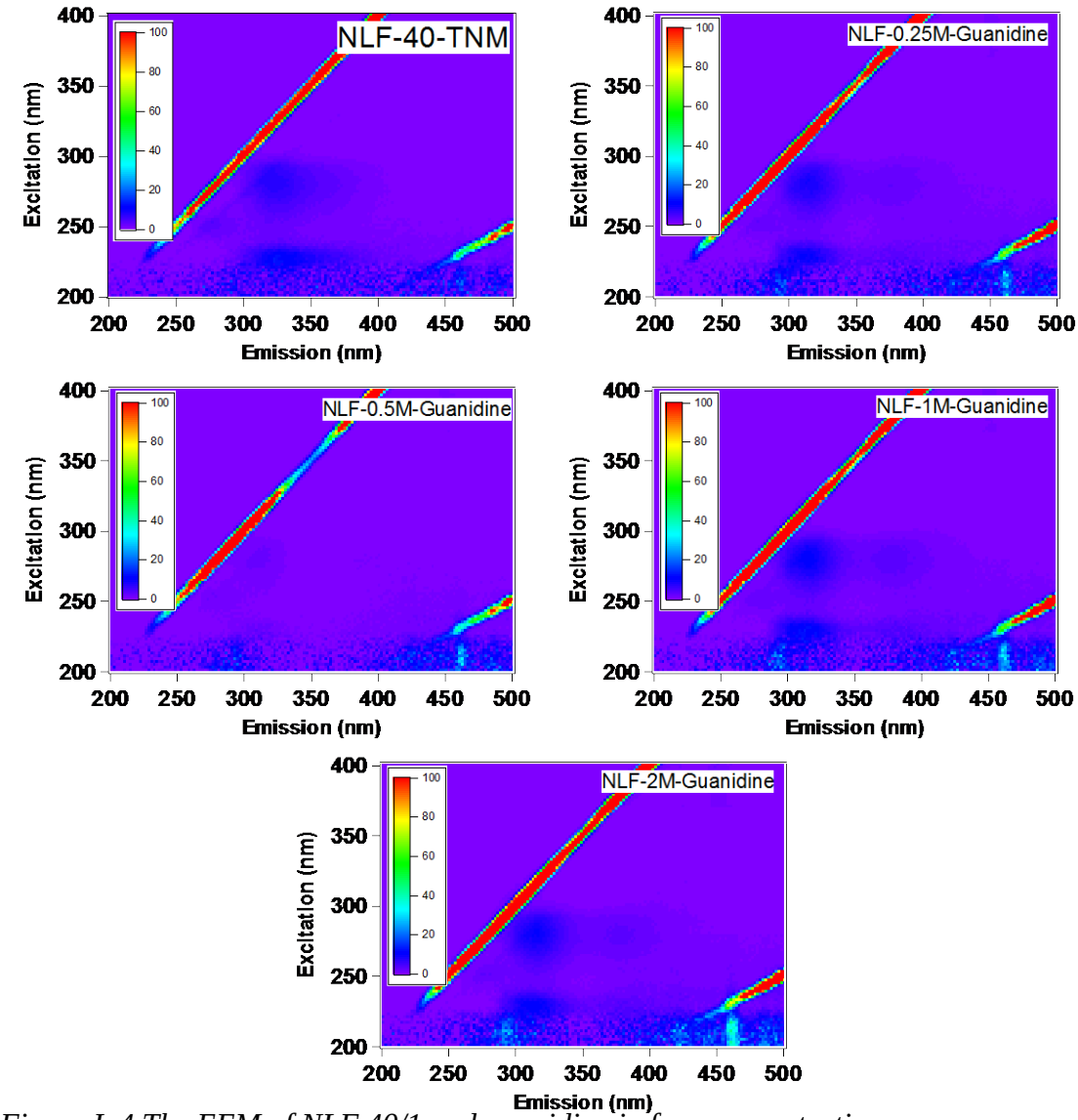

Figure I. 4 The EEM of NLF 40/1 and guanidine in four concentrations.